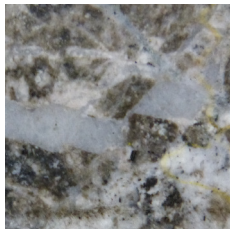
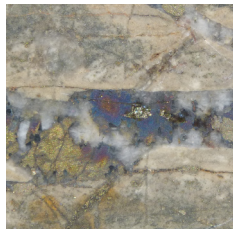
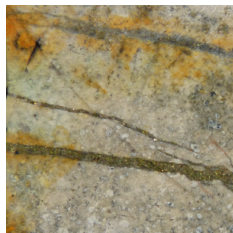





Characteristics of porphyry Cu deposits and their potential as exploration targets in South Australia



Report Book
2013/00019



Characteristics of porphyry Cu deposits and their potential as exploration targets in South Australia

Claire E. Wade

**Geological Survey of South Australia,
Resources and Energy Group, DMITRE**

November 2013

Report Book 2013/00019



Government of South Australia

Department for Manufacturing,
Innovation, Trade, Resources and Energy

Resources and Energy Group

Department for Manufacturing, Innovation, Trade, Resources and Energy
Level 7, 101 Grenfell Street, Adelaide
GPO Box 1264, Adelaide SA 5001
Phone +61 8 8463 3037
Email dmitre.minerals@sa.gov.au
www.minerals.dmitre.sa.gov.au

South Australian Resources Information Geoserver (SARIG)

SARIG provides up-to-date views of mineral, petroleum and geothermal tenements and other geoscientific data. You can search, view and download information relating to minerals and mining in South Australia including tenement details, mines and mineral deposits, geological and geophysical data, publications and reports (including company reports).

www.sarig.dmitre.sa.gov.au

© Government of South Australia 2013

This work is copyright. Apart from any use as permitted under the *Copyright Act 1968* (Cwlth), no part may be reproduced by any process without prior written permission from the Department for Manufacturing, Innovation, Trade, Resources and Energy (DMITRE). Requests and inquiries concerning reproduction and rights should be addressed to the Deputy Chief Executive, Resources and Energy, DMITRE, GPO Box 1264, Adelaide SA 5001.

Disclaimer

The contents of this report are for general information only and are not intended as professional advice, and the Department for Manufacturing, Innovation, Trade, Resources and Energy (and the Government of South Australia) make no representation, express or implied, as to the accuracy, reliability or completeness of the information contained in this report or as to the suitability of the information for any particular purpose. Use of or reliance upon the information contained in this report is at the sole risk of the user in all things and the Department for Manufacturing, Innovation, Trade, Resources and Energy (and the Government of South Australia) disclaim any responsibility for that use or reliance and any liability to the user.

Preferred way to cite this publication

Wade C 2013. *Characteristics of porphyry Cu deposits and their potential as exploration targets in South Australia*, Report Book 2013/00019. Department for Manufacturing, Innovation, Trade, Resources and Energy, South Australia, Adelaide.

CONTENTS

OVERVIEW.....	1
GLOBAL DISTRIBUTION OF PORPHYRY CU PROVINCES, DISTRICTS AND DEPOSITS.....	4
SPATIAL AND TEMPORAL COINCIDENCE	5
TECTONIC SETTINGS AND TECTONO-MAGMATIC CONTROLS	9
MAGMATIC ASSOCIATION	12
REGIONAL AND DISTRICT SCALE CHARACTERISTICS	13
Host rocks.....	13
Porphyry stocks and dykes.....	14
Breccias and veins in porphyry systems.....	16
PORPHYRY EVOLUTION, ALTERATION AND MINERAL ZONING.....	17
ALTERATION.....	22
Early sodic-calcic alteration	22
Potassic (K-silicate) alteration	23
Propylitic alteration (chlorite, epidote, actinolite alteration).....	23
Sericitic-chlorite (green sericite).....	24
Phyllic alteration (sericitic alteration)	24
Advanced argillic alteration (lithocap environment)	24
Intermediate argillic alteration.....	24
Late sodic-calcic alteration	24
Superposition of epithermal over porphyry (telescoping)	25
MINERALISATION	26
Hypogene mineralisation	26
Supergene enrichment – oxidation and upgrading	26
GEOPHYSICAL EXPRESSION OF PORPHYRY CU DEPOSITS.....	27
MAGNETICS	28
GRAVITY.....	28
ELECTRICAL AND ELECTROMAGNETIC METHODS.....	29
ALTERATION FOOTPRINTS.....	30
SPECTRAL MAPPING AND REMOTE SENSING	30
SHORTWAVE INFRARED (SWIR) AND AIRBORNE SWIR	30
ADVANCED SPACEBORNE THERMAL EMISSION AND REFLECTION (ASTER).....	31
GENETICALLY ASSOCIATED MINERAL DEPOSITS.....	32
EPITHERMAL DEPOSITS	33
SKARN DEPOSITS.....	34
CONTINUUM OF IOCG, PORPHYRY AND EPITHERMAL SYSTEMS	34
POTENTIAL OF PORPHYRY SYSTEMS IN SOUTH AUSTRALIA	36
STRATEGY FOR PORPHYRY CU DEPOSITS IN SOUTH AUSTRALIA	41
ACKNOWLEDGEMENTS	47
REFERENCES	48

TABLES

Table 1.	Au-rich porphyry Cu deposits in order of gold tonnage, used in Figures 2 and 3.....	3
Table 2.	Cu-rich porphyry Cu deposits in order of copper tonnage, used in Figures 2 and 3.	4
Table 3.	High and low sulphidation epithermal deposits in order of gold tonnage, used in Figure 4.	5
Table 4.	Summary of ore host and host rocks for selected porphyry and high sulphidation (HS) deposits in central and northern Chile and central Peru.....	14
Table 5.	Vein types and their mineralogy, associated alteration, envelopes or alteration haloes and form associated with Cu, Cu-Mo, Cu-Au and Au-rich porphyry deposits.	20
Table 6.	Summary of main mineralogy, alteration styles and sulphides at selected porphyry Cu and IOCG deposits from South America.	25
Table 7.	Features of porphyry copper deposits and their detectable geophysical techniques and exploration implications after Irvine and Smith (1990). ASTER = advanced spaceborne thermal emission and reflection; VNIR = visual near infra-red; SWIR = short-wave infra-red.	29
Table 8.	Characteristics of the hydrothermal alteration footprint associated with porphyry Cu deposits and their corresponding geophysical technique.....	31
Table 9.	Comparison of characteristics common to IOCG, porphyry and epithermal deposits, including tectonic setting, associated magmas, mineralisation style, alteration assemblage and ore minerals.	36
Table 10.	Summary of exploration activity aimed at porphyry-style mineralisation in South Australia.	38
Table 11.	Examples of methods used to detect specific features related to porphyry Cu deposits and their level of importance in exploration at various scales.	43
Table 12.	Summary of tectonic setting, magma composition, lithology and structural controls of various igneous units in South Australia to assess potential settings for porphyry Cu deposit formation.	45

FIGURES

Figure 1.	Global distribution of porphyry copper, Ag-Pb-Zn-Cu and epithermal deposits after Sillitoe (2010), classified by principal metals, deposit type and age.....	6
Figure 2.	Contained gold metal in Au-rich porphyry Cu deposits listed in Table 1.	7
Figure 3.	Contained copper metal in Cu-rich porphyry Cu deposits listed in Table 2.....	8
Figure 4.	Contained gold metal in high sulphidation and low sulphidation epithermal deposits listed in Table 3.	8
Figure 5.	Favourable geodynamic settings for the formation of porphyry and epithermal deposits.	9
Figure 6.	Series of schematic cross sections illustrating the subduction related (a) and post-collisional tectonic setting (b-d) in the formation of porphyry and epithermal deposits.	10
Figure 7.	Classification of porphyry deposits by metal content after Kesler (1973).....	12
Figure 8.	Conceptual model of porphyry Cu-Au-Mo deposit centred on a multi-phase porphyry intrusion.	15
Figure 9.	Schematic diagrams illustrating the different types of breccias and their hybrids related to porphyry Cu systems, reproduced from Cooke (2013).....	16
Figure 10.	Mineralised breccias from porphyry copper deposits from Chile, South America.	18
Figure 11.	Examples of veins within porphyry copper deposits from Chile, South America.....	19
Figure 12.	Model for an orthomagmatic porphyry Cu system illustrating the generation of Cu-bearing ore fluids during crystallisation of a magma based on observations from the Yerington Batholith after Dilles (1987).....	21
Figure 13.	The porphyry copper model based on Kalamazoo porphyry Cu mine, Arizona after Lowell and Guilbert (1970).	22
Figure 14.	Three porphyry copper models illustrating the lateral and vertical variation in alteration zones surrounding the porphyry intrusion.	23
Figure 15.	Generalised plan in section illustrating the relative position of the hypogene and supergene zones within a porphyry Cu deposit.....	27

Figure 16. Laboratory spectra of muscovite, kaolinite, alunite, epidote, calcite and chlorite resampled to ASTER band passes.	32
Figure 17. The porphyry-epithermal-IOCG spectrum occurring within giant hydrothermal systems of the Great Bear Magmatic Zone, Canada, illustrating the various mineralisation styles present within the system, after Mumin et al. (2010).....	35
Figure 18. Examples of alteration and mineralisation styles at the Netley Hill Prospect, photo source PacMag in Clifford (2008).	40
Figure 19. Location of various igneous units in South Australia which may be potential units that host porphyry Cu deposits, listed in Table 12.....	46

Characteristics of porphyry Cu deposits and their potential as exploration targets in South Australia

Claire E. Wade

OVERVIEW

Porphyry Cu deposits are typically large tonnage (>150 Mt) and low grade (<1%) hypogene deposits (Holliday and Cooke 2007, Sillitoe 2010b). Porphyry Cu deposits are unified by close spatial, temporal and genetic associations between subvolcanic porphyritic intrusive complexes and hypogene mineralisation, with hydrothermal alteration mineral assemblages that occur in and around them (Holliday and Cooke 2007). Hydrothermal alteration associated with porphyry Cu deposits is large volume (10^3 – 10^4 km³), centred on porphyry Cu stocks, plutons or dykes that form above larger batholiths at 6–10 km depth (Sillitoe 2010b). The potential for giant porphyry Cu deposits (i.e. several deposits >1 billion tonnes @ 0.5% Cu, e.g. Bingham Canyon, Utah; Collahuasi, Chuquicamata, La Escondida, El Teniente, Chile; Tables 1–3) makes them valuable exploration targets (Richards 2003). Porphyry Cu deposits are significant in the world's metal supply, accounting for nearly three-quarters of the world's supply of Cu, in addition to other metals such as Mo (approximately half of the world's supply); Au (approximately one-fifth), most of the Re, and minor amounts of other metals such as Ag, Pd, Te, Se, Bi, Zn and Pb (Sillitoe 2010b). Porphyry deposits are most commonly discovered in continental arcs and oceanic arcs of Cenozoic and Quaternary age but have also been discovered in ancient fold belts (Cooke et al. 2005). Porphyry Cu deposits have been generated worldwide since the Archean, although younger examples, Mesozoic to Cenozoic in age are the most abundantly preserved, which may be simply a consequence of younger terranes being less eroded.

The largest Au-rich porphyry deposits are concentrated in the SW Pacific and South America, with other occurrences in Eurasia, British Columbia, Alaska and New South Wales (Figs 1–4). Cu-Mo and Cu-Mo-Au porphyry deposits are concentrated in South America and western United States of America (Figs 1–4).

Porphyry and epithermal deposits form in arc-related settings throughout the world (Fig. 5; Richards 2003, Sillitoe 2010b) with active cross-arc and/or arc-parallel structures. Porphyry Cu systems tend to occur in linear, typically orogen-parallel belts which span from a few tens to hundreds and thousands of kilometres in length e.g. Andes, South America, likely related to the position of the magmatic arc (Fig. 6a; Sillitoe 2010b, Richards 2011b). A small number of systems form in post-collisional and other tectonic settings that develop after subduction ceases (Fig. 6b–d; Sillitoe 2010b, Richards 2011b). Porphyry Cu deposits tend to cluster within mineral provinces which adds weight to the implied critical role that geodynamic setting and crustal architecture play in localising ore deposits.

Porphyry deposits are related to multi-phase porphyritic intrusions successively intruded from a parent magma chamber, typically calc-alkalic to alkalic in composition and belonging to the magnetite series of Ishihara (Ishihara 1981, Holliday and Cooke 2007). Mineralised complexes are typically comprised of multiple pipes, dykes or sills which commonly occur as vertical bodies emplaced at shallow depths (1–4 km; Cooke 2013). Significant mineralisation is usually associated with one or two intermediate stage intrusive phases where mineralisation occurs at depths between 2 and 4 km. Alteration and mineralisation is commonly related to the most felsic phases within the intrusive complexes; one intrusive phase typically contributes most of the magmatic-hydrothermal fluids (Holliday and Cooke 2007). Alteration and mineralisation begins with high-temperature, late magmatic oxidised fluids in the early stages to low or moderate-temperature, more reduced hydrothermal fluids and magmatic and meteoric components in the later stages

(Camus 2005). Each of these hydrothermal stages is broadly related to quartz veins and potassic alteration, sodic-calcic and sodic alteration, calcic alteration, chlorite-epidote-actinolite alteration and sericitic alteration. Metal tenor is influenced by the degree of fractionation in the associated intrusions; less fractionated calc-alkaline intrusions are related to Cu-Au mineralisation while the more fractionated intrusions are related to Cu-Mo mineralisation (Fig. 7; Holliday and Cooke 2007). Metal endowment can also be correlated with tectonic setting and magma composition (Fig. 7).

Ore is generally stockwork, disseminated and breccia-hosted associated with large volumes of hydrothermal alteration. The main ore minerals are chalcopyrite, bornite, gold and molybdenite. In some deposits replacement-style mineralisation predominates. Multiple generations and types of veins are also common in porphyry systems; vein density correlates with grade. Sulphide zonation typically consists of a bornite-rich core (\pm Au), chalcopyrite in the outer central zone and a pyrite halo.

Types and examples of porphyry deposits include:

- Au only (no Cu; Cu <200 ppm) e.g. Maricunga Belt, northern Chile;
- Au-rich (>0.4 g/t Au e.g. Lepanto Far South East, North Luzon; Grasberg, Irian Jaya; Bingham, Utah; and Cadia, New South Wales; Fig. 2);
- Cu-Au (0.1–0.4 g/t Au e.g. Batu Hijau, Indonesia; Pebble, Alaska; Oyu Tolgoi, Mongolia and; Reko Diq, Pakistan; Fig. 3); and
- Cu-Mo (<0.1 g/t Au e.g. Rio Blanco-Los Bronces, central Chile; El Teniente, central Chile; and Chuquibambilla, northern Chile; Fig. 3).

Epithermal deposits are often associated with porphyry deposits. Epithermal deposits occur within 1 km of the surface with a porphyry-epithermal transition and comprise low sulphidation and high sulphidation systems, which is influenced by fluid composition. Low sulphidation epithermal deposits commonly occur in extensional tectonic settings, related to a porphyry, and extend from the surface down to the top of a porphyry system, within the top 1 km of the surface. Low sulphidation fluids comprise reduced, near neutral pH fluids with sulphur occurring as H₂S. Mixing between this fluid and circulating meteoric fluids is an important component of the development of low sulphidation epithermal deposits. High sulphidation epithermal deposits are best developed in magmatic arcs, distal to the porphyry source, either at a distance laterally away from the porphyry source or in some cases above a much deeper porphyry source. High sulphidation fluids are oxidised acidic fluids, where sulphur occurs as SO₂. This hot, acidic fluid evolves and depressurises as it ascends, causing volatiles, including SO₂ to escape from solution in progressively greater quantities. The rising hot fluids become progressively hotter and more acidic as the exsolved SO₂ reacts with water to form H₂SO₄ and condenses. The fluid becomes neutralised and cools as it reacts with permeable host rocks.

Cu-Au porphyry deposits are associated with high sulphidation (HS) epithermal systems e.g. Yanacocha, northern Peru (Sillitoe and Hedenquist 2003); Lepanto, northern Philippines (Cooke and Simmons 2000, Sillitoe and Hedenquist 2003); La Mejicana, northwest Argentina (Cooke and Simmons 2000); and Paradise Peak, Nevada (Sillitoe and Lorson 1994, Cooke and Simmons 2000) and low sulphidation deposits e.g. Hishikari, Japan, Waihi, New Zealand and Kelian, Indonesia. Some intermediate sulphidation (IS) epithermal deposits are spatially associated with porphyry systems e.g. Baguio district, Philippines and the South Apuseni Mountains, Romania (Sillitoe and Hedenquist 2003). The Au content for high sulphidation and low sulphidation epithermal deposits is shown in Fig. 4, for deposits listed in Table 3.

Porphyry Cu deposits are generally formed over a short time interval with individual hydrothermal events spanning 10–500 k.y. (Sillitoe 2010b, Cooke 2013). Alteration associated with porphyry Cu deposits is generally a consistent, broad-scale alteration-mineralisation zoning pattern characterised by several alteration assemblages: potassic, propylitic, phyllic, intermediate argillic, and advanced argillic; each of these assemblages form at discrete points in time and space during the formation of porphyry deposits (Cooke 2013). Propylitic alteration assemblages are zoned laterally outward from the intrusive centre. These widespread and distinctive zones of alteration

provide useful alteration footprints for explorers (Cooke et al., 2005), and alteration mapping has become a key exploration tool for identifying and evaluating porphyry and epithermal systems.

Porphyry Cu-(Au-Mo) and epithermal deposits have two key characteristics that make them readily detectable through the use of geophysics: major regional-scale structural control and large, zoned hydrothermal alteration footprints. Regional-scale surveys such as airborne magnetic and gravity surveys can be used to identify major structures (faults and fault intersections), in addition to locating deep intrusive bodies which may be genetically related to the porphyry system. The large, zoned hydrothermal alteration footprints can be identified by changes in the physical properties of the host rocks where electrical, magnetic and density properties, potassium content, and spectral absorption have been affected. Scale and depth penetration are critical when selecting the most effective geophysical technique for exploring for porphyry Cu and epithermal deposits e.g. district scale versus regional scale.

Table 1. Au-rich porphyry Cu deposits in order of gold tonnage, used in Figures 2 and 3.

	Deposit	Province	Age (Ma)	Tonnage (Mt)	Au (g/t)	Au (t)	Cu (wt %)	Cu (Mt)	Mo (wt %)	Mo (Mt)	Metal	Reference
1	Grasberg	Irian Jaya	3	2480	1.05	2604	1.13	28.02			Cu-Au	1, 2, 3
2	Pebble	Alaska	90	5942	0.35	2100	0.42		0.025		Cu-Au-Mo	4
3	Bingham	Utah	38.8	3228	0.50	1803	0.88	28.46	0.02	0.81	Cu-Au-Mo	1, 2
4	Oyu Tolgoi	Mongolia	411	2467	0.32	1425	0.83	20.57			Cu-Au	5, 6, 7
5	Cadia District	NSW	440	1070	0.77	1400	0.31	3.38			Cu-Au	8
6	Reko Diq	Pakistan	Mioce.?	855	0.33	1390	0.65	5.56			Cu-Au	9
7	Kal'makyr	Uzbekistan	310–294	2700	0.51	1374	0.40	10.80			Cu-Au	2, 10
8	Lepanto-Far South East	North Luzon	1.5– 1.2	685	1.42	973	0.80	5.48			Cu-Au	2, 3
9	Cerro Casale	Chile	13.5	1285	0.70	900	0.35	4.50			Cu-Au	1, 2
10	Panguna	Bougainville	3.5	1415	0.57	799	0.46	6.51			Cu-Au	1, 2
11	Ok Tedi	PNG	1.2–1.1	700	0.64	650	0.64	4.48			Cu-Au	1, 2
12	Batu Hijau	Indonesia	3.7	1644	0.35	572	0.44	7.23			Cu-Au	1, 2, 11
13	Minas Conga	Northern Peru	20	641	0.79	506	0.30	1.92			Cu-Au	1, 3
14	Tampakan	Philippines	3.3–2.2	1400	0.24	506	0.55	7.70			Cu-Au	12, 13
15	Fish Lake	Canada	80	491	0.43	471	0.22				Cu-Au	14
16	La Escondida	Northern Chile	38	2262	0.19	445	1.15	32.49	0.021	0.48	Cu-Au-Mo	2, 5
17	El Teniente	Central Chile	4.8	11845	0.035	437	0.63	94.35	0.02	2.50	Cu-Mo	5
18	Peschanka	Kamchatka	L. Jur.	940	0.42	395	0.51	4.79			Cu-Au	2
19	Dal'neye	Uzbekistan	310–294	545	0.69	376	0.59	3.21			Cu-Au	2, 10
20	Bajo de la Alumbrera	Argentina	8–7	551	0.67	369	0.52	2.87			Cu-Au	1, 2, 15
21	Frieda River	PNG	14–11	1103	0.32	354	0.61	6.73			Cu-Au	1, 2
22	Atlas	Philippines	61	1380	0.24	331	0.50	6.90			Cu-Au	2
23	Sar Cheshmeh	Iran	12.2	1200	0.27	324	1.20	14.40	0.03	0.36	Cu-Au-Mo	1, 2, 3, 16, 17
24	Chuquicamata	Northern Chile	33.6	12066	0.04	301	0.55	66.37	0.024	1.81	Cu-Mo	5
25	Sipilay	Philippines	K-T	884	0.34	301	0.50	4.42	0.01	0.09	Cu-Au	2
26	Prosperity	BC, Canada	79	631	0.46	290	0.25	1.58			Cu-Au	1, 2, 3, 18
27	Refugio	Chile	23	250	1	259	0.03				Cu-Au	14
28	Santo Tomas II	Philippines	1	499	0.7	230	0.375				Cu-Au	14

References: 1 Kirkham and Dunne 2000, 2 Mutschler et al. 1999, 3 Bank of Montreal (BMO; Nesbit Burns unpub. data 2002) in Cooke et al. 2005, 4 Kelley et al., 2011, 5 Camus 2002, 6 Perelló et al. 2001, 7 Ivanhoe Mines 2004, 8 Wilson et al. 2004, 9 Tethyan Copper Company Ltd (unpub. data 2004) in Cooke et al. 2005, 10 Sokolov 1998, 11 Garwin 2002, 12 Sillitoe 1999, 13 Middleton et al. 2004, 14 Sillitoe 1997, 15 Ulrich and Heinrich 2001, 16 Samani 1998, 17 Porter 1998, 18 Cairi et al. 1995. Mioce. = Miocene; L. Jur. = Late Jurassic; K-T = Cretaceous-Tertiary.

In South Australia porphyry-style mineralisation is associated with various Cambrian and Neoproterozoic successions of the Adelaide Geosyncline and Stuart Shelf e.g. porphyry Cu deposit at Burra and Cu-Mo porphyry-style mineralisation at Anabama Hill, Nackara Arc. Hydrothermal alteration/iron-metasomatism and copper mineralisation is associated with Hiltaba Suite granites in the Myall Creek area and Lake Charles Diorites in the Benagerie Ridge, suggesting Mesoproterozoic granites and volcanic rocks associated with IOCG mineralisation may also represent a continuum to porphyry-style mineralisation. Hydrothermal assemblages in magmatic rocks at Billeroo, Curnamona Province, display many similarities to alkali porphyry Cu-Au systems (Rutherford et al., 2003), with the potential for mesothermal Fe-oxide Cu-Au and skarn replacement-style mineral systems.

Table 2. Cu-rich porphyry Cu deposits in order of copper tonnage, used in Figures 2 and 3.

	Deposit	Province	Age (Ma)	Tonnage (Gt)	Cu (wt %)	Cu (Mt)	Mo (wt %)	Mo (Mt)	Au (g/t)	Au (t)	Metal	Reference
1	Río Blanco-Los Bronces	Central Chile	5.4	6.99	0.75	204.30	0.018	1.26	0.035	244.7	Cu-Mo	1
2	El Teniente	Central Chile	4.8	12.48	0.63	94.35	0.02	2.50	0.035	437	Cu-Mo	1
3	Chuquicamata	Northern Chile	33.6	7.52	0.55	66.37	0.024	1.81	0.04	300.8	Cu-Mo	1
4	Butte	Montana	61	5.23	0.67	35.11	0.03	1.44	0.042	217.0	Cu-Mo	2, 3, 4, 5
5	La Escondida	Northern Chile	38	2.26	1.15	32.49	0.021	0.48	0.19	429.8	Cu-Au-Mo	6
6	Cananea	Mexico	58	7.14	0.42	30.00	0.01	0.57	0.012	82.0	Cu-Mo	3, 7, 8
7	Bingham	Utah	38.8	3.23	0.88	28.46	0.02	0.81	0.497	1603	Cu-Au-Mo	2, 3
8	Grasberg	Irian Jaya	3	2.48	1.13	28.02			1.05	2604	Cu-Au	2, 3, 9
9	Los Pelambres-El Pachón	Central Chile	10	4.19	0.63	26.88	0.016	0.67	0.02	83.86	Cu-Mo	1
10	Rosario	Northern Chile	34.1	3.11	0.82	25.49	0.024	0.75	0.01	31.08	Cu-Mo	1
11	Lone Star	SW Arizona	58	5.53	0.45	24.74					Cu-Mo	2, 3, 10, 11
12	Morenci-Metcalf	SW Arizona	56.6	4.69	0.52	24.59		0.086	0.006	30.0	Cu-Mo	2, 3
13	Oyu Tolgoi	Mongolia	411	2.47	0.83	20.57			0.32	790.2	Cu-Au	12
14	Cerro Colorado	Panama	4.3	4.50	0.45	20.25			0.11	160.71	Cu-Au	2, 3, 13, 6
15	Radomiro Tomic	Northern Chile	32.7	4.98	0.39	19.93	0.015	0.75			Cu-Mo	1, 14
16	La Granja	Northern Peru	10	3.20	0.61	19.52	0.013	0.08	0.04	128	Cu-Mo	2, 3, 9
17	Cujaone	Southern Peru	52.3	2.17	0.60	17.14	0.03	0.65			Cu-Mo	1, 15
18	Sar Cheshmeh	Iran	12.2	1.20	1.2	14.40	0.03	0.36	0.27	324	Cu-Au	2, 3, 16, 17
19	Escondida Norte	Northern Chile	39–36	1.62	0.87	14.05					Cu-Mo	1
20	Pima	SW Arizona	58–57	1.90	0.69	13.06		0.03			Cu-Mo	3
21	Aktogay-Aiderly	Kazakhstan	?Carb	3.13	0.4	12.50	0.01				Cu-Mo	2, 18
22	El Salvador	Northern Chile	41	0.97	0.63	11.29	0.022	0.21	0.1	97.4	Cu-Au-Mo	1
23	Toki	Northern Chile	39–36	2.41	0.45	10.85					Cu-Mo	19
24	Ray	SW Arizona	61–60	1.58	0.68	10.79		0.04	0.002	3.20	Cu-Mo	2, 3
25	Kal'makyr	Uzbekistan	?Carb	2.70	0.39	10.64			0.51	1,374.3	Cu-Au	3, 18

References: 1 Camus 2002, 2 Kirkham and Dunne 2000, 3 Mutschler et al. 1999, 4 Meyer et al. 1968, 5 Brimhall 1977, 6 Clark et al. 1977, 7 Salas 1991, 8 Bushnell 1988, 9 Bank of Montreal (BMO; Nesbitt Burns, unpub. data 2002) in Cooke et al., 2005, 10 Langton and Williams 1981, 11 Bouse et al., 1999, 12 Ivanhoe Mines 2004, 13 Kesler et al. 1977, 14 Cuadra and Camus 1998, 15 Clark et al. 1990, 16 Samani 1998, 17 Porter 1998, 18 Sokolov 1998, 19 Camus 2005. Carb. = Carboniferous.

GLOBAL DISTRIBUTION OF PORPHYRY CU PROVINCES, DISTRICTS AND DEPOSITS

The worldwide distribution of porphyry Cu-Mo, Cu-Mo-Au and Cu-Au deposits, porphyry and major skarn/carbonate replacement Ag-Pb-Zn-Cu deposits and high-sulphidation epithermal ± porphyry deposits are shown on Fig. 1. The majority of the world's porphyry Cu deposits outline Phanerozoic orogenic belts (Seedorff et al. 2005) and are located within circum-Pacific orogenic belts (Sillitoe 1972, Sillitoe 2010b). Porphyry Cu systems typically occur in linear, orogen-parallel belts that range from a few tens to thousands of kilometres (e.g. Andes, western South America (Fig. 1;

Sillitoe 2010b)). Porphyry Cu systems tend to occur in clusters and may attain densities of 15 per 100 000 km³ (Sillitoe 2010b). Major deposits also occur in isolation e.g. Bingham, Utah; Pebble, Alaska and Butte, Montana (Fig. 1; Cooke et al. 2005, Sillitoe 2010b). Porphyry Cu systems are linked to a time-equivalent magmatic event and were formed during well-defined metallogenic epochs (Cooke et al. 2005, Sinclair 2007, Sillitoe 2010b). The spatial distribution of porphyry Cu belts suggests arc migration, and that steepening or shallowing of subducted slabs occurred between each of the magmatic-metallogenic epochs, spatially separating each of the belts rather than superimposing them (Sillitoe and Perelló 2005).

Table 3. High and low sulphidation epithermal deposits in order of gold tonnage, used in Figure 4.

	Deposit	Province	Age (Ma)	Au (t)	Ag (t)	Deposit type	Reference
1	Pueblo Viejo	Dominican Republic	130 or 77	1364		High sulphidation	1
2	Yanacocha	Peru	10.9	868		High sulphidation	2, 3
3	Baguio	Philippines	0.6	800	900	Low sulphidation	4, 5, 6
4	Cripple Creek	Creek USA	32-31	755		Low sulphidation	7
5	Porgera	PNG	6-5.6	600		Low sulphidation	8
6	Ladolam	PNG	0.35-0.1	595		Low sulphidation	9
7	Pascua-Lama	Chile-Argentina	9.4–8.1	509		High sulphidation	10
8	Round Mountain	USA	26	413		Low sulphidation	11, 12
9	Far South East	Philippines	1.5-1.2	400		High sulphidation	13, 14
10	Tayoltita	Mexico	40	312	116500	Low sulphidation	15
11	El Indio	Chile	7.6–6.2	310		High sulphidation	16, 17, 18
12	Comstock Lode	Lode USA	13.7	260		Low sulphidation	19, 20, 21
13	McDonald	USA	39-37	251		Low sulphidation	22
14	Hishikari	Japan	1.25-0.6	250		Low sulphidation	23, 24, 25, 26
15	Pachuca-Real del Monte	Mexico	21-20	235		Low sulphidation	27
16	Waihi	New Zealand	7	230		Low sulphidation	28
17	Pierina	Peru	14	224		High sulphidation	29
18	Kelian	Indonesia	E. Miocene?	200		Low sulphidation	30
19	Chelopech	Bulgaria	78–74	195		High sulphidation	31, 32
20	Goldfield	Nevada	21	160		High sulphidation	33, 34
21	Bor	Serbia	85	150		High sulphidation	35, 36
22	Lepanto	Philippines	1.5-1.2	123		High sulphidation	37, 38, 39
23	La Copeia	Chile	24–20	96		High sulphidation	40
24	Potosi	Bolivia	13.8		86000	High sulphidation	41, 42

References: 1 Russell and Kesler 1991, 2 Harris et al. 1994, 3 Harvey et al., 1999, 4 Sawkins et al., 1979, 5 Cooke and Bloom 1990, 6 Cooke et al., 1996, 7 Thompson 1992, 8 Richards and Kerrich 1993, 9 Moyle et al., 1990, 10 Bissig et al. 2002, 11 Tingley and Berger 1985, 12 Sander and Einaudi 1990, 13 = Mutschler et al. 1999, 14 Hedenquist et al. 1998, 15 Smith et al. 1982, 16 Jannas et al. 1999, 17 Muntean et al. 1990, 18 Siddeley and Araneda 1986, 19 Vikre et al. 1988, 20 Vikre 1989a, 21 Hudson 1993, 22 Bartlett et al. 1995, 23 = Izawa et al. 1990, 24 Izawa et al. 1993, 25 Shikazano and Nagayama 1993, 26 Shikazano et al. 1993, 27 Geyne et al. 1963, 28 Brathwaite and Blattner 1995, 29 Rainbow et al., 2005, 30 van Leeuwen et al. 1990, 31 Bonev et al. 2002, 32 Moritz et al. 2002, 33 Ashley 1974, 34 Vikre 1989b, 35 Jankovic et al. 2002, 36 Bailly et al. 2002, 37 Garcia 1991, 38 Arribas et al. 1995, 39 Hedenquist et al. 1994, 40 Oviedo et al. 1991, 41 Sillitoe et al. 1998, 42 Steele 1996.

SPATIAL AND TEMPORAL COINCIDENCE

Giant porphyry deposits tend to cluster within mineral provinces, which implies that geodynamic setting and crustal architecture played an important role in localising the giant deposits (Cooke et al. 2005). Porphyry and epithermal deposits occur in arc-related settings of various ages throughout the world, most commonly in continental and oceanic arcs of Cenozoic and Quaternary age (Cooke et al. 2005). Two principal factors are believed to control the time-space distribution of porphyry Cu deposits: 1. The level of exposure of a plutonic-volcanic chain, which is largely dependent on erosion rate; and 2. The time and location of magma generation in a subduction zone and the quantity of metals within the magma (Sillitoe 1972).

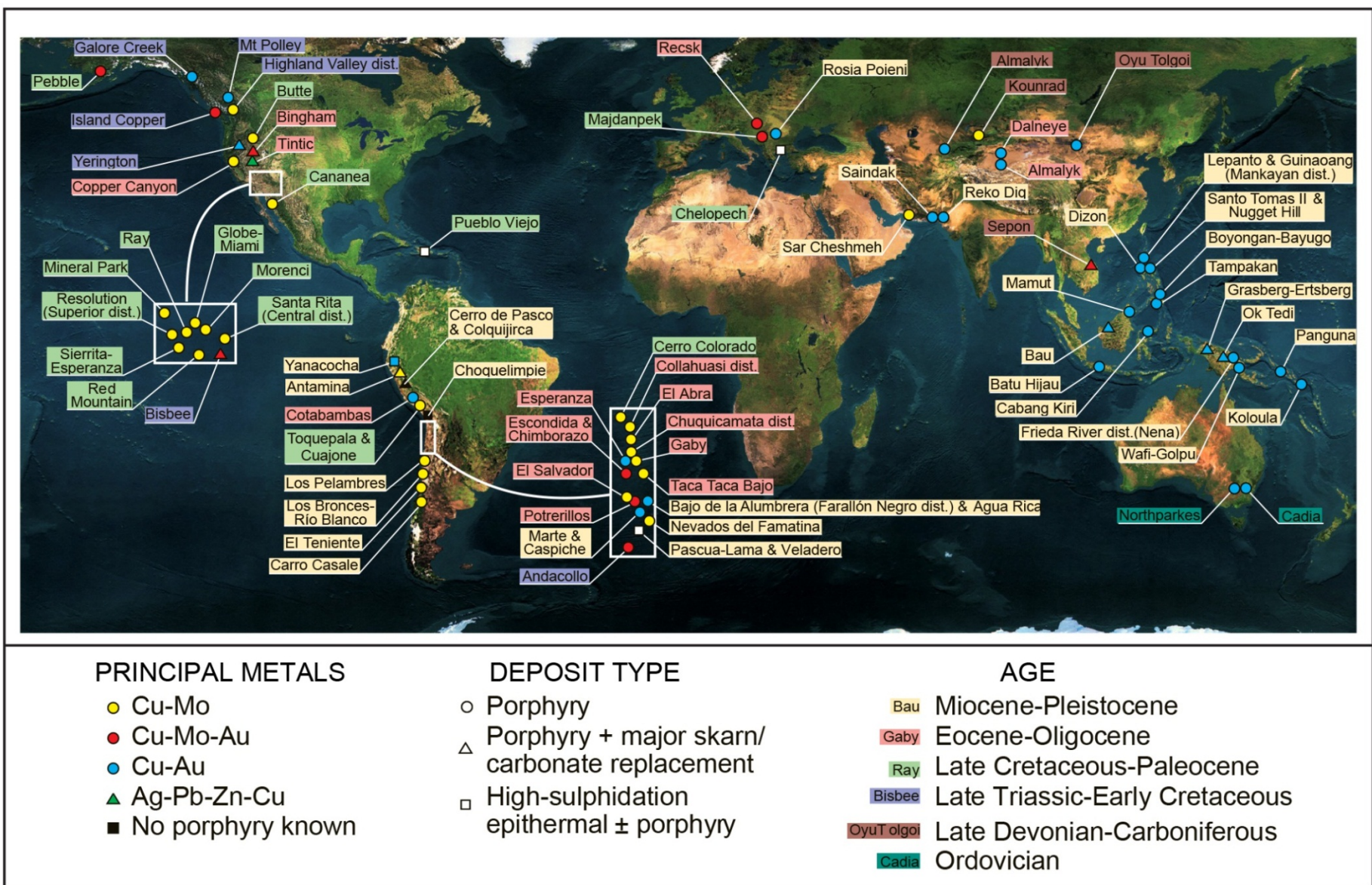


Figure 1. Global distribution of porphyry copper, Ag-Pb-Zn-Cu and epithermal deposits after Sillitoe (2010), classified by principal metals, deposit type and age.

Image source <http://auxilium-cornerstone.com/wp-content/uploads/2012/04/earth-map-dual-monitor.jpg>

Ore deposits related to older orogenic belts are less common, which is attributed to the effects of Mesozoic to Cenozoic erosion. Giant mineral deposits are restricted to only a few mineral provinces and three main time periods:

1. Central Chile Province, late Miocene to Pliocene. Contains three of the largest deposits: Rio Blancos-Los Broncos, El Teniente and Los Pelambres-El Pachón (Tables 1 and 2; Figs 2 and 3; Cooke et al. 2005, Cooke 2013).
2. Northern Chile Province, Eocene to Oligocene. Contains Chuquicamata, La Escondida, Rosario, Radomiro Tomic, Escondida Norte, El Salvador and Toki (Tables 1 and 2; Figs 2 and 3; Cooke et al. 2005, Cooke 2013).
3. South-western Arizona and Mexico, Palaeocene to early Eocene. Includes Ray, Pima, Cananea, Lone Star and Morenci-Metcalf (Table 2; Fig. 3; Cooke et al. 2005, Cooke 2013).

Archaean and Palaeoproterozoic porphyry deposits occur in Canada, although these deposits contain small to moderate quantities of metal compared to the younger deposits (Seedorff et al. 2005).

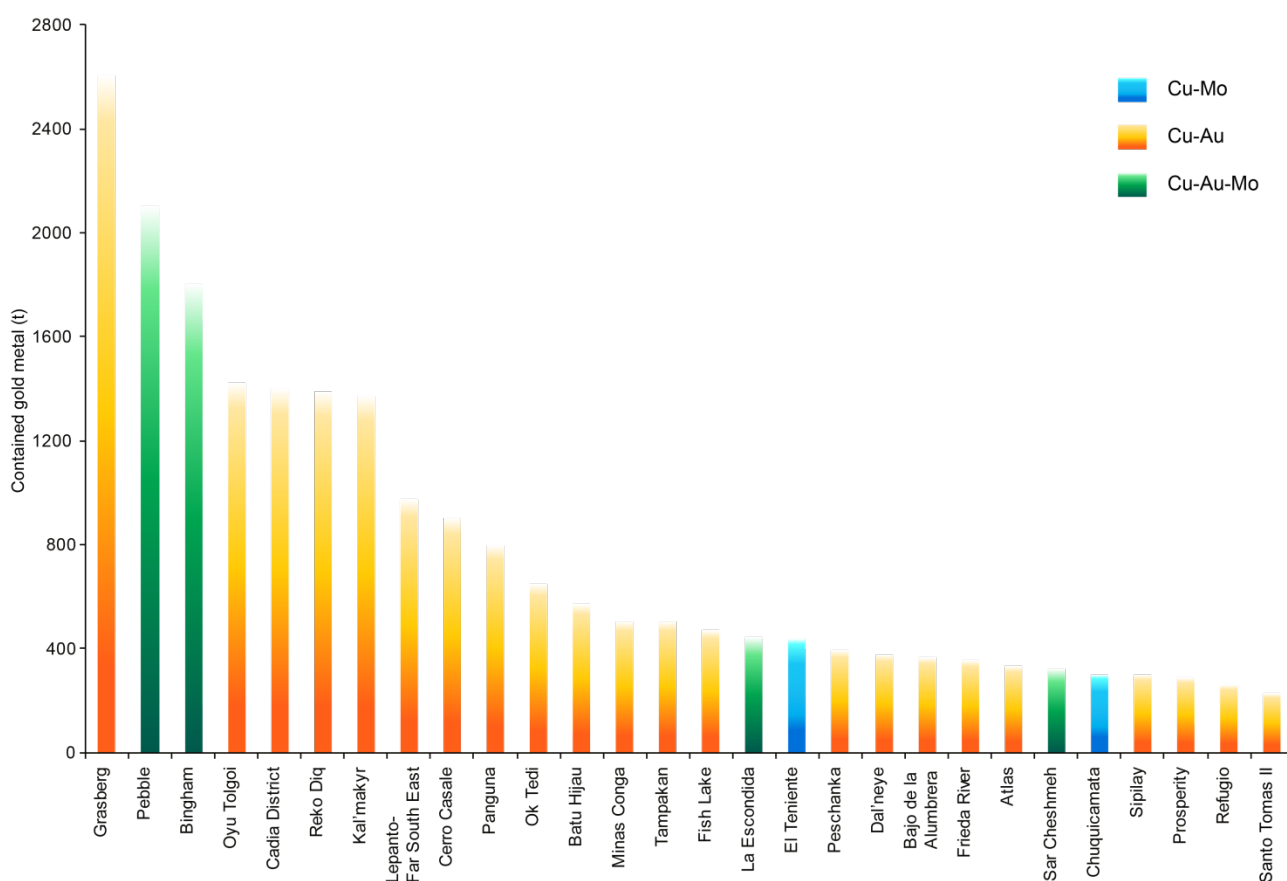


Figure 2. Contained gold metal in Au-rich porphyry Cu deposits listed in Table 1.
Data compiled from references in Table 1 and Cooke et al. 2005.

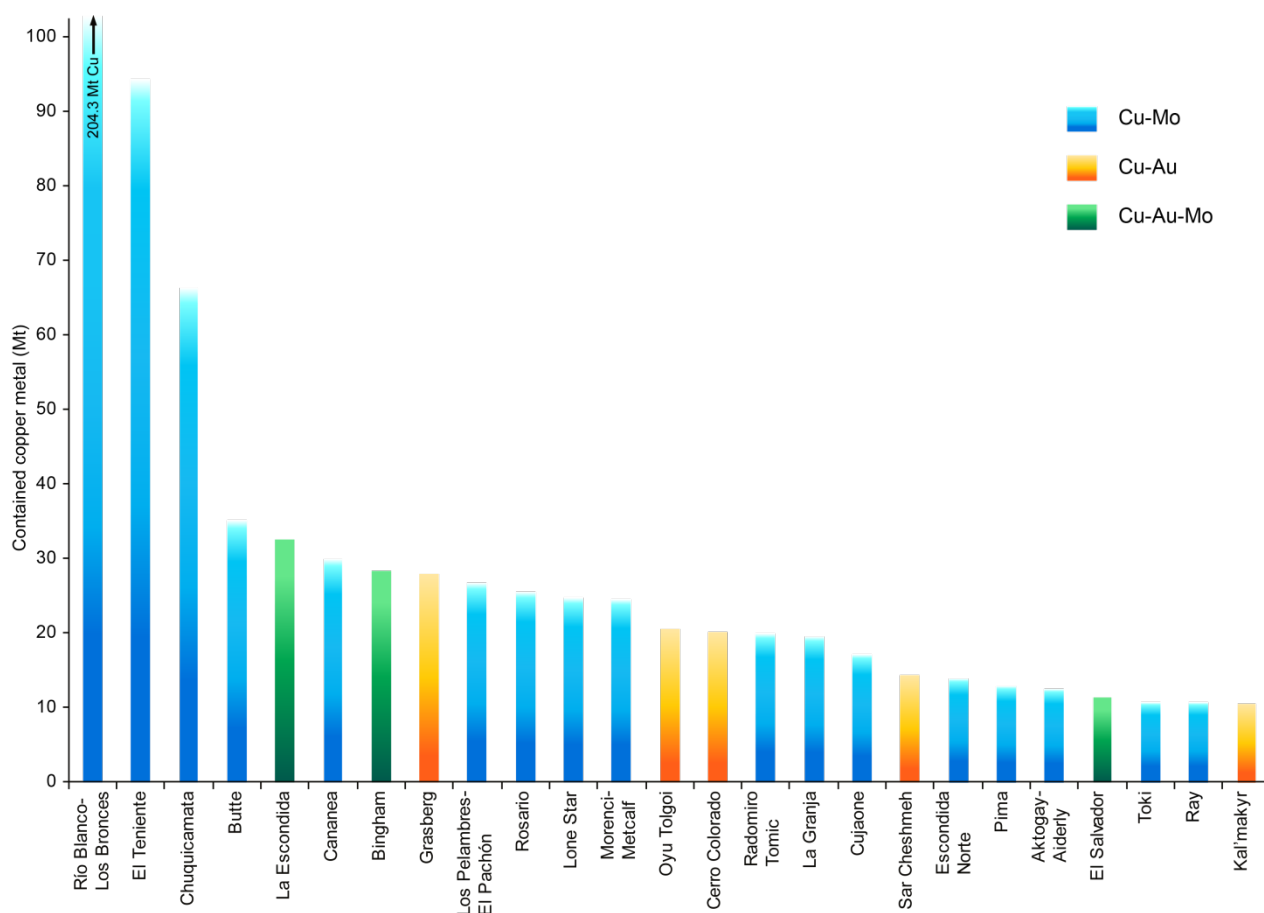


Figure 3. Contained copper metal in Cu-rich porphyry Cu deposits listed in Table 2.
Data compiled from references in Table 2 and Cooke et al. 2005.

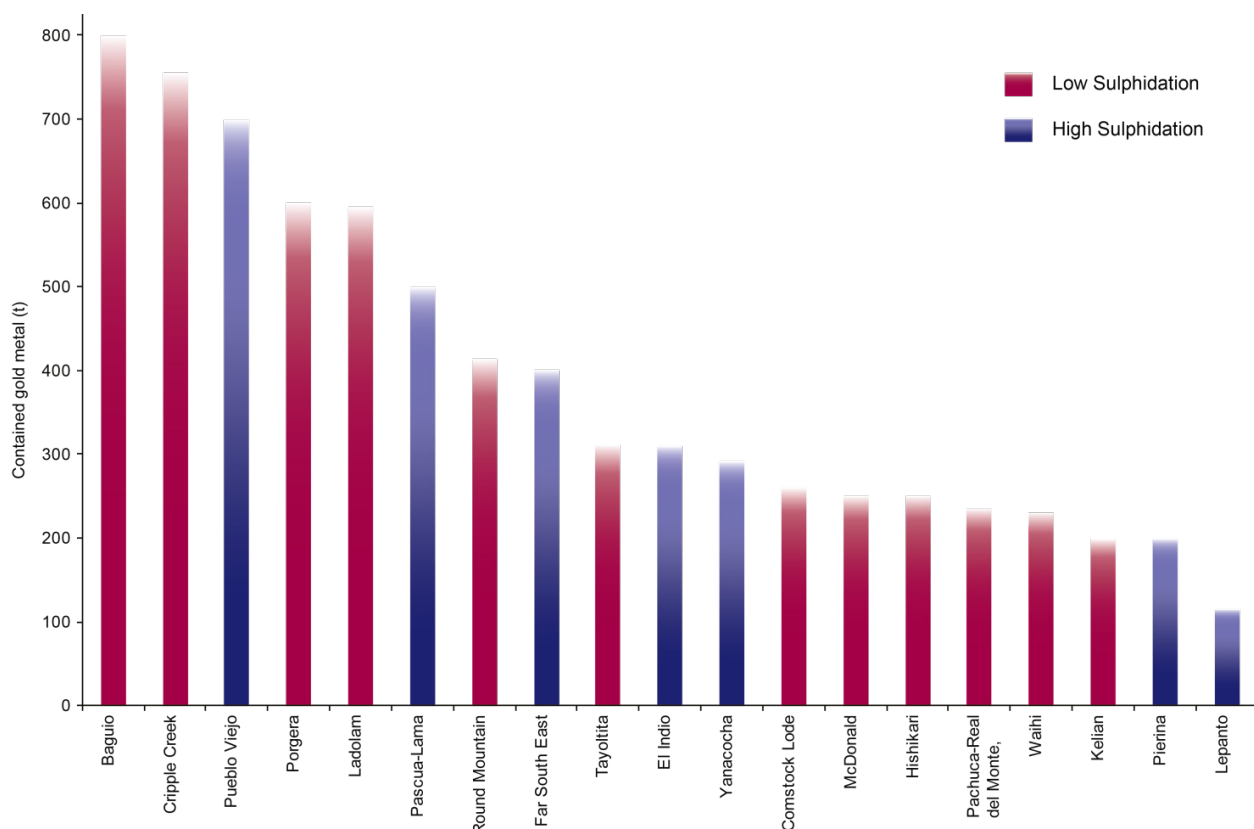


Figure 4. Contained gold metal in high sulphidation and low sulphidation epithermal deposits listed in Table 3.
Data compiled from references in Table 3 and Cooke et al. 2005.

TECTONIC SETTINGS AND TECTONO-MAGMATIC CONTROLS

Porphyry Cu(-Mo-Au) and epithermal systems are typically generated in magmatic arc environments (Fig.5; Sillitoe 2010b) and form at discrete moments in the evolution of the magmatic arc often triggered by tectonic perturbations. There are clear correlations in time between a porphyry system, a change in tectonic regime and magmatism (Richards 2003) e.g. Triassic arc development and formation of porphyry Cu systems, British Columbia (Tosdal 2012), magmatic events of latest Cretaceous to early Oligocene and Eocene to Oligocene porphyry Cu deposits in El Salvador (Cornejo et al. 1997), middle to late middle Miocene volcanic rocks and porphyries in Argentina (Halter et al. 2004), late Eocene to late Miocene magmatism and mineralisation, Cerro de Pasco and Huancayo, Peru (Bissig et al. 2008, Cooke 2013), and Pliocene volcanism and porphyry Cu-Au and high-sulphidation epithermal mineralisation in northern Luzon, the Philippines (Arribas et al. 1995).

Within magmatic arcs, regional stress regimes may range from moderately extensional through to oblique-slip contractional (Fig. 5), while strongly extensional settings lack significant porphyry Cu systems (Tosdal and Richards 2001). Post-collisional porphyry deposits (e.g. Fig. 6b-d) are found in south-west China where collision commenced at 65 Ma and porphyry deposits cluster at 40 Ma, 35 Ma and 25 Ma (Cooke 2013).

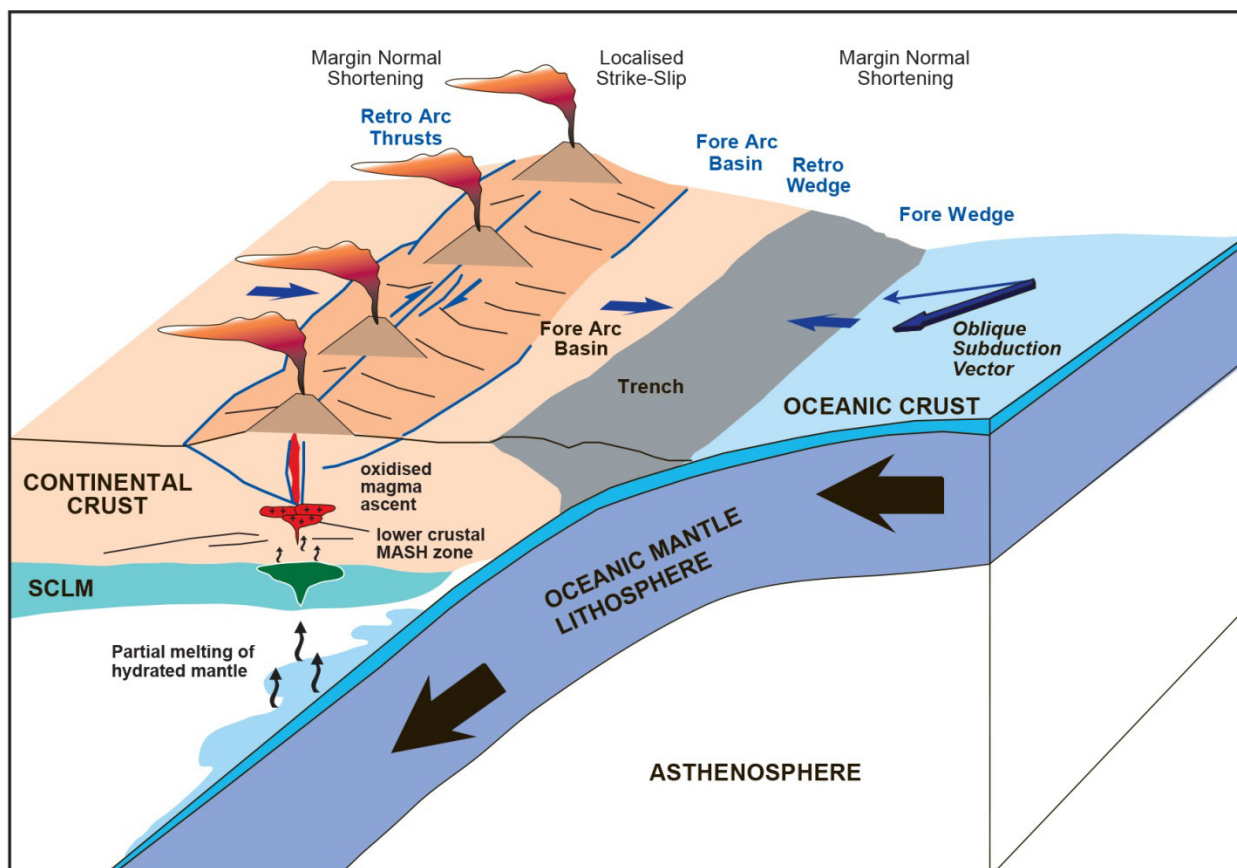


Figure 5. Favourable geodynamic settings for the formation of porphyry and epithermal deposits.

Settings include island arc, Andean Arc, accreted arc, post orogenic belt and behind-belt magmatic centres. Also indicated are the structure and processes that occur beneath the volcanic arc to produce the oxidised magma which is an integral part in the formation of porphyry Cu and epithermal deposits. Lower crustal Melting, Assimilation, Storage and Homogenisation (MASH) zone represents a multistage process for the petrogenesis of magma by blending of subcrustal, deep crustal and sub-continental lithospheric mantle (SCLM) magmas in zones at the mantle-crust transition. Figure modified from Jorge Skarmeta in Cooke (2013) and Richards (2011b).

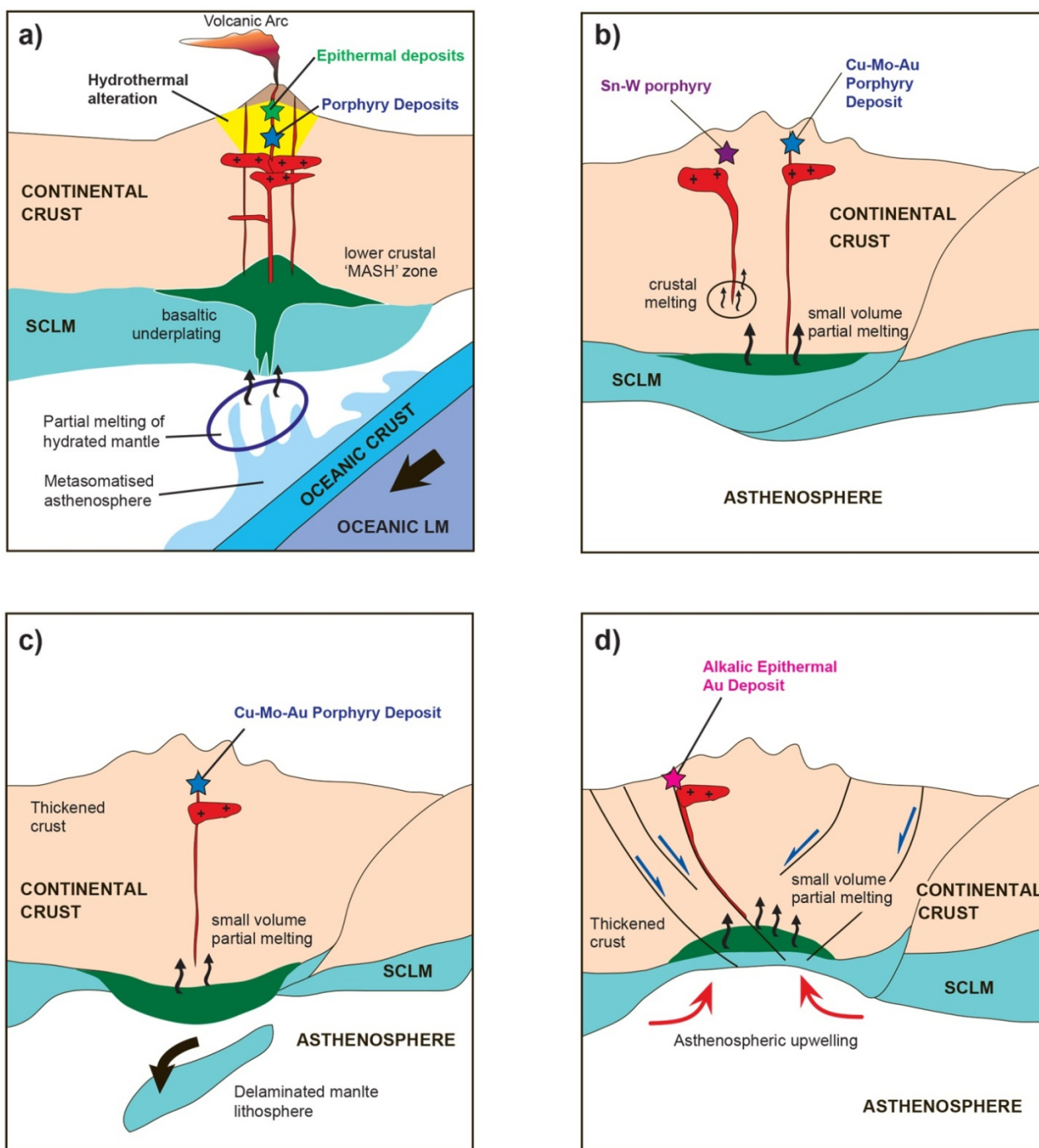


Figure 6. Series of schematic cross sections illustrating the subduction related (a) and post-collisional tectonic setting (b-d) in the formation of porphyry and epithermal deposits.

a) Section through a volcanic arc showing the process of magma generation beneath the arc. Metasomatised asthenosphere and partially melted hydrated mantle ascend to the sub-continental lithospheric mantle (SCLM) and form a basaltic underplate to the lower continental crust. The lower crustal MASH (melting, assimilation, storage and homogenisation) zone occurs at this transition, producing evolved, oxidised, andesitic magmas which ascend and pool in the mid-to upper crust forming a batholitic complex. Cu-Mo porphyry deposits and epithermal deposits may form at shallower levels above these batholitic complexes; **b-d)** post-subduction processes where small volume partial melting of previously subducted SCLM or lower crustal zones produce magmas that may remobilise Au, Cu and Mo left behind by arc magmatism forming porphyry Cu-Mo-Au and epithermal Au deposits; **b)** post-collisional thermal rebound; **c)** sub-continental lithospheric mantle delamination; **d)** post-collisional extension. Figure modified from Richards (2011b).

The changes in tectonics may promote changes in the subduction angle (i.e. flat to normal, then a return to flat: James and Sacks 1999, Gutscher et al. 2000, Kerrich et al. 2000, Cooke et al. 2005), crustal thickening, uplift and erosion, and magmatism coeval with the formation of well-endowed porphyry and/or epithermal mineral provinces (Cooke et al. 2005, Sillitoe and Perelló 2005, Sillitoe and Mortensen 2010). Thus an empirical relationship exists between contractional tectonic settings, crustal thickening, surface uplift and rapid exhumation and high-grade porphyry Cu deposits.

Regions where low-angle or flat-slab subduction, particularly of aseismic ridges, seamount chains and oceanic plateaus beneath oceanic island and continental arcs, are favourable for porphyry and epithermal deposit formation (e.g. northern Peru and central Chile, Fig. 5; Cooke et al. 2005). Tectonic change is therefore an important trigger for porphyry ore formation and some perturbation of the prevailing tectonic regime triggers the formation of porphyry systems (Cooke et al. 2005). Topographic and thermal anomalies on the down-going slab appear to act as tectonic triggers for porphyry ore formation. Other factors such as sutures in the overriding plate, permeability architecture of the upper crust, efficient processes of ore transport, i.e. fluids or permeable wall rocks, and deposition and in some cases formation of and preservation of supergene enrichment blankets are also vital for the development of high-grade giant ore deposits (Cooke et al. 2005).

Five key attributes which contribute to the formation of porphyry Cu deposits have been identified:

1. Volcanism is inhibited as a result of horizontal compression in the lithosphere impeding magma ascent through the upper crust;
2. The resultant shallow magma chambers are larger than those beneath extensional arcs and pooling in deep-crustal sill complexes is favoured where the magma can evolve and interact with the lower crust;
3. Further fractionation of the magma, volatile saturation and generation of large volumes of hydrothermal-magmatic fluids can occur, as a result of the inability of the magma to erupt;
4. The number of apophyses can form on the roof of the large magma chamber is restricted by compression, providing better, more efficient fluid focussing into a single stock rather than a cluster of intrusions i.e. structurally controlled extensional pathways; and
5. Abrupt decompression, rapid uplift and erosion promote the efficient extraction and transport of magmatic-hydrothermal fluids from depth.

While tectonic triggers appear to play an important role in the formation of porphyry deposits, direct evidence may be consumed by plate subduction within a few million years (Cooke et al. 2005). Moreover, whilst no unique process is required for porphyry deposit formation, tectono-magmatic processes may affect the size, grade and location of the resulting deposits (Richards 2003).

Porphyry Cu systems are commonly localised along fault systems which are typically arc-parallel and arc-oblique; these fault systems need not be active during deposit formation, e.g. the Bingham deposit is Eocene in age emplaced along a Palaeoproterozoic suture zone as a series of stocks. The fault system allows oxidised magma and hydrothermal fluid to rise and provide an environment for ore formation.

While the tectono-magmatic association may indicate that porphyry Cu deposits are linked to arc magmatism (implying exploration should solely focus on eroded magmatic arcs), porphyry deposits only represent very small point features within an arc (Richards 2003, Cooke et al. 2005). Important similarities exist between porphyry Cu deposits worldwide, suggesting that their mechanism formation must be reproducible, requiring no unique processes or magma types (Richards 2003). Convergence and optimisation of various contributing factors likely affect the size and grade of porphyry Cu deposits (Richards 2003). These include:

- Partial melting in the mantle wedge overlying the subducting plate;
- Magma interaction with the lithosphere;
- Mechanisms for magma emplacement; and
- Mechanisms for volatile exsolution in the upper crust.

MAGMATIC ASSOCIATION

Porphyry Cu deposits are spatially related to calc-alkaline magmatic rocks, intermediate to felsic composition, generally erupted 0.5–3 m.y. prior to stock intrusion and mineralisation (Bissig et al. 2008, Sillitoe 2010b). These volcanic rocks are typically formed in association with active subduction processes at convergent plate boundaries (e.g. Figs. 5 and 6). The geochemical characteristics of these igneous rocks represent a sub-arc mantle source, e.g. Cretaceous to mid-Miocene volcanic rocks of central Chile have enriched LREE, negative Nb anomalies on primitive mantle normalised diagrams and La/Ta ratios that exceed 25 (Kay and Mpodozis 2002, Hollings and Cooke 2005), supporting an arc setting. Convergent margin settings are also capable of generating large volumes of moderately hydrous, oxidised magmas, which are essential in the formation of porphyry Cu deposits. Metal tenor is influenced by the degree of fractionation in the associated intrusions; less fractionated calc-alkaline intrusions are related to Cu-Au mineralisation while the more fractionated intrusions are related to Cu-Mo mineralisation (Fig. 7; Holliday and Cooke 2007).

Porphyry Cu deposits display varied relationships with precursor plutons, which are typically multi-phase, equigranular intrusions commonly of batholithic dimensions and dioritic to granodioritic compositions (Sillitoe 2010b). Not only spatially related, porphyry Cu deposits are also temporally and probably genetically related to these intrusions as well (Bissig et al. 2008). The precursor plutons may also host porphyry Cu deposits, as single deposits, an alignment of coalesced deposits or as clusters of two or more deposits (Sillitoe 2010b). The porphyry Cu stocks and the precursor pluton are typically separated by 1–2 million years. The porphyritic intrusions in porphyry Cu deposits are exclusively I-type and magnetite-series magmatic rocks, typically metaluminous and medium-K calc-alkaline, but may range to high-K calc-alkaline or alkaline fields (Cooke et al. 2005). The porphyritic intrusions range in composition from calc-alkaline diorite and quartz diorite, granodiorite, quartz monzonite, and alkaline diorite to monzonite to (uncommonly) syenite. The more felsic intrusions are usually associated with Mo-rich porphyry Cu deposits, while the more mafic end members are generally associated with Au-rich porphyry Cu deposits (Fig. 7).

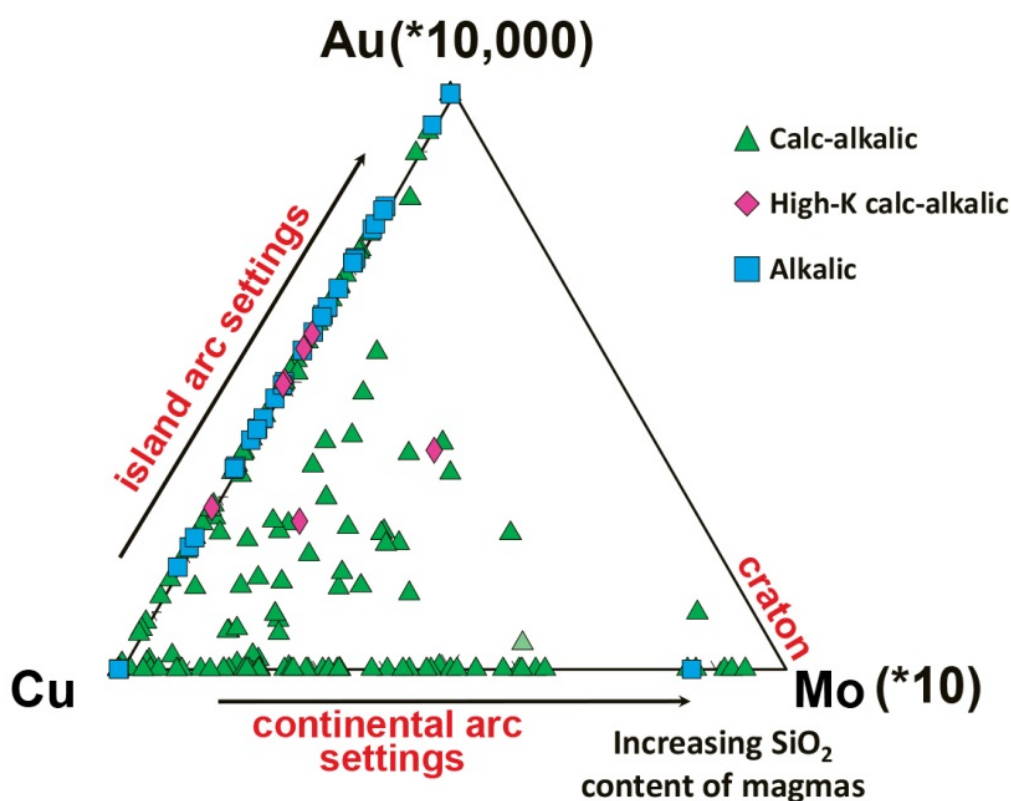


Figure 7. Classification of porphyry deposits by metal content after Kesler (1973).
Also indicated are tectonic settings which host the different porphyry deposits and their associated magma compositions.

The phenocryst assemblage of the porphyritic intrusions typically includes hornblende, biotite, magnetite and titanite. Hornblende and biotite are indicative of a hydrous magma which is conducive to porphyry formation. Magnetite and titanite are indicative of an oxidised system which is critical for achieving high concentration of sulphur (>1000 ppm) in the form of SO₂ in the magma. The presence of sulphur is critical in the formation of porphyry deposits. *Maintaining the oxidation state of the magma as it ascends through the crust is a critical step in the formation of a porphyry deposit.* The porphyritic intrusions usually contain a fine-grained, commonly aplitic groundmass. This aplitic groundmass is ascribed to pressure quenching during rapid ascent and consequent volatile loss.

Magmatic rocks associated with porphyry Cu deposits are often referred to as 'adakites' or of an 'adakitic' composition. While the term refers to magmas formed by subducted oceanic crust undergoing eclogite facies metamorphism, similar geochemical characteristics are readily formed in normal asthenospheric mantle-wedge derived magmas (Richards 2011a). The 'adakite-like' trace element composition of porphyry related igneous rocks can be achieved by fractionation of hornblende ± garnet ± titanite in the hydrous, oxidised magma derived from partial melting of the metasomatised asthenospheric mantle wedge above the subduction zone (e.g. Fig 5 and Fig. 6a; Richards 2011a). In mature arcs the primary basaltic magmas stall at density barriers in the mantle or levels within the crust where they undergo wall rock Assimilation and Fractional Crystallisation (AFC; Depaolo 1981) or MASH processes (Melting, Assimilation, Storage and Homogenisation) in the lower crust (Fig. 5 and Fig. 6a; Richards 2011a). While the mafic magma is ponded in the mantle or at the base of the crust, crystallisation of ultramafic or gabbroic cumulates occurs, where garnet is the early fractionating or residual phase forming andesitic to dacitic magmas. These resulting, intermediate magmas are calc-alkaline in composition and will have heavy rare earth element (REE)-depleted REE patterns and consequently high La/Yb and Sr/Y ratios. For this reason many porphyry-related igneous rocks commonly have high Sr/Y and La/Yb ratios and low Y and Yb contents (Richards 2011a). These ratios also suggest the suppression of plagioclase occurred which is indicative of a hydrous magma.

REGIONAL AND DISTRICT SCALE CHARACTERISTICS

Host rocks

A wide variety of host rocks exist for porphyry Cu-Mo, Cu-Mo-Au and Cu-Au deposits (Table 4); many are hosted within sub-volcanic basement sequences. Volcanic rocks may be older and unrelated or broadly related to the mineralised magmatic system, generally predating the mineralising porphyries and occurring as wall rocks to the porphyries (Seedorff et al. 2005). Plutonic rocks may also be unrelated to the mineralising system e.g. Proterozoic granites and batholiths a few million years older than mineralisation at Butte, and those more closely linked in time to the porphyry system can also host the porphyry deposits e.g. Bingham, Los Pelambres and Yerington (Seedorff et al. 2005). Many of the giant epithermal Au deposits are also associated with breccia pipes and breccias, e.g. Yanacocha, Chelopech, Baguio, Lepanto, Pueblo Viejo and Pascua Lama (Sillitoe and Hedenquist 2003, Cooke 2013). One of the largest system, Rio Blanco-Los Bronces, is a breccia-hosted porphyry Cu-Mo system.

The wide variety of rocks that host porphyry Cu deposits suggests the wall rocks play a non-influential role in the system (Sillitoe 2010b). However, some lithologies may enhance the grade development in porphyry systems and related deposits (Sillitoe 2010b). High-grade ore formation is favoured where host rocks are massive carbonate sequences, or poorly fractured fine-grained rocks which can allow impermeable seals around and/or above the porphyry Cu deposit (Sillitoe 2010b). High-grade porphyry Cu mineralisation is also favoured by ferrous Fe-rich lithologies, which have the capacity to effectively precipitate Cu transported in oxidised magmatic fluids (Sillitoe 2010b).

Table 4. Summary of ore host and host rocks for selected porphyry and high sulphidation (HS) deposits in central and northern Chile and central Peru.

Deposit	Deposit type	Ore host	Ore bodies	Mineralisation age (Ma)	Host rock	Host rock age (Ma)
Rio Blanco-Los Bronces- Sur Sur	Breccia-hosted porphyry Cu-Mo	biotite cement breccia, biotite-altered rock flour matrix breccia, tourmaline cement breccia	Breccia	5–7	Granodioritic San Francisco Batholith	12–8
El Teniente	Porphyry Cu-Mo	andesites and dacites, dacite porphyry dyke with breccia-hosted anhydrite-cement and biotite breccias	Stockwork veins, breccia	4.7–4.0	Strongly altered mafic to intermediate sills, stocks, lavas and volcanoclastic rocks of the Farallones Formation	11–8.9
Caspiche	Stockwork-hosted Au-Cu porphyry, associated with HS epithermal*	Quartz diorite porphyry	Stockwork veins		Siliciclastic sediments, red beds, volcanic sandstone and siltstone, volcanic breccia	12–8
Sierra Gorda	Breccia-hosted Cu-Mo-(Au) porphyry	Hydrothermal breccia, tourmaline breccia	Breccia	57	Andesites and tuffs from the Quebrada Mala Formation, Sierra Gorda Monzodiorite	<94
Chuquicamata	Porphyry Cu-Mo	Chuquicamata Intrusive Complex (monzogranite to monzodiorite)	Veins, veinlets, microveinlets, micro-breccias, disseminated	~33	Andesitic volcanics and volcanoclastics, Fortuna Granodiorite Complex	39–38
Radomiro Tomic	Porphyry Cu-Mo	Chuquicamata Intrusive Complex (monzogranite to monzodiorite - East Porphyry (34.8 Ma), Fine Porphyry (34.8 Ma))	Veins, veinlets, microveinlets, micro-breccias, disseminated	~34	Elana Porphyry	37.7
Colquijirca	HS volcanic- and carbonate-hosted Cu-Au-Ag-Zn-Pb-Bi	Marcapunta Volcanic Complex (breccia and andesite domes, lava flows and pyroclastics)		11.3	Limestone and clastic units and basal conglomerates of the Pocobamba Formation (~40 Ma), and Pucara Group (~195–85 Ma)	~40 and ~195–85

*telescoped system

Porphyry stocks and dykes

Porphyry Cu deposits are centred on porphyry intrusions that range in shape and form from vertical, plug-like stocks which are circular to elongate in plan ≤ 1 km in diameter, to dyke arrays and small, irregular bodies ≤ 1 km in length (Fig. 8; Sillitoe 2010b). Larger porphyritic intrusions may act as hosts to mineralisation and can range in length from ≤ 4 to ≥ 14 km and have vertical extents > 2 to ≥ 4 km. The size of the stocks, however, do not appear to bear any direct relationship to the size of the deposit and their Cu contents (Sillitoe 2010b). Porphyry Cu deposits are typically sub-circular to sub-elliptical and rarely elongate in shape. The intrusions related to porphyry deposits are multiphase intrusions, emplaced before, during, near the end and after the alteration and mineral events (Cooke et al. 2005, Sillitoe 2010b, Vry et al. 2010, Cooke 2013). In general, the earliest porphyry intrusions and their host rocks contain the highest grade of mineralisation, the porphyries typically become less mineralised as they progressively become younger with late and post intrusive phases often being barren (Cooke et al. 2005, Sillitoe 2010b, Cooke 2013). Diatremes are also often late additions to the porphyry system and are associated with phreatomagmatic eruptive activity, commonly ≥ 1 km in near-surface diameter and greater than 2 km in vertical extent (Fig. 8; Sillitoe 2010b).

There is potential for the system to be terminated or any existing mineralisation to be removed or downgraded by later, barren intrusive phases or if the system erupts via phreatomagmatic explosion e.g. Braden Pipe, El Teniente, Chile. However, while diatremes may either post-date or crosscut porphyry mineralisation at depth, they may overlap with related high sulphidation events at shallower epithermal levels (Fig. 8; Sillitoe 2010b), i.e. terminate the porphyry but initiate the development of a high sulphidation system due to fluid evolution off the porphyry.

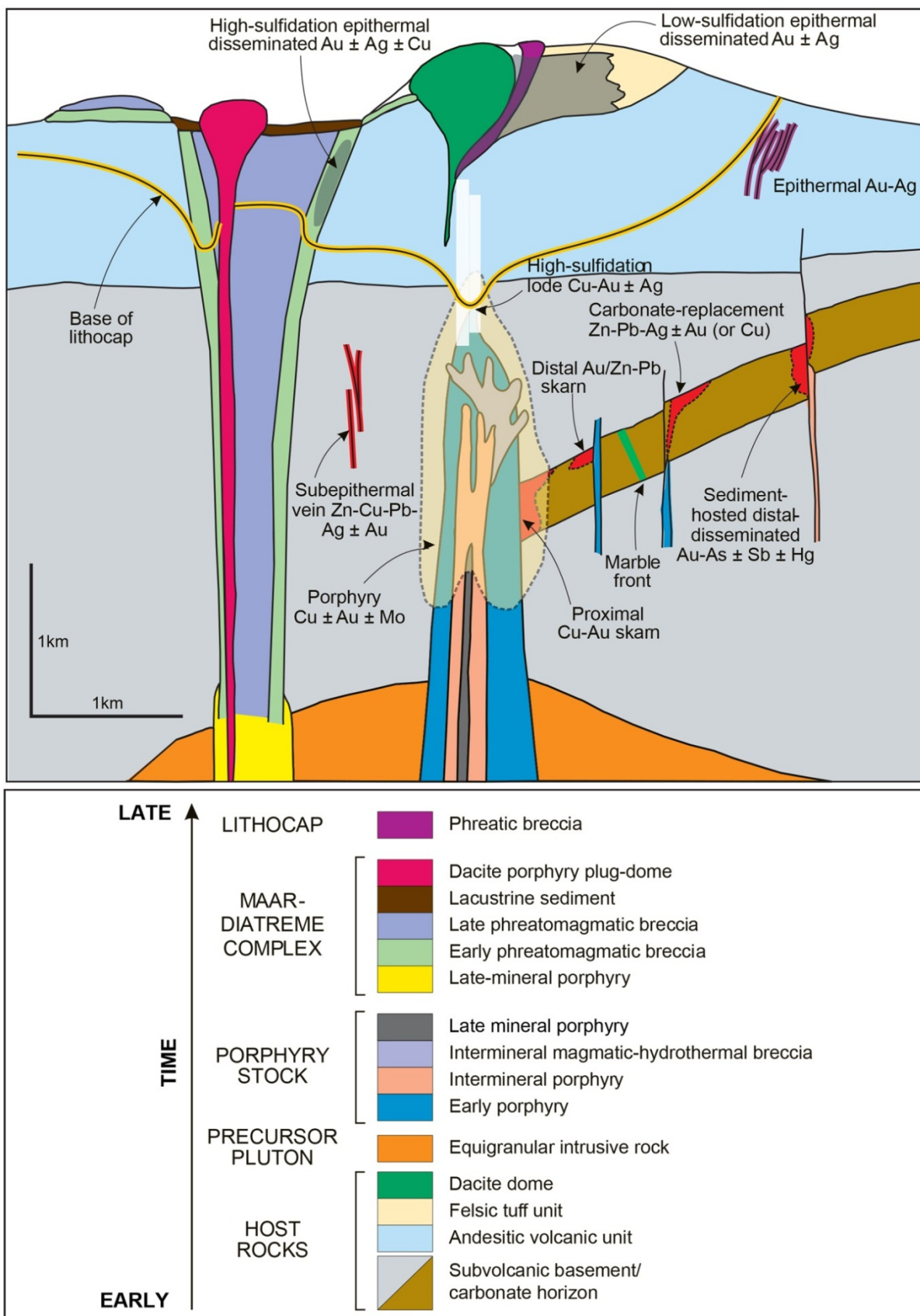


Figure 8. Conceptual model of porphyry Cu-Au-Mo deposit centred on a multi-phase porphyry intrusion.

Illustrated are the relationships between multiple intrusive and breccia phases and the host rocks and their relative temporal relationship displayed in the legend. Also shown are the related mineralisation styles that can be associated with porphyry Cu-Au-Mo deposits, although all of the indicated styles uncommonly occur together. Figure reproduced from Sillitoe (2010b).

Breccias and veins in porphyry systems

Several different types of breccias are observed in porphyry Cu systems. Breccia types include hydrothermal breccias, magmatic breccias, volcanic breccias, phreatic breccias, hydraulic breccias and tectonic breccias, and many hybrid breccias of these (Fig. 9). Of the hydrothermal breccias associated with porphyry systems, hydrothermal-magmatic breccias are the most common breccias found in the deeper parts of the system. Magmatic-hydrothermal breccias are the products of release of over-pressurised magmatic fluids, commonly during porphyry intrusion (Sillitoe 2010b).

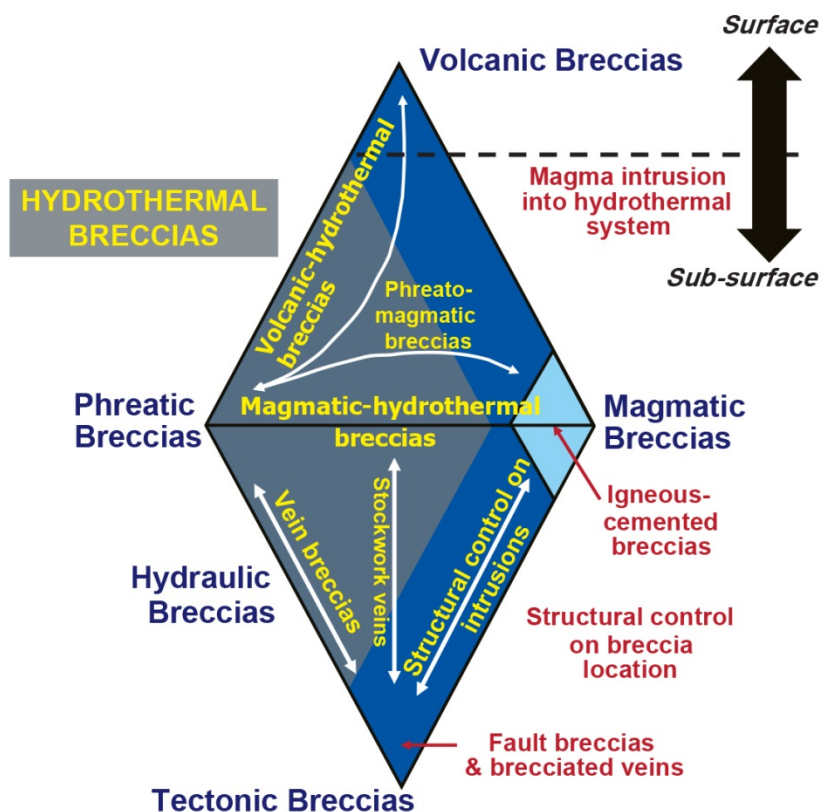


Figure 9. Schematic diagrams illustrating the different types of breccias and their hybrids related to porphyry Cu systems, reproduced from Cooke (2013).

Phreatomagmatic breccias form part of the maar-diatreme system, forming late in the magmatic system. Magmatic-hydrothermal breccias represent the locus of greatest fluid flow and permeability and often contain a large proportion of the deposited ore minerals and high-grade mineralisation as well as being able to precipitate abundant, well-mineralised cement (Seedorff et al. 2005, Sillitoe 2010b, Cooke 2013). Such hydrothermal cement is locally abundant and comprised of biotite, tourmaline, quartz and sulphides (Fig. 10). In contrast, phreatomagmatic breccias associated with the maar-diatreme breccia complex are commonly poorly mineralised (Sillitoe 2010b) e.g. Braden Breccia, El Teniente.

Breccias associated with deeper hydrothermal systems are often associated with deposit types including porphyries, IOCG, skarn and MVT, while epithermal deposits are associated with breccias in shallow hydrothermal systems. Magmatic-hydrothermal breccias and phreatomagmatic breccias can be distinguished from each other by several features including texture, clast form and composition, clast to matrix ratios, matrix to cement ratios and alteration type (Sillitoe 2010b). The orientation, mineralogy, textures, location and abundance of veins and breccias therefore provide valuable information about the evolution of fluid composition and flow.

Ore minerals in porphyry deposits are typically found in veins, veinlets and as disseminations throughout the rock (Cooke et al. 2005, Seedorff et al. 2005, Sillitoe 2010b). Veins typical of porphyry deposits are generally only a few millimetres wide but can be as wide as a few centimetres (Fig. 11; Seedorff et al. 2005). Veins are commonly orthogonal or orthogonal-

conjugate arrays or sheeted arrays with a single dominant orientation. Vein geometry is ultimately influenced by the shape of the porphyry intrusion and veins are formed through the interaction between magmatic and far-field stresses.

Veins associated with porphyry Cu deposits may be broadly categorised into three groups:

1. early quartz-sulphide-free veins often containing actinolite, magnetite (M type), (early) biotite (EB type) and K-feldspar;
2. sulphide-bearing quartz-dominated veins (A and B types); and
3. late, crystalline quartz-sulphide veins with feldspar-destructive alteration selvages (D type).

("A", "B" and "D" nomenclature is based on observations from El Salvador by Gustafson and Hunt (1975); Gustafson and Hunt 1975, Sillitoe 2010b; Table 5).

The first two groups are mainly emplaced during potassic alteration while the third group is associated with chlorite-sericite, sericitic and deep advanced argillic overprints (Table 5; Sillitoe 2010b). The quartz-dominated veins (A- and B-type) contain much of the metal which is also disseminated within the potassic-altered rocks. The late quartz-sulphide veins and their wall rocks may also contain significant amounts of metal. Multiple generations of veins exist in porphyry Cu deposits and the number of generations and vein mineralogy is often deposit specific, e.g. 15 vein types are identified at El Teniente, Chile. While vein types may be deposit specific, it is the relationships between veins, including crosscutting relationships and their offset, that provide valuable evidence for the relative ages of hydrothermal alteration at particular locations (Seedorff et al. 2005). Vein density is concentrated in the core of the system and decreases outwards. Therefore, vein density is also an important tool as this is generally correlated to grade and can be used as vectors towards high grade mineralisation, particularly in Au-rich deposits. However, there are examples of porphyry Cu-Au deposits devoid of veins and veinlets, e.g. in British Columbia.

PORPHYRY EVOLUTION, ALTERATION AND MINERAL ZONING

Porphyry genesis is onset by the emplacement of granite to granodiorite porphyry dykes that are successively intruded from the parent magma chamber (Fig. 12). Successive fracturing and upward flow of high-density saline ore fluids occurs contemporaneously as the dykes propagate from the magma chamber. Crystallisation occurs from the outside of the magma chamber inwards causing the final dykes to originate from the centre of the magma chamber (Fig. 12). The dykes propagating from the magma chamber cause alteration zonation by thermally driven-off fluid on the flanks of the intrusion. The main stage of mineralisation is usually associated with an intermediate stage porphyry emplacement where the porphyry dykes are mineralised at depths 2–4 km immediately above where they intruded through the carapace of the chamber. Lower T assemblages overprint early high T assemblages as the system begins to crystallise and collapse. As the magma rises it reaches neutral buoyancy where crystallisation begins. This leads to increased fluid pressure which in turn leads to catastrophic fracturing and quench crystallisation. These multiple igneous events are associated with multiple hydrothermal events.

Alteration and mineralisation in porphyry Cu systems are related to the most felsic phases within these multiphase intrusive complexes (Fig. 12; Camus 2005). While no two systems are alike, many share similar hydrothermal characteristics. The evolution of the alteration and mineralisation in porphyry systems begins with high-temperature, late magmatic oxidised fluids in the early stages to low or moderate-temperature, more reduced hydrothermal fluids and magmatic and meteoric components in the later stages (Camus 2005). Each of these hydrothermal stages is broadly related to quartz veins and potassic alteration, sodic-calcic and sodic alteration, calcic alteration, chlorite-epidote-actinolite alteration and sericitic alteration.

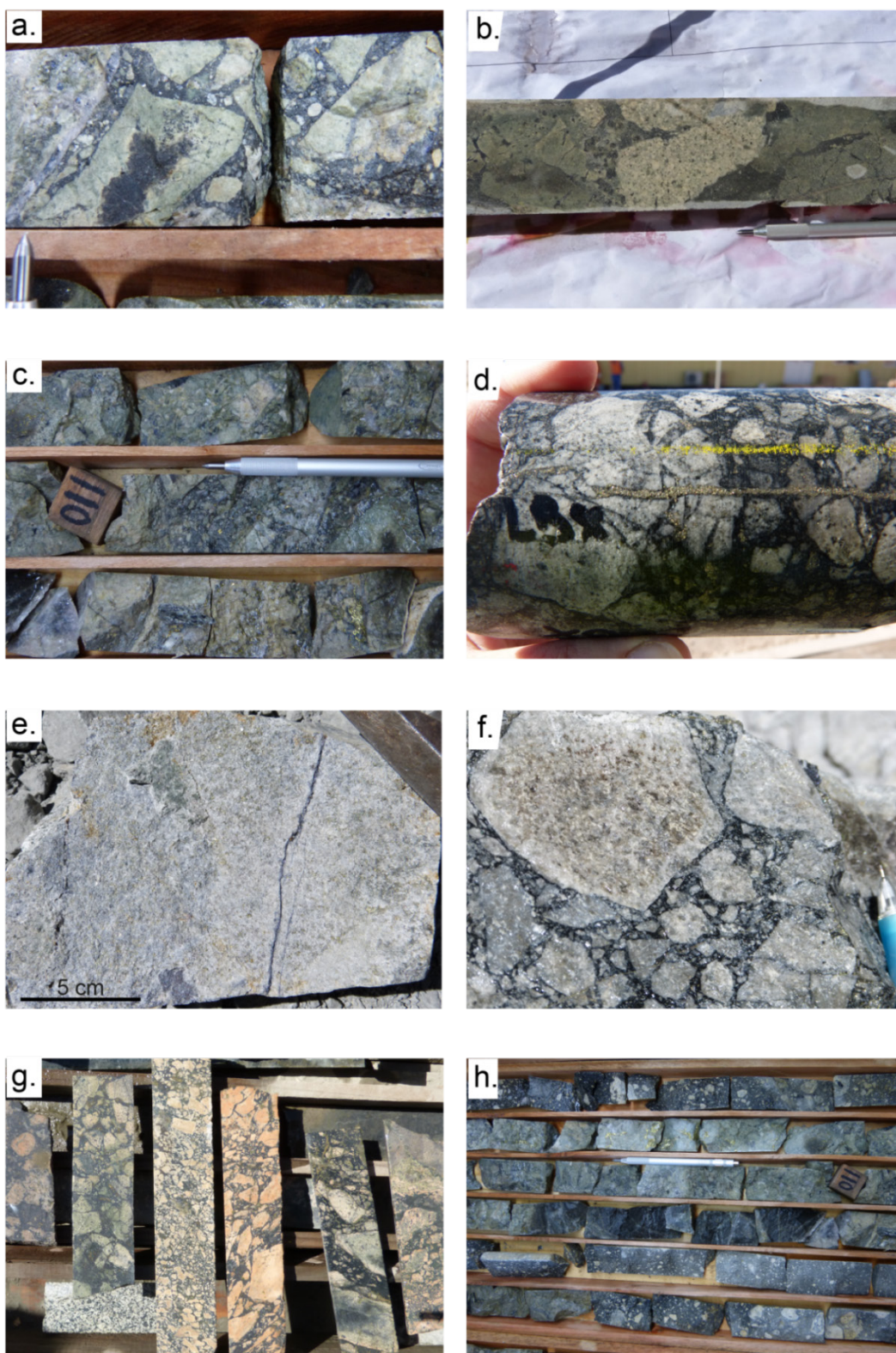


Figure 10. Mineralised breccias from porphyry copper deposits from Chile, South America. **a)** altered breccia clasts from El Teniente; **b)** breccia, Sierra Gorda; **c)** altered and mineralised breccia, El Teniente; **d)** mineralised breccia from Sierra Gorda, sulphides are disseminated within the matrix and occurs as veins which crosscut breccia clasts; **e)** tourmaline breccia crosscut by molybdenite veins, Rio Blanco; **f)** tourmaline breccia, Rio Blanco; **g)** K-feldspar breccias, Candelaria; **h)** El Teniente breccias above and below mineralised zone within altered breccia and quartz veining. (Photos 413598–413605)

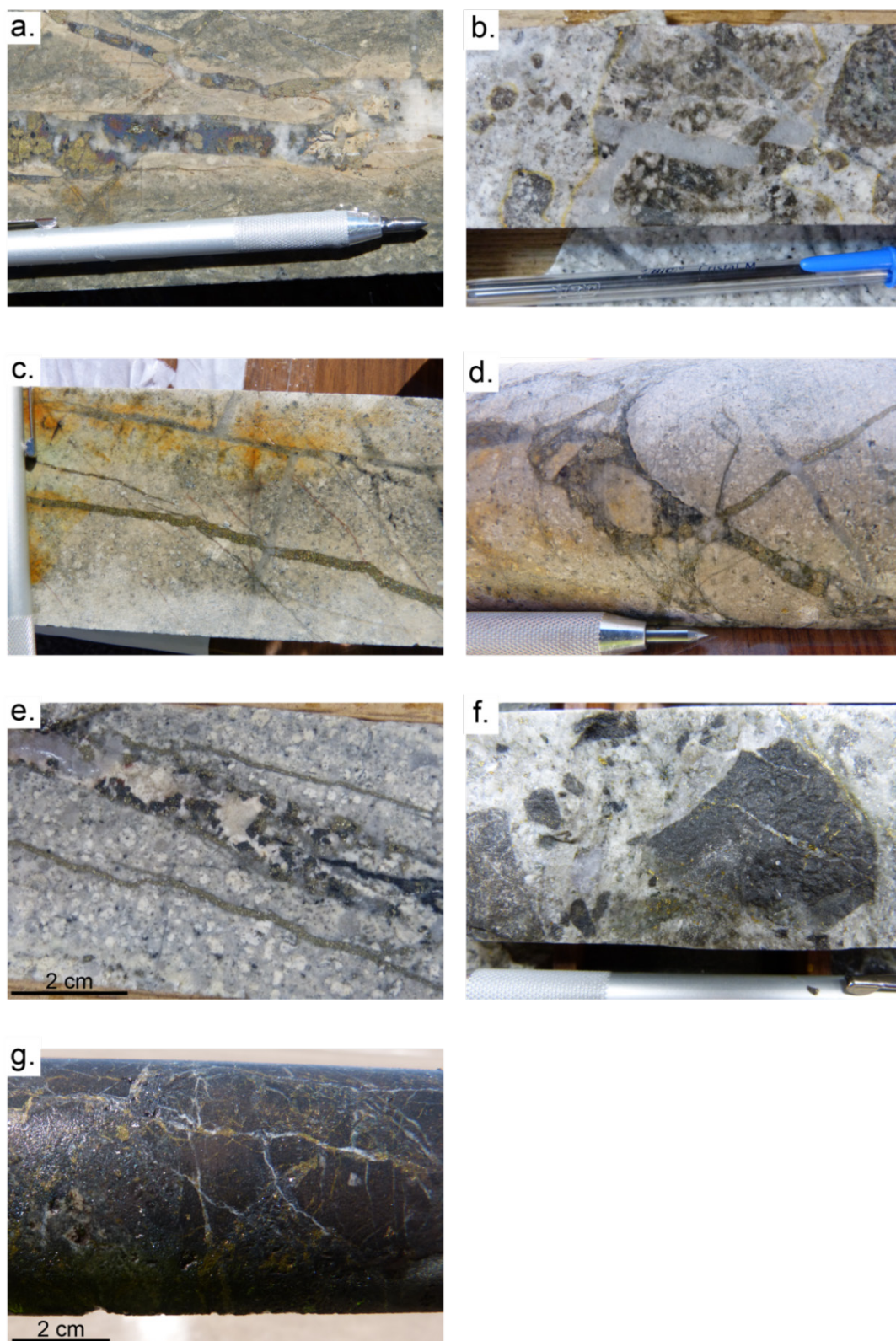


Figure 11. Examples of veins within porphyry copper deposits from Chile, South America.
a) bornite-chalcopyrite-quartz vein in a dacitic porphyry, Sierra Gorda. Early cpy-py vein crosscut by bn-cpy-qtz vein. Mo veins formed late in the system and crosscut the cpy-py veins;
b) granodiorite porphyry clasts crosscut by quartz veins within a dacitic porphyry, Rio Blanco. Granodioritic and dacitic porphyry are both crosscut by late quartz veins **c)** cross-cutting vein relationships in dacitic porphyry at Sierra Gorda; **d)** cross-cutting vein relationships in porphyry at Sierra Gorda; **e)** py-mg replacement in quartz vein in porphyry, Rio Blanco **f)** mineralised veins within breccia clasts, El Teniente; **g)** breccia clasts with pre-existing mineralised veins crosscut by later mineralised quartz veins at Manto Verde. Disseminated sulphide mineralisation is present within the matrix. Sulphide mineralisation is concentrated along the clast edges. (Photos 413606–413612)

Table 5. Vein types and their mineralogy, associated alteration, envelopes or alteration haloes and form associated with Cu, Cu-Mo, Cu-Au and Au-rich porphyry deposits.

TIMING	TYPE	VEIN MINERALOGY/ COMPOSITION	ASSOCIATED ALTERATION	ENVELOPES, HALOES, SELVEDGES	FORM/ MORPHOLOGY	ASSOCIATED PORPHYRY TYPE	PROXIMITY
EARLY	M	mt-act ± qtz ± tm ± plag	Sodic calcic		banded	Au-rich Cu	In and around porphyry extending to wall rocks
		mt-amph-plag	Sodic ferric				
			Sodic calcic	Plagioclase		Cu-(Au-Mo)	
			mt-bt ± qtz-cpy		K-feldspar	hairline	
		mt-rich			hairline	Mo	
	EB	bt ± mt ± sul	Potassic (K-silicate)			Cu and Au; W and Mo	In and around porphyry
		Green mica (qtz poor) green bt, K-feld, and, mu, cd				Cu	
	A	qtz-mg-sul (py-cp-bn ± Au)	Potassic (K-silicate)		Stockworks to sub- parallel sheeted arrays	Au-rich	In and around porphyry
		Sugary qtz ± mt-cpy	Potassic (K-silicate) Transitional potassic-advanced argillic (high T, mod T, low T)	K-feldspar, anhydrite, chalcopyrite, bornite, apatite, rutile	Random, discontinuous, wispy, irregular, segmented	Cu Au	
			Granular qtz – K feldspar-anh- sul	Transitional potassic-advanced argillic			
	B	qtz-mo-py-cpy, anh ± tm	Potassic (K-silicate)	Absent; occasionally K-feld, albite, biotite, sericite, andalusite or corundum with increasing depth	Banded, planar	Cu-Mo	In and around porphyry
		qtz-mg	Transitional potassic-sericitic	Absent	banded	Au	
	C	qtz bearing bt-ser ± K-feld, and	Transitional potassic-sericitic- advanced argillic	Sericite, biotite ± K-feldspar, andalusite		Cu-Mo	In and around porphyry
LATE	D	qtz-py-sul-tm	Sericite (phyllic, qtz-ser-py)	Sericitic, sericite + chlorite; pyrite, quartz, anhydrite, rutile, feldspar destructive selvages, phyllic alteration haloes	Continuous systematic orientations	Cu-Mo	Wall rocks outside porphyry intrusion
		py-qtz					
		py-bn-cpy-en-ten-sp-gal					
	Ep	ep-py-qtz	Sodic calcic, propylitic	K-feldspar replaced by albite; bt replaced by chlorite, vermiculite and epidote; magnetite is destroyed Albite-chlorite-sericite		Cu	Distal

act = actinolite; amph = amphibole; anh = anhydrite; and = andalusite; Au = gold; bn = bornite; bt = biotite; cc = chalcocite; cd = corundum; chl = chlorite; cpy = chalcopyrite; en = enargite; ep = epidote; gal = galena; k-feld = k feldspar; mo = molybdenite; mt = magnetite; mu = muscovite; plag = plagioclase; py = pyrite; qtz = quartz; ser = sericite; sp = sphalerite; sul = sulphides; ten = tennantite; tm = tourmaline.

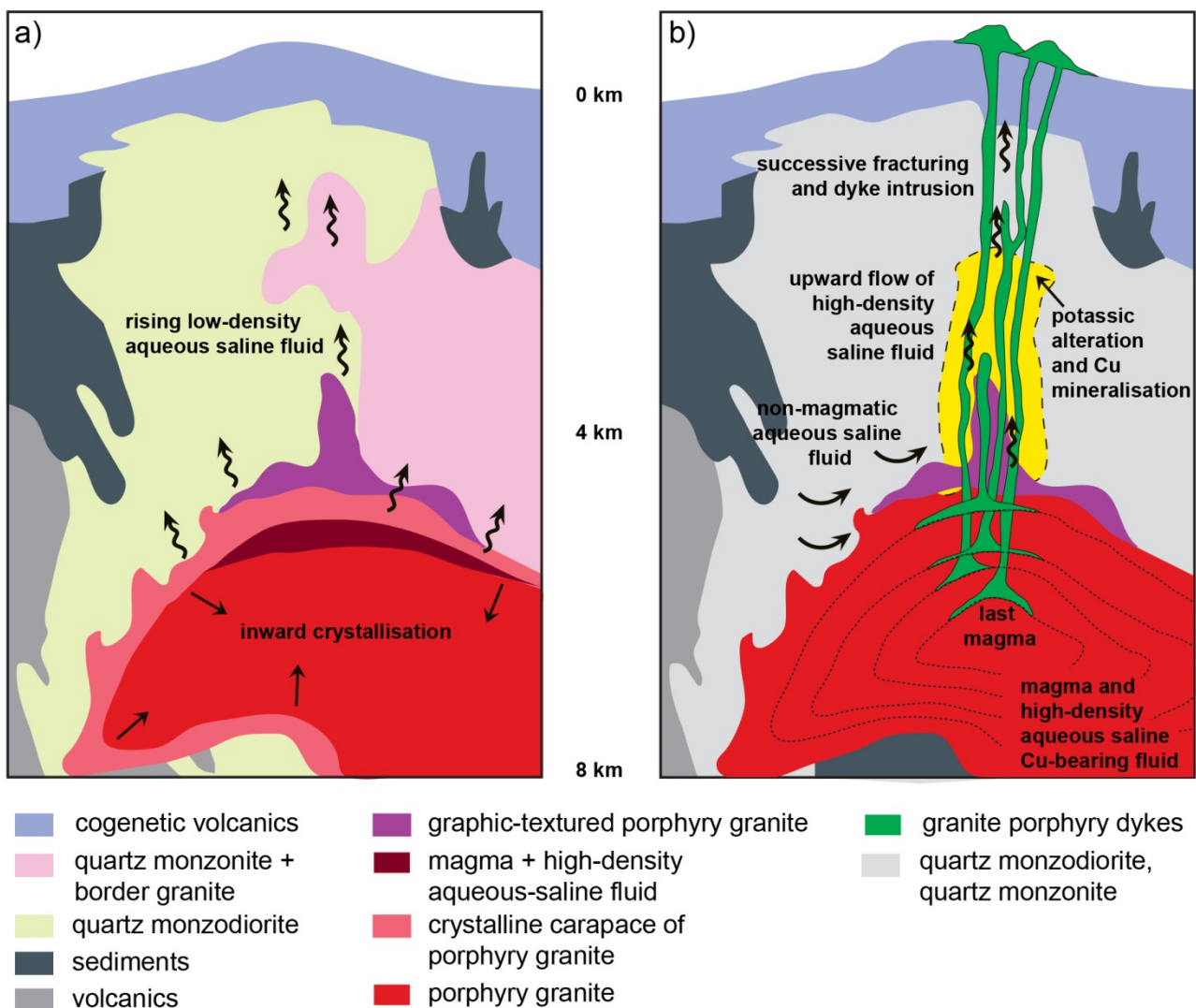


Figure 12. Model for an orthomagmatic porphyry Cu system illustrating the generation of Cu-bearing ore fluids during crystallisation of a magma based on observations from the Yerington Batholith after Dilles (1987).

a) early porphyry granite crystallisation where water saturation occurred producing the graphic-textured porphyry granite on the apex of the granite cupola and low-density aqueous saline fluid ascends from the magma chamber; **b)** early to late porphyry granite crystallisation where granite porphyry dykes and magmatic hydrothermal fluids are emplaced upward and in successive pulses causing multiple mineralising events. The high-density fluid within the magma is enriched in Na, K, Ca, Fe, Cu and S. A second non-magmatic fluid is proposed to flow upward along the hot, highly permeable granite dykes shortly after they were emplaced.

The porphyry Cu model (Fig. 13) has largely been based on that proposed by Lowell and Guilbert (1970) for the Kalamazoo porphyry copper mine in Arizona, USA, and while it may be applicable to other deposits such as Morenci, Butte and Bingham, it does not apply to all porphyry Cu deposits. Other proposed alteration models for other deposit styles are illustrated on Fig. 14. Common to all porphyry Cu systems, is a vertical and lateral zonation of alteration (Fig. 13 and Fig 14) and mineralisation (Fig. 13b and 13c).

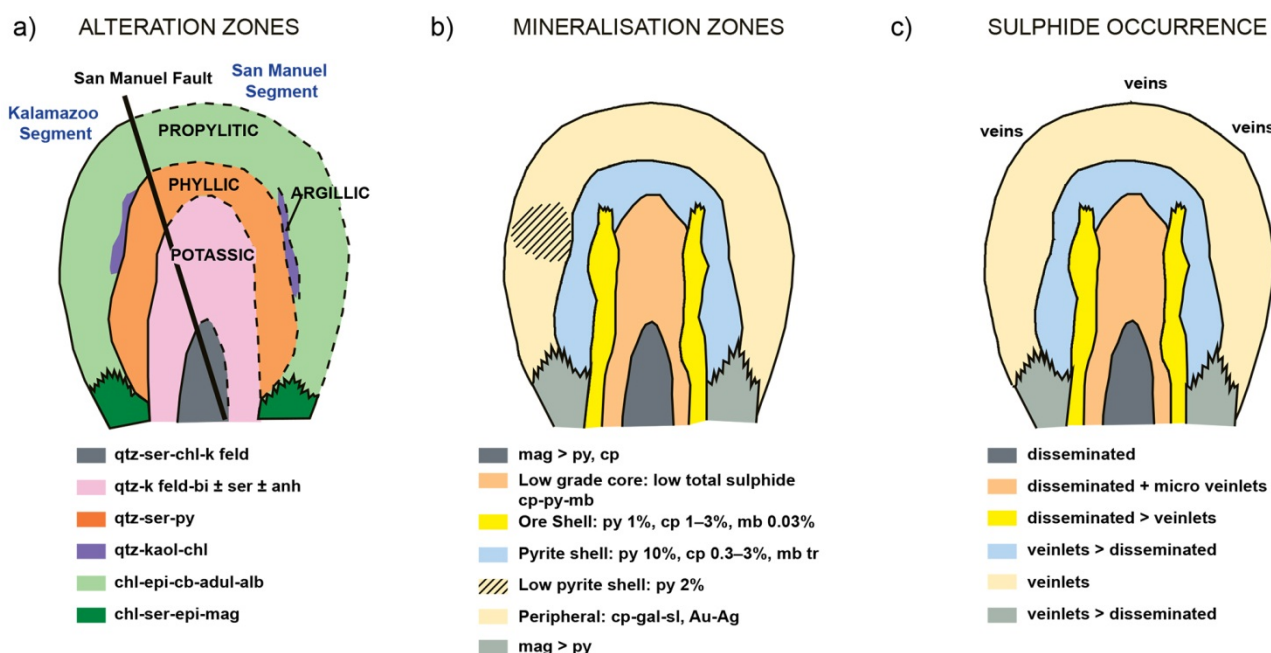


Figure 13. The porphyry copper model based on Kalamazoo porphyry Cu mine, Arizona after Lowell and Guilbert (1970).

a) alteration zones observed at Kalamazoo mine, illustrating the concentric distribution of potassic, phyllic, argillic and propylitic alteration; **b)** mineralisation zones displaying the concentric distribution of sulphides. Note the close correlation of sulphide tenor and alteration zones; **c)** sulphide occurrence observed at Kalamazoo mine ranging from a disseminated core, to microveinlets, veinlets and veins in the distal regions. alb = albite; adul = adularia; anh = anhydrite; bi = biotite; cb = carbonate; chl = chlorite; cp = chalcopyrite; epi = epidote; gal=galena; kaol = kaolinite; k feld = k feldspar; mag = magnetite; mb = molybdenite; py = pyrite; qtz = quartz; ser = sericite; sl = sulphide.

ALTERATION

Alteration associated with porphyry Cu deposits is generally a consistent, broad-scale pattern of alteration-mineralisation zoning, both lateral and vertical, characterised by several alteration assemblages as illustrated by Figures 13 and 14. Characterising this alteration footprint is essential in the exploration for porphyry Cu-(Au-Mo) deposits to both outline the ore zones and understand the ore formation processes. Zoned upward, alteration ranges from barren, early sodic-calcic, potentially ore-grade potassic, chlorite-sericite, sericite, to advanced argillic (Fig. 14; Sillitoe 2010b). Advanced argillic alteration constitutes the lithocap, including minerals such as quartz (partly residual, vuggy), alunite, dickite, pyrophyllite, and kaolinite. High sulphidation Au, Ag and/or Cu epithermal deposits may occur in the lithocaps above porphyry Cu deposits. Each of the alteration assemblages form at discrete points in time and space during the formation of porphyry deposits (Table 6). The alteration is typically widespread, affecting several cubic kilometres of rock and the distinctive zones of alteration provide useful alteration vectors to mineralisation for explorers (Cooke et al. 2005).

Early sodic-calcic alteration

Early sodic-calcic alteration may occur deep within, including below, some porphyry Cu deposits (e.g. Pangua, Papua New Guinea and El Teniente, Chile; Fig. 14c) and is characterised by albite/orthoclase, actinolite and magnetite (Sillitoe 2010b). This alteration is typically sulphide-free but may be locally ore-bearing in Au-rich porphyry Cu deposits e.g. Nugget Hill, Philippines. Magnetite ± actinolite veinlets (M type) can be associated with this alteration event.

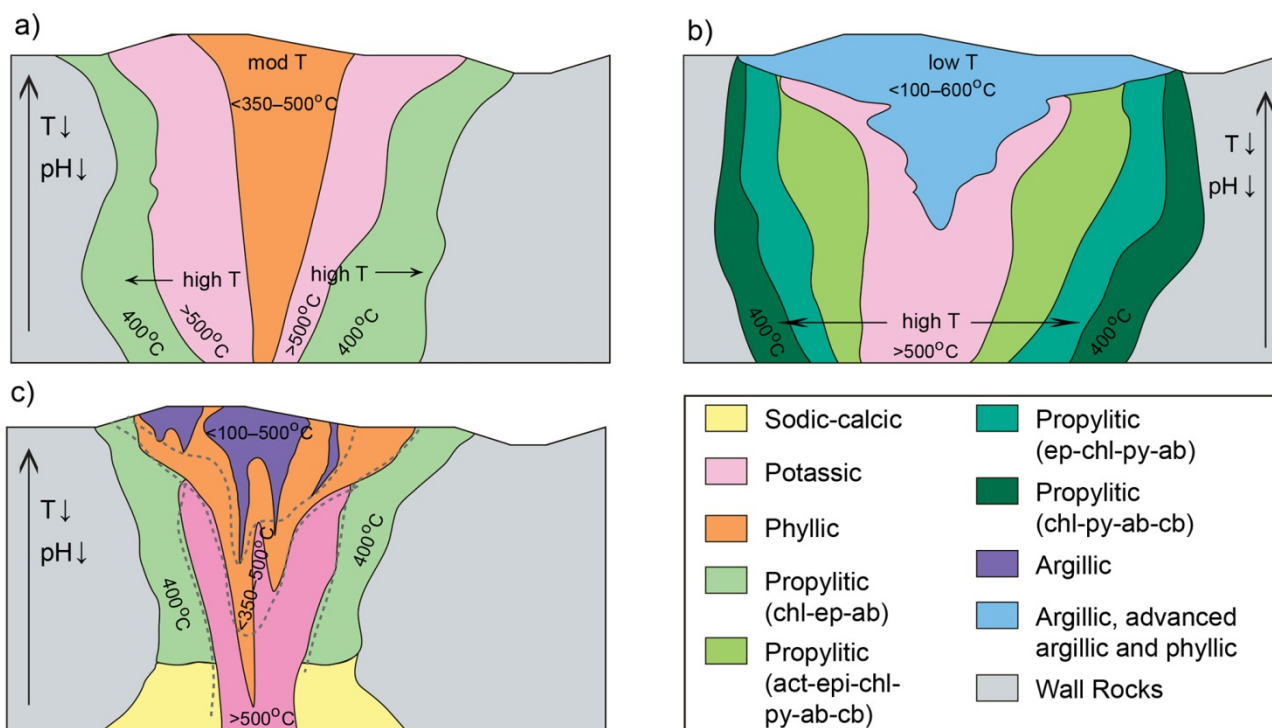


Figure 14. Three porphyry copper models illustrating the lateral and vertical variation in alteration zones surrounding the porphyry intrusion.

a) South American model after Cooke (2013), with phyllic alteration envisaged to overprint the potassic alteration in the central core; chlorite-epidote-albite propylitic alteration is still present in distal zone; **b)** calc-alkalic porphyry model after Holliday and Cooke (2007) indicating three propylitic subzones dominated by actinolite (proximal), epidote and chlorite (distal). Argillic, advanced argillic and phyllic alteration constitutes a lithocap which overprints the porphyry and can contain a domain of HS epithermal mineralisation; and **c)** distribution of alteration facies in the Yerington Batholith after Cohen (2011).

Potassic (K-silicate) alteration

Potassic alteration or K-silicate alteration is a high temperature alteration event that occurs early in the hydrothermal system. Potassic alteration affects early porphyry intrusions and decreases in intensity from older to younger porphyry phases (Sillitoe 2010b). In relatively mafic porphyry intrusions potassic alteration is predominantly biotite-bearing while in more felsic porphyry intrusions K-feldspar increases in abundance (Sillitoe 2010b). The potassic zone typically hosts the main ore minerals, commonly chalcopryrite and bornite (e.g. El Teniente, Chile) and digenite ± chalcocite where the sulphidation state is sufficiently low (Sillitoe 2010b). Mineral assemblages often observed in the potassic zone include magnetite-biotite-pyrite; chlorite after biotite-chalcopryrite; K-spar-biotite-magnetite; quartz-biotite-K-spar-sericite; and quartz-anhydrite-K feldspar-biotite. Potassic alteration is also commonly associated with biotite (EB) veins, quartz-sulphide-magnetite (A) veins and quartz-molybdenite-pyrite-chalcopryrite (B) veins.

Propylitic alteration (chlorite, epidote, actinolite alteration)

Propylitic alteration is contemporaneous with high temperature fluids entering the core of the porphyry system and forms in the country rocks producing the biggest alteration halo of the system. High temperature fluids travel along the margin of the plume driven by the thermal energy of the causative (parent) batholiths during late magmatic alteration. Propylitic alteration is characterised by the combination of epidote, albite, calcite, chlorite, pyrite, actinolite and illite clay and at higher temperature by abundance of epidote and actinolite. Propylitic alteration can be divided into three main sub-types: actinolite, epidote, and chlorite and these assemblages are zoned laterally outward from the intrusive centre (actinolite → epidote → chlorite) in marginal parts of the system and below lithocaps (Fig. 14b). More mafic lithologies are characterised by the

presence of epidote, chlorite, calcite and minor albite, and prehnite, while felsic lithologies contain widespread calcite in groundmass aggregates and as replacements of feldspars, as observed in porphyry Cu-Mo deposits in the Collahuasi District, northern Chile (Djouka-Fonkwé et al. 2012). The propylitic zone is often barren, however pyrite may be dominant within this zone.

Sericite-chlorite (green sericite)

Sericite-chlorite alteration is widespread in shallower parts of porphyry Cu deposits, particularly Au-rich deposits, where it overprints potassic alteration. This alteration is a transition stage between potassic and sericite (phyllic) alteration, characterised by chlorite intergrown with phengitic muscovite (Sillitoe 2010). Mafic minerals are partially to completely replaced by chlorite, plagioclase to sericite/illite, and magnetite to hematite as martite and/or specularite (Sillitoe 2010b). Pyrite and chalcopyrite are the principal sulphides associated with this alteration.

Phyllic alteration (sericitic alteration)

Phyllic or sericitic alteration is characterised by the removal of Na, Ca and Mg from calc-alkalic rocks with pervasive replacement of silicates generally at moderate temperatures (<350–500°C). The typical assemblage is sericite-quartz-pyrite ± chlorite. Sericitic alteration often occurs in the upper parts of porphyry Cu systems where it overprints and wholly or partially destroys the earlier potassic and chlorite-sericite alteration assemblages (Sillitoe 2010b). Sericite alteration is contemporaneous with quartz-pyrite-sulphide veinlets (D veins) and while commonly barren, may constitute ore where appreciable copper remains with pyrite, either as chalcopyrite or HS assemblages (pyrite-bornite, pyrite-chalcocite, pyrite-covellite, pyrite-tennantite and pyrite-enargite (Sillitoe 2010b)).

Advanced argillic alteration (lithocap environment)

Advanced argillic alteration is characterised by the complete replacement of feldspar minerals by clay minerals (kaolinite, smectite, dickite, pyrophyllite, montmorillonite, alunite and illite) and generally occurs at low, although broad, temperatures (<100–600°C) and at low pH. At higher temperatures, argillic alteration grades into phyllic alteration. Argillic alteration is representative of lithocap environments, e.g. quartz-alunite epithermal systems and above porphyry systems, and the supergene environment. The low pH (i.e. elevated acidity of fluids) is a key control on alteration.

Intermediate argillic alteration

Intermediate argillic alteration is weaker and occurs at lower temperature (<250°C) than sericitic alteration, and relatively low pH (although not as acidic as advanced argillic alteration). Intermediate argillic alteration is characterised by relict alkali feldspar in K-rich rocks and the replacement of biotite or plagioclase by kaolinite, illite and smectite (Seedorff et al. 2005).

Late sodic-calcic alteration

Na-Ca alteration occurs deep in the porphyry system where the influx of brine into the porphyry system removes most elements and precipitates Na-rich plagioclase and Ca-bearing minerals (at high temperature actinolite; at low temperature epidote, although T <400°C). This alteration is dominated by albite ± chlorite ± epidote mineral assemblages. The grade of the porphyry system may be destroyed by Na-Ca alteration e.g. Jersey deposit where a Ca-rich fluid stripped out metals.

Table 6. Summary of main mineralogy, alteration styles and sulphides at selected porphyry Cu and IOCG deposits from South America.

EARLY		LATE		
El Teniente	Pre-mineralisation	Late magmatic stage	Principal hydrothermal	Late hydrothermal
Mineralogy	mt, qtz	qtz-anh-cpy, bn, mo, k-feld; bt, chl, tm	qtz-anh-cpy, bn, mo, py	+ carb-tm-sul; qtz, anh, cpy, py, bn, tn; gy, chl
Alteration	mt-qtz-act-anh-plag ± ep; tm, ser, chl, mt	Na-K feld, bt, chl, ser	ser-chl, qtz	ser-chl, qtz
Sulphides		cpy, bn	cpy	cyp, py

Candelaria	Iron oxide stage	Sulphide stage	Late stage
Mineralogy	bt, mt, qtz	qtz, mt, amph, pyr, sp, mo, el, cpx, haem	cal, chl, clays
Alteration	alb-qtz-bt- k-feld- haem-mt	Ca amph, qtz, anh, Na scap, pyx, gnt	qtz, cal, haem
Sulphides		cpy, pyr, py, el, mo, sp	cpy, py,

Manto Verde	K and Fe metasomatism	Chlorite-sericite-quartz	Specular haematite-chalcopryrite	Late calcite veins
Mineralogy	K-feld, qtz, mt, orth, bt, tm, ti, qtz	orth, chl-ser, qtz, mu, chl, ser, anh, scap, ru, ep, haem	qtz, chl, ep, haem, sid, cal	cal, qtz
Alteration	K-feld, Fe	chl-ser-qtz	haem	cal
Sulphides	py	py	py, cpy, Au	

Mantos Blancos	Phyllic	Potassic	Sodic	Propylitic
Mineralogy	cpy, bn, py, qtz, ser	K-feld, qtz, tm, bi-chl, mt, cpy, dg, py	alb, haem, py, cpy, Ag-rich dg ± qtz	qtz, chl, ep, cal, alb, ser, haem, cpy, gal, py
Alteration	qtz, ser	K-feld	alb	qtz, ser, chl, ep, cal, haem ± alb
Sulphides	py, cpy, bn	py, cpy ± dg	py, cpy, dg	± py ± gal

Chuquicamata	Early: propylitic and potassic	qtz-Mo: ser over K	Main stage: qtz-ser over K sil	Late stage: qtz-ser
Mineralogy	qtz, k-feld, bt, anh; chl-ep-spec	qtz-Mo, K sil	py, qtz, Cu-Fe sul, en, tn, sp, mo	cv, dg, qtz, py, haem, sp, en
Alteration	chl, alb	K-sil, ser, qtz cc ± cv ± cpy ± dg; cv-cpy-dg ± cc;	qtz-ser	qtz-ser
Sulphides	cpy>bn, dg ± cv; bn, dg, cpy ± cv; py, haem, spec	cpy-bn, dg ± cv; bn, cpy ± cv ± dg	py-cv ± dg; py-cpy-bn-cv	py-cv-en, cc, cc + cpy, dg-cv

act = actinolite; alb = albite; amph = amphibole; anh = anhydrite; Au = gold; bn = bornite; bt = biotite; cal = calcite; carb = carbonate; cc = chalcocite; chl = chlorite; cpx = clinopyroxene; cpy = chalcopryrite; cv = covellite ;dg = digenite; el = electrum; en = enargite; ep = epidote; gnt = garnet; gy = gypsum; haem = haematite; k-feld = k feldspar; mo = molybdenite; mt = magnetite; mu = muscovite; orth = orthoclase; plag = plagioclase; py = pyrite; pyr = pyrrhotite; qtz = quartz; ru = rutile; scap = scapolites; ser = sericite; sp = sphalerite; spec = specularite; sul = sulphides; ti = titanite; tm = tourmaline.

Superposition of epithermal over porphyry (telescoping)

Telescoping is the process of overprinting early, deep, high T (>400°C) mineralisation by late, shallow, low T (~300°C) mineralisation (Sillitoe 1994), i.e. a younger event superimposed on the earlier mineral system. Telescoping is generally an epithermal style mineralisation, commonly in veins characterised by high-sulphidation type minerals, e.g. bornite, chalcocite enargite and covellite and is present in rocks dominated by sericitic alteration. The high sulphidation state minerals are precipitated as the fluid composition evolves as a result of decreasing temperature, increased fluid/rock ratio and time to reach a higher sulphidation state (Einaudi et al. 2003).

Telescoping results from lowering palaeosurfaces and associated palaeowater tables during the lifespan of the hydrothermal system. This may occur as a result of rapid erosion under fluvial conditions, sector collapse of volcanic edifices (Sillitoe 1994) or exhumation of the porphyry system, each of which bring the porphyry environment closer to the surface changing the physicochemical environment of ore deposition. The palaeosurface may be lowered up to 1 km causing vertical compression of any contained ore by at least 1 km (Sillitoe 1994). Telescoping is a common feature in many porphyry Cu and Cu-Mo deposits, e.g. Butte, Chuquicamata, El Salvador,

Escondida and Collahuasi and occurs late in the hydrothermal evolution of the porphyry system, up to 2 m.y. after the potassic alteration phase.

Telescoping needs to be taken into account during exploration for intrusion-centred porphyry systems, especially where HS epithermal deposits are being explored as the porphyry Cu and/or Au mineralisation may be concealed at shallower depths than anticipated (Sillitoe 1994).

MINERALISATION

Hypogene mineralisation

The emplacement of the porphyry intrusion develops a hydrothermal alteration system in which potassic, inner propylitic and outer propylitic alteration forms around the source intrusion and is accompanied by the initiation of quartz-sulphide veins (A-type) or sheeted quartz-magnetite-sulphide veins (M-type; Corbett 2009). This early mineralisation is commonly represented by pyrite-chalcopyrite-bornite \pm Au. As the intrusion cools, large bodies of hot acid ground water are formed by volatiles (H_2O and SO_2) venting from the cooling intrusions, promoting the development of more acidic phyllic to cooler less acidic argillic alteration (Corbett 2009). These hot acid waters collect in the upper parts of the hydrothermal system and can mix with mineralised fluids rising from the magma source at depth. This promotes Cu-Au deposition, typically within B-type quartz veins (Corbett 2009). The majority of mineralisation is deposited in quartz-sulphide veins (B-type), mainly as pyrite and chalcopyrite, which overprint the earlier quartz-sulphide and quartz-magnetite-sulphide veins.

The main ore minerals in porphyry deposits are chalcopyrite, bornite, gold and molybdenite. Gangue minerals include quartz, orthoclase, anhydrite, magnetite, biotite \pm sericite \pm pyrite. Sulphide zonation typically grades from a bornite-rich core through chalcopyrite to an outer pyrite halo. Zonation patterns may be complicated by late-stage veins with abundant pyrite and base metal sulphides.

Supergene enrichment – oxidation and upgrading

Supergene enrichment zones represent a low tonnage, high grade component to the hypogene Cu system, occurring either spatially above or adjacent to the hypogene mineralisation, e.g. Quellaveco, Cuajone, Toquepala, Santa Rosa, Chuquicamata, Sierra Gorda and Manto Verde, Chile. Supergene enrichment occurs close to surface, within the uppermost several hundred metres, and mineralisation is often flat-lying forming an enrichment blanket (Fig. 15). Supergene enrichment zones are attractive exploration targets due to higher Cu grades relative to primary ore zones and their relative ease of processing and metal extraction. Common Cu oxide-zone ore minerals include atacamite, brochantite, native Cu, malachite, chalcocite, covellite, bonattite, chalcantite, chrysocolla and pitch limonite.

Supergene processes occur in punctuated events over tens of millions of years and are best preserved in highly weathered and permeable host rocks with some neutralising capacity. The formation of supergene enrichment is dependent on the sulphur content, in particular as pyrite, and the availability of reduced sulphur. High pyrite content yields the potential for enrichment due to high acid generation capacity. Supergene enrichment is best achieved in areas of stable erosion/exhumation and semi-arid climates e.g. Andes, south-west USA. In areas of high erosion rates and wet climates, exhumation is too rapid for significant enrichment to occur. Mo and Au will be present in the residual leached cap and Au may be enriched to higher grade due to mass removal. Deep supergene enrichments may occur due to faults and fault intersections; late to post-mineralisation structures may control the form of the supergene zone.

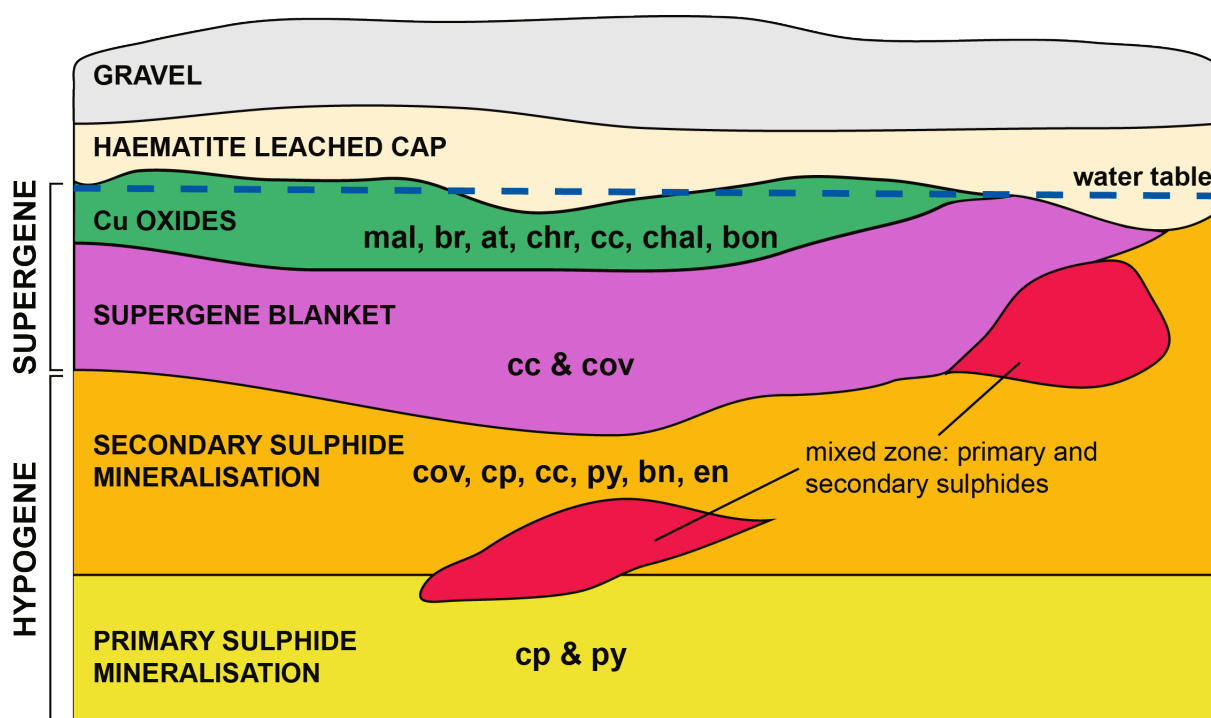


Figure 15. Generalised plan in section illustrating the relative position of the hypogene and supergene zones within a porphyry Cu deposit.

The hypogene zone contains the primary and secondary sulphide mineralisation comprised of chalcopyrite (cp) and pyrite (py) in the primary zone and covellite (cov), chalcopyrite (cp), chalcocite (cc), pyrite (py), bornite (bn) and enargite (en) in the secondary zone. Occurrences of mixed primary and secondary zones may exist. The supergene blanket is predominantly chalcocite and may contain covellite. The copper oxide zone may consist of malachite (mal), brochantite (br), atacamite (at), chrysocolla (chr), chalcocite (cc), chalcantite (chal) and bonattite (bon).

GEOPHYSICAL EXPRESSION OF PORPHYRY CU DEPOSITS

Geophysical methods are widely used in the exploration for and the characterisation of porphyry Cu deposits. Regional-scale surveys such as airborne magnetic and gravity surveys can be used to identify the broad crustal structure and magmatic framework that hosts mineralisation (John et al. 2010), including major structures (faults and fault intersections), in addition to locating deep intrusive bodies which may be directly related to the porphyry system. Features related to porphyry Cu deposits and their corresponding geophysical and spectral techniques are listed in Table 7. In addition to major regional structures, porphyry Cu and epithermal deposits have large, zoned hydrothermal alteration footprints, also detectable by geophysics. The large, zoned hydrothermal alteration footprints can be identified by changes in the physical properties of the host rocks where electrical, magnetic and density properties, potassium content, and spectral absorption will be affected (Table 8).

Scale and depth penetration are critical when selecting the most effective geophysical technique for exploring for porphyry Cu and epithermal deposits e.g. district scale vs. regional scale. Level of erosion and exhumation within a porphyry system will influence the geophysical response and thus the preferred geophysical technique. Most exposed porphyry Cu systems have been discovered already and consequently exploration is now focussed on covered deposits, mainly using indirect geophysical methods and geochemical information from distal exposures (Richards 2003). Hence knowledge of the level of erosion is important in assessing the potential roles for various exploration approaches, particularly when searching for targets beneath cover. Furthermore, given porphyry and epithermal systems are extremely diverse in form, host rock lithologies and structural settings, making general predictions about specific geophysical characteristics is not possible.

Therefore, exploration strategies require knowledge of the regional geological history and an understanding of porphyry Cu genesis within the broader context of tectono-magmatic arc processes and deposit-scale ore-forming processes (Richards 2003), e.g. variability in alteration, metal distribution and possible post-mineral modification.

Regional-scale features that provide insights into the broad structural and magmatic framework that host porphyry-related mineralisation (e.g. faults, fault intersections, intrusive bodies and bulk rock properties), can be detected using aeromagnetics, gravity, resistivity/conductivity and remote sensing techniques (John et al. 2010). Seismic reflection and seismic tomography may be useful in identifying lithologies surrounding or capping porphyry deposits.

Deposit-scale features that can be distinguished geophysically in porphyry Cu systems include magnetite destruction or magnetite-rich zones, enhanced potassium levels, clay mineralogy and alteration, supergene alteration, sulphide distribution and the hydrothermal alteration footprint (Table 7). These deposit-scale features may be detected using detailed magnetics, airborne electromagnetic, and ground electrical and electromagnetic techniques. Sulphide distribution and mineralisation may be characterised in three dimensions at a deposit-scale by a combination of aeromagnetic, ground magnetic, electromagnetic and induced polarisation surveys.

MAGNETICS

Regional magnetics can be used to identify regional structural corridors and major structures controlling emplacement of porphyry deposits. Intersections of regional faults can be delineated to identify target zones within recognised metallogenic belts. Regional magnetics will provide information about the physical bulk-rock properties, including host rock sequences, e.g. mafic volcanic sequences. Deep intrusive bodies and the extent of the host sequences can also be detected using magnetic surveys. Porphyry Cu districts in northern Chile are located within, or within close proximity to transverse magnetic anomalies, suggesting a connection between the magma source(s) of these regional magnetic anomalies and the sources for porphyry Cu deposits (Behn et al. 2001).

Detailed magnetic surveys are able to map anomalism associated with alteration systems in porphyry deposits and can identify magnetic 'bulls-eyes' where potassic cores are preserved near surface, or where hydrothermal magnetite alteration zones within ore bodies at depth are preserved. Detailed magnetic surveys will map the outer non-magnetic propylitic and phyllic zones which occur adjacent to the magnetic porphyry and magnetite-rich potassic zone in the core of the system; by comparison, surrounding host rocks may show characteristic noisy data. A magnetic porphyry and magnetite-rich potassic zone will be readily identified in detailed magnetic survey data. Where pervasive epithermal overprinting exists, a magnetic low within the volcanic host may be recognised. The magnetic response of porphyry deposits can be complicated by telescoping of the early, deep mineralisation with overprinting by late shallow mineralisation or by magnetite destruction. Magnetite is unstable at temperatures below 300°C (Allis 1990). Magnetite destruction is typically in the phyllic alteration zone and is caused by hydrothermal fluids, including relatively cool CO₂, and will produce a low magnetic response or demagnetisation anomalies (Allis 1990).

GRAVITY

Gravity surveys are effective for interpreting the crustal architecture associated with mineralisation. At a regional-scale, gravity is useful for identifying marked density differences that may exist between hydrothermally altered and unaltered rocks host rocks within the porphyry system. Small features such as veins and alteration zones associated with porphyry systems cannot be effectively identified using gravity modelling and inversion methods due to the level of spatial resolution required. Gravity highs may be associated with silicification or surface exposures of altered rock where cementation of pore space in the host rock has occurred (Irvine and Smith 1990). Density changes in the host rocks due to the destruction of primary and secondary magnetite by sericite alteration can also be mapped using gravity surveys. On a regional-scale,

gravity surveys are also useful to delineate the depth-to-basement which may help identify basin-bounding structures. Identification of deep intrusive bodies and the extent of the host sequence under cover can also be achieved using regional gravity surveys.

Table 7. Features of porphyry copper deposits and their detectable geophysical techniques and exploration implications after Irvine and Smith (1990). ASTER = advanced spaceborne thermal emission and reflection; VNIR = visual near infra-red; SWIR = short-wave infra-red.

	FEATURE	GEOPHYSICAL TECHNIQUES	EXPLORATION IMPLICATION
REGIONAL-SCALE FEATURE	Major structures including faults, structural corridors, basement structures, depth to basement	<ul style="list-style-type: none"> Airborne magnetics Gravity Magnetotellurics Electromagnetics 	<ul style="list-style-type: none"> Delineate major structural intersections and fluid conduits Locate oblique structures and juxtaposition of variable lithologies Delineate broad basement structures
	Deep intrusives	<ul style="list-style-type: none"> Airborne magnetics Gravity Magnetotellurics Seismic reflection and tomography 	<ul style="list-style-type: none"> Locate and identify potential source pluton to porphyry system
	Volcanic host sequences and bulk rock properties (including host rocks)	<ul style="list-style-type: none"> Airborne magnetics Gravity Magnetotellurics Seismic reflection and tomography 	<ul style="list-style-type: none"> Characterise host rocks, identify host rock lithologies i.e. mafic vs. felsic volcanics, identify alteration and or mineralisation zones within host rocks
DEPOSIT-SCALE FEATURE	Enhanced/depleted potassium content	<ul style="list-style-type: none"> Ground and airborne gamma ray spectrometry (radiometrics) 	<ul style="list-style-type: none"> Identify/map potassic core in alteration system, vector towards high grade mineralisation in core of system
	Magnetite destruction	<ul style="list-style-type: none"> Ground and airborne magnetics Magnetic susceptibility measurements 	<ul style="list-style-type: none"> Differentiate hydrothermal alteration zones due to magnetite destruction Identify magnetite-rich zones where potassic alteration is preserved near surface. Identify pervasive epithermal overprinting (magnetic low)
	Increased or reduced density	<ul style="list-style-type: none"> Gravity 	<ul style="list-style-type: none"> Characterise host rock sequences, differentiate hydrothermal alteration within different host rocks i.e. increased density due to volume of fractures/dissolution vs. decreased density due to hydrothermal silicification
	Supergene alteration (oxides)	<ul style="list-style-type: none"> ASTER VNIR SWIR 	<ul style="list-style-type: none"> Identify enrichment blanket above hypogene mineralisation
	Clay alteration (reduced resistivity)	<ul style="list-style-type: none"> Ground and airborne electromagnetics Ground resistivity Magnetotellurics 	<ul style="list-style-type: none"> Differentiate alteration zones associated with argillic alteration
	Clay mineralogy	<ul style="list-style-type: none"> SWIR 	<ul style="list-style-type: none"> Differentiate alteration zones and argillic alteration zones
	High silica content (high resistivity)	<ul style="list-style-type: none"> High resolution resistivity Controlled source audiomagnetotellurics Induced polarisation Transient electromagnetic 	<ul style="list-style-type: none"> Distribution of silica alteration, locate and identify silicified zones and quartz veins hosting mineralisation
	High sulphide content and haloes (high conductivity and chargeability)	<ul style="list-style-type: none"> Induced polarisation Electromagnetics 	<ul style="list-style-type: none"> Differentiate pyrite, chalcopyrite and bornite dominant zones
	Hydrothermal alteration footprint	<ul style="list-style-type: none"> ASTER SWIR Radiometrics Electromagnetics Gravity Magnetics Ground and airborne magnetic 	<ul style="list-style-type: none"> Differentiate alteration zones (core-distal): potassic, phyllic, propylitic, argillic and advanced argillic (See Table 8 for more detail)

ELECTRICAL AND ELECTROMAGNETIC METHODS

Both airborne electromagnetic and ground electrical and electromagnetic (EM) methods can be used in porphyry and epithermal exploration due to the distinctive electrical resistivity of rocks and minerals associated with these deposits. Quartz, and igneous and metamorphic rocks are highly

resistive, whereas clay minerals, sulphides, graphite and saline fluids are conductive. Sedimentary rocks, weathered rocks, non-sulphide alteration zones and freshwater are moderately resistive. Airborne EM is therefore used to effectively map both conductive and resistive zones associated with alteration and mineralisation. In this respect airborne EM can be used to test for sulphides where stockwork veins have good connectivity, thus strong conductive responses are generally coincident with mineralisation. Alteration zones can be mapped due to the distribution and relative conductivity of clays and sulphides. The sericite alteration zone which has the most intense fracturing and fluid flow can readily be identified as a low resistivity response. At a broader scale, conductivity information can also be used to map structural fabrics and to map and identify intrusive bodies, which are usually more resistive as a result of coherency.

Ground electrical and EM methods such as resistivity, induced polarisation (IP), magnetotellurics (MT) and transient EM (TEM) can also be effective in targeting conductive hydrothermally altered zones enclosing or capping a deposit or resistive zones associated with quartz veins or silicified zones. Strong chargeability (IP) and conductive responses (TEM) are coincident with mineralisation.

Induced Polarisation (IP) is suitable to detect sulphide distribution, particularly in narrow quartz veins, and peripheral pyrite haloes, with the strongest IP response correlating to the quartz-sericite-pyrite alteration. The central potassic alteration zone and the distal propylitic alteration zone typically have low pyrite contents hence show weaker IP responses than the sericite alteration zone (John et al. 2010). Disseminated sulphides may produce broad IP responses but with adequate geological control IP can still provide valuable information (Irvine and Smith 1990). IP techniques can also be used to map the depth to hypogene sulphides (high chargeability) and distribution of silica alteration as resistivity high.

ALTERATION FOOTPRINTS

Alteration associated with porphyry Cu deposits occurs in zones, producing predictable spatial patterns that can be detected using ground electrical and EM methods (Table 8). Differing magnetic properties within these zones can be mapped by detailed high resolution aeromagnetic and ground magnetic surveys (John et al. 2010). Iron and sulphide distribution (pyrite, chalcopyrite, chalcocite and bornite) can be identified using modern electrical and electromagnetic techniques which measure their relative resistivity and conductivity. Induced polarisation methods are also suitable for porphyry systems due to the dispersed nature of sulphide minerals.

SPECTRAL MAPPING AND REMOTE SENSING

Airborne, spaceborne, multispectral and hyperspectral imaging systems can be used to map alteration mineral associations and their spatial relationship to porphyry Cu systems (John et al. 2010), and is particularly useful in areas of good exposure with sparse vegetation. The primary mineralogy in porphyry Cu deposits is strongly modified at surface by weathering processes, therefore the signatures in airborne and satellite systems is highly dependent on the nature of the regolith. Spectral mapping is particularly useful in mapping hydrothermal minerals characteristic of sericitic, intermediate and advanced argillic, and propylitic alteration; iron oxides and hydroxides, and silica can be remotely mapped using their distinctive absorption features in the visible-near infrared through shortwave infrared and thermal infrared wavelengths (John et al. 2010).

SHORTWAVE INFRARED (SWIR) AND AIRBORNE SWIR

Shortwave Infrared data has sufficient resolution to differentiate the spectral signatures for advanced argillic (alunite-kaolinite), sericitic (muscovite), propylitic (chlorite-epidote-calcite) and supergene mineral assemblages (John et al. 2010). Therefore SWIR is able to map spectral zonation that corresponds to the alteration system. SWIR can be used to identify the clay minerals associated with argillic alteration. SWIR used in conjunction with chemistry can assist to refine the interpretation of mineral alteration patterns. SWIR can be used to identify which minerals are present and the chemistry used to assess how much of the mineral is present. Together, spectra

and chemistry can be used to map mineralogy that can assist with predictions of ore distribution, mining method, milling and recovery issues. A limitation of SWIR is the restricted range of minerals that can be identified and inability to penetrate thin coatings, e.g. hematite dusting on mineral surfaces. Spectral identification of alteration minerals can be used for temperature estimates and therefore provide a depth estimation of the system related to the alteration zone.

Table 8. Characteristics of the hydrothermal alteration footprint associated with porphyry Cu deposits and their corresponding geophysical technique.

Alteration	Position in system	Key minerals	Principal sulphide assemblages	Physical properties and geophysical response	Corresponding geophysical technique
Potassic (K-silicate)	Core zones of deposit	bi-K-spar ± act ± ep ± ser ± and-alb ± carb ± tm ± mt	mt-ru, py-cp, cp ± bn, bn ± dg ± cc	Magnetic high, increased K content, conductive, high chargeability, low resistivity	IP, magnetic, airborne EM, radiometrics, MT
Phyllic (sericitic)	Upper parts of deposit	qtz-ser ± pp ± carb ± tm ± spec	py ± cp, py-en ± ten, py-bn ± c, py-sp, rt-cp-mo	Conductive, magnetic low, high chargeability, low resistivity (higher than potassic), strong IP	IP, magnetic, airborne EM, MT
Argillic	Above deposit, constitutes lithocap	kaol-mm-ser-chl	none	Conductive, kaolinite has distinct Al-OH absorption feature	EM, TEM, IP, MT, SWIR
Intermediate Argillic	Above deposit, constitutes lithocap	kaol-chl-ser ± mm ± il ± sm ± cal ± ep ± bt	py-pyr-cp-haem	Conductive, kaolinite has distinct Al-OH absorption feature	EM, TEM, IP, MT, SWIR
Advanced argillic	Above deposit, constitutes lithocap	qtz-pp-kaol-dk-alun ± and ± cd ± tz	py-en, py-cc, py-cv	Conductive, kaolinite and alunite have distinct Al-OH absorption features	EM, TEM, IP, MT, SWIR
Propylitic	Marginal parts of system, below lithocaps	chl-ep-act-alb-carb ± haem ± mt	py-sp-haem-cp-gal-ten-tet	Resistive, low chargeability	Airborne EM, IP

act = actinolite; alb = albite; alun = alunite; and = andalusite; bn = bornite; bt = biotite; cal = calcite; carb = carbonate; cc = chalcocite; chl = chlorite; cp = chalcopyrite; cv = covellite; dg = digenite; dk = dickite; en = enargite; ep = epidote; gal = galena; haem = haematite; il = illite; kaol = kaolinite; mo = molybdenite; mt = magnetite; mm = montmorillonite; pp = pyrophyllite; py = pyrite; pyr = pyrrhotite; qtz = quartz; ru = rutile; ser = sericite; sm = smectite; sp = sphalerite; ten = tennantite, tet = tetrahedrite.

ADVANCED SPACEBORNE THERMAL EMISSION AND REFLECTION (ASTER)

Advanced Spaceborne Thermal Emission and Reflection (ASTER) provides high resolution images of land surface temperature, reflectance and elevation in the visible through thermal infrared spectrum. ASTER allows the discrimination and identification of hydrothermal alteration minerals in the SWIR region of the electromagnetic spectrum; vegetation and iron oxide minerals are detectable through visible and near infrared (VNIR) and thermal infrared (TIR) can map carbonates and silicates (Pour and Hashim 2011, 2012). ASTER data have been widely and successfully used in minerals exploration and lithological mapping, specifically mapping hydrothermal alteration systems associated with porphyry systems. The spectral absorption properties of unique mineral assemblages in these hydrothermal alteration systems make ASTER data particularly effective in mapping broad alteration patterns (Fig. 16). As previously mentioned imaging such as ASTER is most effective in areas of sparse vegetation and abundant exposed bedrock. Ground validation is required to confirm the minerals responsible for the pattern of spectral response in ASTER data as there is limited ability to differentiate minerals due to poor spectral resolution in the data (only 8 available channels).

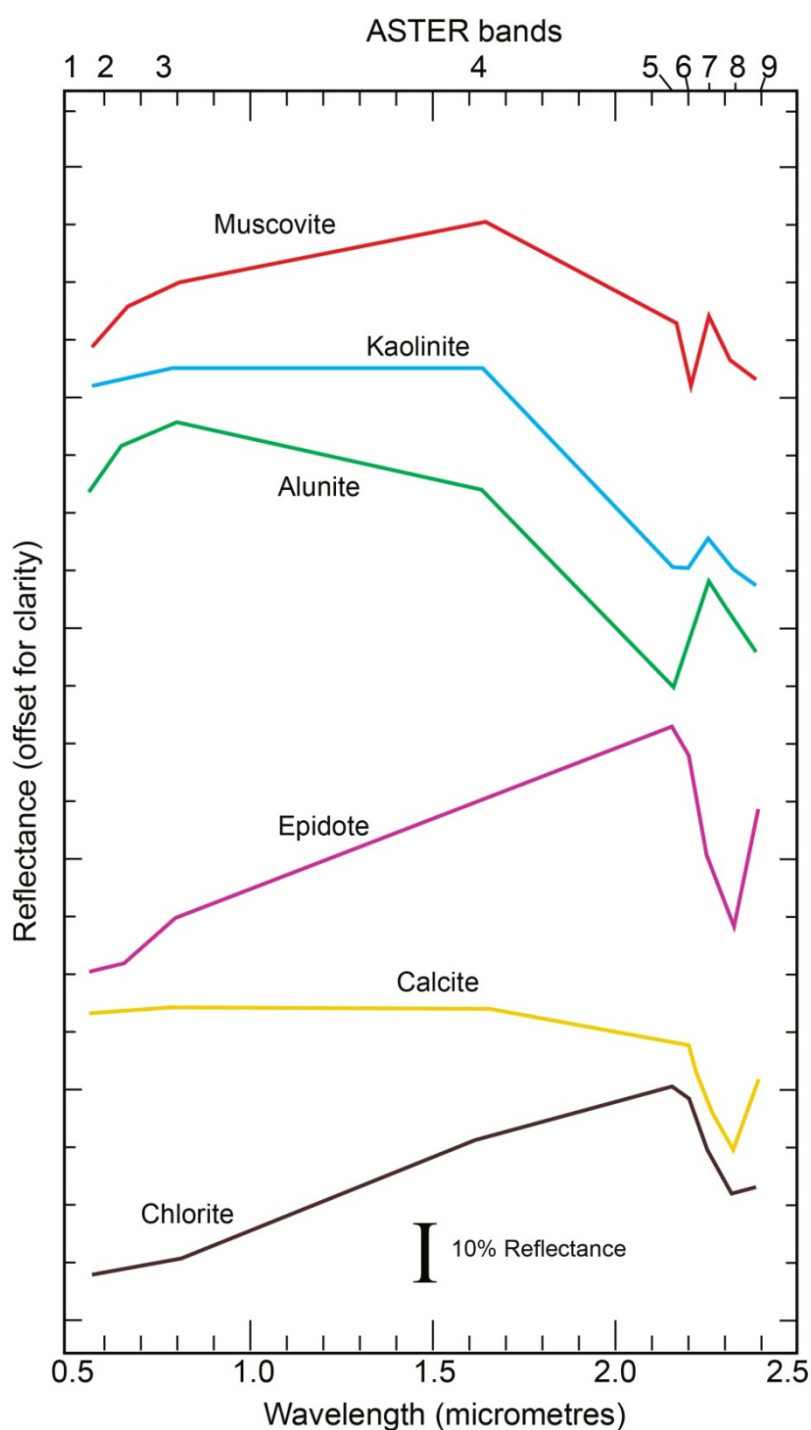


Figure 16. Laboratory spectra of muscovite, kaolinite, alunite, epidote, calcite and chlorite resampled to ASTER band passes.

Muscovite is typical in phyllic alteration (2.2 μm); kaolinite and alunite are typical of argillic alteration (2.17 μm); epidote, calcite and chlorite are typical of propylitic alteration (2.35 μm). Image source: Clarke et al. 1993.

GENETICALLY ASSOCIATED MINERAL DEPOSITS

There is a wide variety of mineral deposits that may be genetically related to porphyry Cu deposits as indicated by Fig. 8. These include:

- Sub-epithermal vein Zn-Cu-Pb-Ag \pm Au
- Proximal Cu-Au skarn
- Distal Au/Zn-Pb skarn

- Carbonate-replacement Zn-Pb-Ag ± Au or Cu
- Sediment-hosted distal disseminated Au-As ± Sb ± Hg
- High-sulphidation Au ± Ag ± Cu
- Low-sulphidation Au-Ag

Within the porphyry system it is unlikely that all of these mineralisation styles will occur together, although well-endowed examples include the Bingham District with porphyry Cu-Au-Mo, Cu-Au skarn, carbonate replacement Zn-Pb-As-Au and sediment hosted Au deposits, and the Lepanto District with high sulphidation Cu-Au-Ag and epithermal Au-Ag-Cu associated with the porphyry Cu-Au deposit (Sillitoe 2010b). Mineralisation elsewhere in the porphyry system is largely influenced by rock type; skarn, carbonate replacement and sediment-hosted mineralisation types are dependent on the presence of reactive carbonate rocks, while large-tonnage high-sulphidation deposits are favoured by permeable rock packages, e.g. pyroclastic or epiclastic rocks (Sillitoe 2010b). The position within the magmatic arc and the evolution of associated fluids may also influence mineralisation style within the porphyry system. Similarly the presence of one or several of these mineralisation styles does not preclude or indicate the presence of a nearby porphyry Cu deposit. Nonetheless recognition of weakly developed mineralisation of a single type may vector towards potentially higher grade mineralisation elsewhere in the system.

EPITHERMAL DEPOSITS

Epithermal Au and Au-Ag deposits are relatively shallow, magma-related hydrothermal systems which commonly form in subaerial volcanic arcs. There are two major deposit types: high and low sulphidation, which are dependent on the composition and mixing of related fluids, which are influenced by the position of the system within the magmatic arc. Low sulphidation epithermal Au-Ag deposits commonly form above porphyries, within the upper 1 km of the surface. Low sulphidation epithermal Au-Au deposits are derived from a dilute, near-neutral chloride fluid with sulphur as H₂S. Low sulphidation epithermal deposits form two end members; magmatic arc low sulphidation epithermal Au and extensional low sulphidation epithermal Au-Ag deposits. High sulphidation epithermal mineralisation occurs at high crustal levels and displays a dominant magmatic component. The fluid in high sulphidation systems evolves from a hot, near-neutral fluid to a hot, extremely acidic (pH 1–2) fluid at shallow levels. The epithermal system may form above, e.g. low sulphidation epithermal quartz Au ± Ag, or to the side, e.g. high sulphidation epithermal Au such as; Lepanto and Far South East, Luzon (Chang et al. 2011), which are examples of a coeval porphyry system overprinting porphyry Cu deposits.

Low sulphidation epithermal Au-Ag mineralisation within the magmatic arc produces quartz-sulphide Au ± Cu, carbonate-base metal Au and, at shallower levels, epithermal quartz Au ± Ag mineralisation. Low sulphidation epithermal quartz-sulphide Au ± Cu deposits typically have Au-rich pyrite and occur deeper and closer to the porphyry, e.g. Kelian, Indonesia; Mineral Hill, Australia; Hamata, Papua New Guinea, and Copiapo, Chile, and may represent a transition between porphyry and epithermal deposits e.g. Cadia, Australia and Maricunga Belt, Chile. Carbonate-base metal Au deposits e.g. Kerimenge, Papua New Guinea and the El Indio district, Chile, are commonly high-grade Au deposits due to the mixing of bicarbonate waters with metal-bearing fluids which destabilises Au and provides an efficient deposition mechanism. As the fluid evolves epithermal quartz Au ± Ag deposits may form, which contain high fineness Au with minor Ag.

In extensional environments of the magmatic arc i.e. back-arc or intra arc extension, a range of mineralisation styles are associated with low sulphidation epithermal mineralisation which include quartz-sulphide, polymetallic Ag-Au or chalcedony-ginguro Au-Ag veins (ginguro refers to black bands hosting electrum and Au recognised by Japanese miners; ginguro bands have also been called adularia-sericite or quartz-adularia veins). Polymetallic Ag-Au deposits commonly occur as fissure veins in Latin America as Ag-rich end member of carbonate-base metal mineralisation. Polymetallic Ag-Au deposits are commonly banded veins associated with the intersection of steep listric faults and competent host rocks. Chalcedony-ginguro Au-Ag forms in the upper portion of polymetallic deposits and evolve from the Ag-Au fissure veins. Chalcedony-ginguro Au-Ag deposits

occur in the SW Pacific Rim e.g. Gosowong, Japan e.g. Hishikari, western USA e.g. McLaughlin, and northern Australia e.g. Cracow.

High-sulphidation Au, Ag ± Cu deposits are characteristic in the lithocap environment of porphyry Cu deposits; however, the preserved parts of many lithocaps are essentially barren (Sillitoe 2010b). High sulphidation epithermal deposits form in magmatic arc environments and are common in the Andes extending into Mexico and western USA, and are also found in the SW Pacific Rim. There is usually a spatial separation (commonly ≥ 1 km) between the porphyry source and the high sulphidation deposit in which fluid evolution takes place. The fluid in high sulphidation epithermal Au mineralisation rises rapidly up a structure as a volatile-rich, near-neutral hot fluid, which becomes increasingly depressurised as it ascends to higher crustal levels, causing volatiles such as SO₂ to exsolve and react with water to form H₂SO₄ and condense. The fluid becomes increasingly acidic at shallow levels and cools and is neutralised as it reacts with permeable wall rocks or entrained ground waters, which results in zoned hydrothermal alteration. High sulphidation epithermal Au-Cu-Ag deposits are characterised by enargite-barite-alunite veins e.g. La Coipa, Chile and residual or vuggy silica.

SKARN DEPOSITS

Skarn deposits can form in a broad range of geologic environments, associated with a variety of rock types and are best developed in permeable rock units e.g. limestone, marls, dolomite and volcanics. The development of skarn deposits occurs in stages, producing zonation in alteration and mineralisation, similar to a porphyry system. Three stages have been identified in the evolution of skarn deposits and are related to the porphyry system evolution. The first stage comprises contact metamorphism in the wall rocks caused by the heat source and is called isochemical skarn. The second stage is a metasomatic skarn which develops by circulating hydrothermal cells transferring magmatic volatiles (H₂O, Al, Si and Fe) into carbonate rocks while Ca, CO₂ and Mg are removed. The third stage is the development of a retrograde skarn where ground waters entering the cooling skarn environment cause hydrous retrograde minerals to replace anhydrous prograde minerals.

Other types of skarns include exoskarn and endoskarn. These skarns are classified according to the rock type replaced. Exoskarns develop outside the related intrusion i.e. by replacing carbonates, and are classified according to the dominant mineralogy which reflects the composition of the carbonate rock being replaced. The majority of the world's economic skarn deposits occur in calcic exoskarns. Garnet and pyroxene are the dominant minerals in calcic exoskarns (Einaudi and Burt 1982). Endoskarns occur inside the related intrusion. In deep systems, the endoskarn only forms in narrow zones at the immediate intrusive contact (Einaudi and Burt 1982). Endoskarn is best developed where fluid flow is dominantly into the pluton or upward along its contacts with carbonates, producing metasomatic fronts.

Skarns provide significant sources of Cu-Au, Mo and W with the potential for higher grade epithermal overprints. Skarn alteration and mineralisation can also be used as vectors towards porphyry Cu-Au mineralisation e.g. Ertsberg-Grasberg, Philippines; Cadia-Ridgeway, New South Wales; and Ok Tedi-Frieda, Papua New Guinea.

CONTINUUM OF IOCG, PORPHYRY AND EPITHERMAL SYSTEMS

In giant hydrothermal systems, a continuum of alteration and mineralisation between spatially and genetically linked IOCG, porphyry and epithermal systems may exist, e.g. Great Bear Magmatic Zone, Canada (Mumin et al. 2010). The continuum between IOCG, porphyry and epithermal deposits can be plotted on a ternary diagram due to relative temperature and depth of mineralisation, alteration assemblage and metal enrichments of each of the end members (Fig. 17; Mumin et al. 2010). The geological characteristics common to porphyry, epithermal and IOCG deposits are summarised and compared in Table 9. As discussed by Mumin et al. (2010) the continuum of IOCG, porphyry and epithermal systems should be an expected and logical outcome of large and complex hydrothermal systems associated with felsic to intermediate volcano-plutonic

complexes. While IOCG deposits are considered to be hotter, deeper seated and more regionally developed than porphyry Cu systems, both systems are associated with strong temperature gradients ranging from magmatic temperatures to near-surface ambient temperatures (Mumin et al. 2010, Sillitoe 2010a). The associated alteration assemblages and textures may also reflect these temperature differences. For example in the Great Bear Magmatic Zone (GBMZ) porphyry systems are distinguished from IOCG and epithermal deposits by potassic-phyllitic-propylitic alteration zoning; epithermal deposits are characterised by lower temperature assemblages, and near surface textures located distal or peripheral to high-temperature alteration assemblages; and IOCG deposits are characterised by alkali-iron metasomatism and hydrothermal iron-oxides.

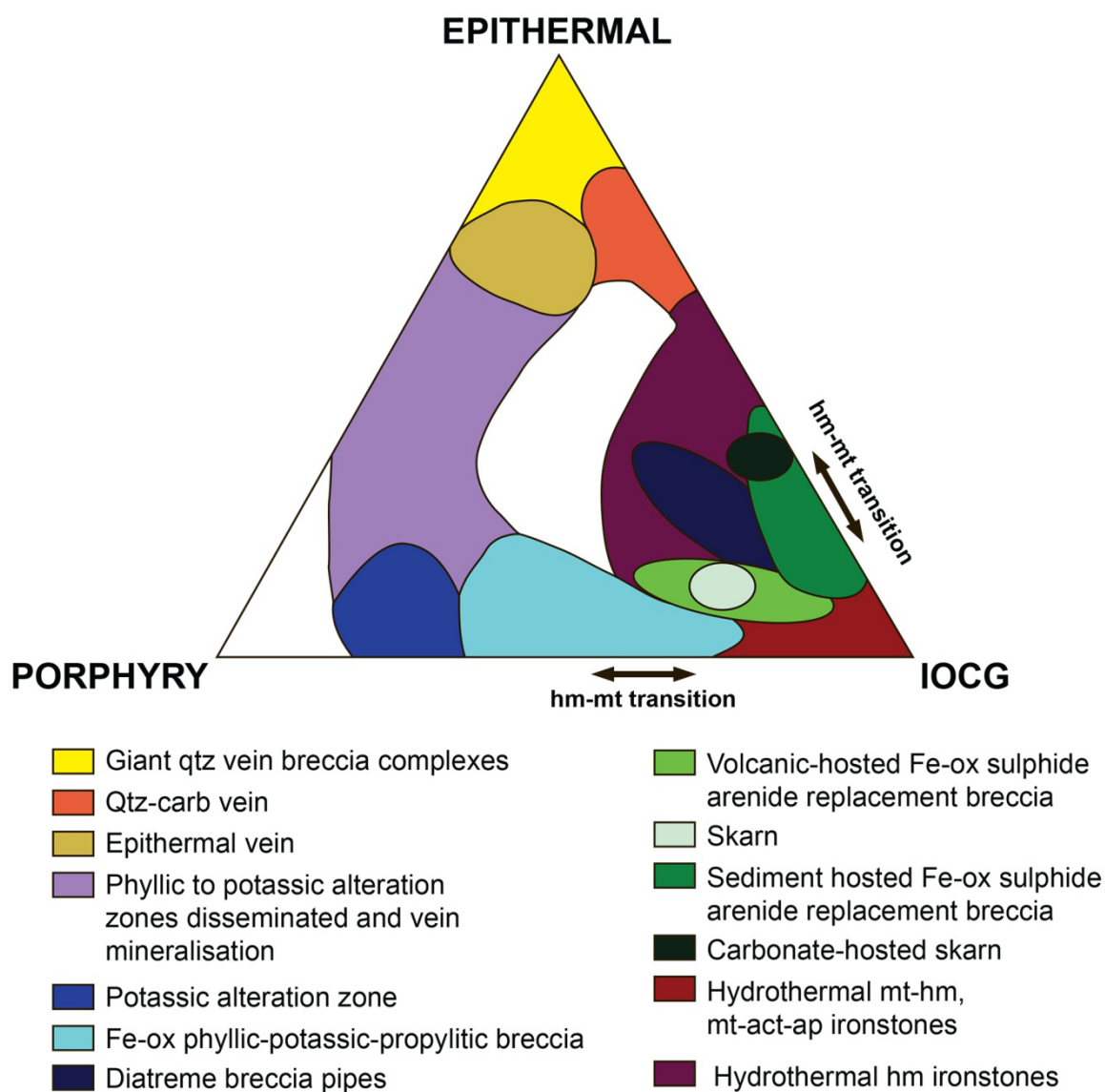


Figure 17. The porphyry-epithermal-IOCG spectrum occurring within giant hydrothermal systems of the Great Bear Magmatic Zone, Canada, illustrating the various mineralisation styles present within the system, after Mumin et al. (2010).

Table 9. Comparison of characteristics common to IOCG, porphyry and epithermal deposits, including tectonic setting, associated magmas, mineralisation style, alteration assemblage and ore minerals.

	IOCG	PORPHYRY	EPITHERMAL
Age/time period	Archaean to Mesozoic and Cenozoic	Archaean to Cenozoic, predominantly Mesozoic to Cenozoic	Archaean to Recent, commonly Cenozoic to Recent
Tectonic setting	Extensional, back-arc, continental rift, ?anorogenic	Arc settings, post-collisional	Volcanic arcs to convergent plate margins, intra-arc, back-arc post-collisional rift settings
Structural control	Strong structural control, faults and shear zones	Fault intersections, oblique to faults	Faults and fractures
Associated magmas	Tholeiitic to calc-alkaline, mantle-derived gabbros to granodiorites Single-phase intrusions	Calc-alkaline to alkaline pipes, sills and dykes Multiphase intrusions	Calc alkaline to alkaline andesite to rhyolite, tholeiitic bimodal basalt to rhyolite
Mineralisation style	Veins Hydrothermal breccias Tectonic breccias Replacement Calcic skarns Composite	Stockwork Veins and veinlets Disseminated Breccias	Veins, vein swarms Stockwork Hydrothermal breccias Strata-bound disseminated
Classification	Magnetite-rich Haematite-rich	Au only Au-rich Cu-Au Cu-Mo	Neutral pH: quartz-calcite-adularia-illite Low sulphidation: arsenopyrite-loellingite-pyrrhotite, pyrrhotite, Fe-rich sphalerite-pyrite Acid pH: quartz-alunite-pyrophyllite-dickite-kaolinite High sulphidation: pyrite-enargite-luzonite-covellite-digenite-famatinite-orpiment
Alteration assemblage	Iron (magnetite, haematite); potassic (K-feldspar, sericite, biotite); sodic (albite, scapolite) Magnetite-rich: actinolite-biotite-K-feldspar-quartz Haematite-rich: K-feldspar-chlorite-sericite-epidote-carbonate-quartz-actinolite-scapolite	Potassic: K-feldspar-biotite-sericite-anhydrite-tourmaline-magnetite Phyllic: quartz-sericite-pyrite Propylitic: chlorite-epidote-actinolite Argillic: quartz-kaolinite-alunite-sericite-clays	Propylitic: quartz, k feldspar (adularia), albite, illite, chlorite, calcite, epidote, pyrite Argillic: illite, smectite, chlorite, clays, pyrite, calcite (siderite), chalcedony Advanced argillic: opal, alunite, kaolinite, pyrite, marcasites; quartz, alunite, dickite, pyrophyllite; alunite, kaolinite, halloysite, jarosite, Fe-oxides
Alteration zoning (upwards and outwards)	Magnetite-actinolite-apatite to scapolite-haematite-chlorite-sericite	Potassic – Phyllic – Propylitic – Argillic	Propylitic – clay, carbonate, zeolite minerals – quartz, adularia, illite, pyrite
Formation conditions	?>4km	2-4 km	<1.5 km; <300 °C
Ore minerals	Haematite-rich: chalcopryite-pyrite-bornite Magnetite-rich: chalcopryite	Chalcopryite, bornite, Au, molybdenite	Electrum, acanthide, silver sulfosalts, silver selenites, Au-Ag tellurides, sphalerite, galena, chalcopryite
Examples	Olympic Dam, Ernest Henry, Candelaria, Manto Verde, Mantos Blancos	Chuquicamata, El Teniente, Bingham, Butte, Parkes	Baguio district, Lepanto, El Indio, Pueblo Viejo, Yanacocha, Potosi

POTENTIAL OF PORPHYRY SYSTEMS IN SOUTH AUSTRALIA

The exploration for porphyry-style Cu deposits in South Australia commenced in the early 1960s (Table 10) with the main focus on the Cambrian-aged Anabama Granite and related granites in the Nackara Arc portion of the Adelaide Geosyncline. Exploration has also been undertaken in the central Flinders Ranges for porphyry-related deposits in Neoproterozoic-aged rocks. Yorke Peninsula and northern Eyre Peninsula have been the focus for porphyry systems in Palaeoproterozoic to Mesoproterozoic rocks altered by igneous activity related to the Gawler Range Volcanics-Hiltaba Suite granites and the Moonabie Formation. Exploration has also

focussed on Palaeoproterozoic and Mesoproterozoic successions in the Curnamona Province, particularly in the Benagerie Ridge area.

Early focus on the porphyry-style Cu-Mo mineralisation associated with the Anabama Granite in the Nackara Arc, identified promising indications of alteration but yielded no economically significant results. Porphyry-style Cu-Mo mineralisation associated with the Anabama Granite was first recognised in 1966 by A. H. Blissett and M. G. Mason at Netley Hill (Morris 1981). Subsequent drilling confirmed anomalous copper and molybdenum associated with hydrothermally altered granite at Netley and Anabama Hills (Morris 1981). Mineralisation in this region is Palaeozoic in age and located in the eastern Nackara Arc.

The Anabama Granite occurs in a region where a thick Neoproterozoic sequence of Adelaide Geosyncline strata are separated from the Palaeoproterozoic Willyama Supergroup of the Curnamona Province (to the northeast) by the MacDonald Shear Zone, and from the Murray Basin to the southeast by the Anabama-Redan Fault Zone (Morris 1981). The Anabama Granite (ca. 450 Ma), is a large (65 km x 9 km), elliptical-shaped granite body that lies parallel to the northeast regional strike of the Adelaidean metasediments and was likely emplaced during the Delamerian Orogeny (Morris 1981). Additional granites of similar age were intruded at Bendigo, Palmer, Victor Harbor, Kangaroo Island and in the area between Murray Bridge and Naracoorte. The Anabama Granite is a coarse-grained, biotite granite to granodiorite with interlayered micro-granodiorites and is cross-cut by quartz porphyry and porphyritic microgranite dykes, a dacite porphyry dyke and a pebble dyke (Morris 1981). In the upper parts the granitic rocks have been almost completely hydrothermally altered to greisen; hydrothermal alteration decreases with depth where patches of greisens occur and muscovite/sericite replacement of feldspar and chlorite and epidote replacement of biotite are observed. The base of the granite hill is relatively unaltered, except for greisen envelopes around quartz veins (Morris 1981). Primary and secondary sulphides are rare; traces of disseminated pyrite and chalcopyrite occur within porphyritic microgranite and scattered flakes of molybdenite are intergrown with pyrite, while malachite and chrysocolla are associated with pyrite in one or two quartz veins (Morris 1981). Indications of copper oxides are present as cubic cavities or pseudomorphs of limonite, and goethite after pyrite is abundant; jarosite is also present (Morris 1981).

PacMag Metals Limited and Giralia Resources NL hold a JV project (EL3438) that comprises the Blue Rose-Olary Project and includes the Netley Hill and Blue Rose Prospects (Clifford 2008). At Netley Hill the host to mineralisation is a muscovite-quartz pyrite rock (greisen) which grades to biotite granite (Clifford 2008). A strong IP anomaly 3 km x 1 km was drill- tested with four *PACE* funded diamond drill-holes which showed pervasive dissemination and vein-hosted sulphide mineralisation (chalcopyrite, molybdenite and pyrite) to be the cause of the IP anomaly (Clifford 2008). Highlights from this drilling include 40 metres @ 0.05% molybdenum and 1g/t silver from 11 metres below surface (Clifford 2008). Drilling at Netley Hill has indicated the thickness of molybdenum mineralisation has increased above and to the east of the IP anomaly and the extent of molybdenum mineralisation will be tested by additional drilling (Clifford 2008).

Strong alteration consists of two types at Netley Hill: potassium feldspar selvage around quartz-pyrite veinlets and fractures; and sericite-pyrite veins and selvage that overprints the earlier K-feldspar alteration (Fig. 18; Clifford 2008). The alteration is predominantly stockwork veins and fractures with zones developed above very fine micro-veins (Fig. 18).

Blue Rose Prospect was discovered in 1997 within covered Neoproterozoic pelites, schists and calc-silicate rocks, and is partially hosted within two monzonite dykes, with the majority of the copper and gold sulphide mineralisation located in skarns, pelites and schists in the hanging wall of the dykes (Clifford 2006). Sulphide mineralisation consists of chalcopyrite-bornite with accessory molybdenite and gold mineralisation (Clifford 2006). A linear magnetite skarn is located 1 km east of the porphyry target at Blue Rose Prospect where encouraging copper and gold grades (up to 48 m @ 1.01 g/t Au and 0.82% Cu) are associated with magnetite-rich calc-silicate rocks; the limits of the skarn mineralisation are yet to be defined (Clifford 2006).

Table 10. Summary of exploration activity aimed at porphyry-style mineralisation in South Australia.

Operator	Location	Year(s)	Tenement	Reference	Stratigraphy	Target	Feature/Anomaly	Follow Up & Result
South Alligator Uranium NL, Metals Exploration NL	Central Flinders Ranges: Blinman, Woorumba and Oraparinna	1965–1967	SML00086	ENV 00620	Callanna Group	Porphyry-type Cu deposit associated with diapiro breccia	IP anomaly and soil geochemical anomalies	Iron-bearing heavy minerals or graphite responsible for IP anomalies
Yunta Copper Pty Ltd; Noranda Exploration Co. Ltd; Ausminda Pty Ltd	Nackara, Oodla Wirra	1965–1966	SML00100; SML00103	ENV 00634	Tapley Hill Formation, Skillogalee Dolomite	Old copper workings	IP anomaly ~460 m long x 60–120 m wide	Geological mapping, stream and sediment geochemical sampling and diamond drilling failed to prove economic copper mineralisation present
The Broken Hill Pty Co Ltd	Anzac Dam, north-eastern Eyre Peninsula	1969–1970	SML00204	ENV 01174	Gawler Range Volcanics, Moonabie Formation	Porphyry Cu deposit	Magnetic anomaly akin to porphyry copper deposits; fault intersections with dykes or faults	IP survey, mapping and geochemical drainage sampling failed to evidence of mineralisation
Bureau de Recherches Geologiques et Minieres (France); Societe Le Nickel; Serem (Aust.) Pty Ltd	Cultana area, north-east Eyre Peninsula	1971	-	ENV01722	Moonabie Formation, Cultana Subsuite	Porphyry Cu style mineralisation	Copper mineralisation at surface	Soil geochemistry
South Australian Department of Mines	South Dam, Burra	1972–1973	EL00012	ENV 02165	Bendigo Granite	Porphyry Cu-Mo	Two magnetic anomalies related to granites underlying gravels and clays	IP and resistivity surveys, shallow pattern drilling revealed weakly anomalous Cu and Zn values
South Australian Department of Mines	Anabama Hill, Netley Hill, Adelaide Geosyncline	1980	EL00016	ENV 02175	Anabama Granite	Porphyry Cu-Mo	Anomalous Cu and Mo associated with quartz veins, porphyry dykes and greisen	Rock chip and soil geochemistry showed low grade Cu-Mo mineralisation
South Australian Department of Mines	Anabama Hill and Cronje Dam, Adelaide Geosyncline	1977	EL00173	RB 77/00051; ENV 03054	Anabama Granite	Porphyry Cu-Mo	Coincident geochemical, magnetic and IP anomalies associated with greisens zone; hydrothermal alteration, sulphide assemblage and rock types show affinity to porphyry Cu deposits	Rotary percussion drilling tested coincident IP and soil anomalies. Best intersections: 5 m @ 0.1% Cu and 4 and 5.5 m 0.1% Mo; 14 m @ 0.12% Cu
Asarco Pty Ltd	Anabama Hill, Adelaide Geosyncline	1980	ELA 65/80	ENV 3854	Anabama Granite	Porphyry Cu-Mo	Coincident zoned hydrothermal alteration, breccia pipes and Cu-Mo mineralisation	Deep, near vertical diamond drilling recommended but not carried out
CSR Ltd	Anabama Hill, Adelaide Geosyncline	1980–1982	EL00753	ENV 04029	Anabama Granite	Porphyry Cu-Mo	Further test Cu-Mo mineralisation associated with Anabama Granite	79 m near vertical diamond drill-hole; target high grade ore body not located. Best intersections: 24 m @ 0.06% Mo, 27 m @ 0.19% Cu and 29 m @ 3 g/t Ag
BHP Minerals Ltd	Scott Hill, central-eastern Flinders Ranges	1982–1983	EL00971	ENV 4716	Umberatana Group, Burra Group	Olympic-Dam style mineralisation	Coincident magnetic and gravity anomaly	Rock chip sampling, mapping, ground magnetic and gravity surveys revealed insignificant mineralisation

Operator	Location	Year(s)	Tenement	Reference	Stratigraphy	Target	Feature/Anomaly	Follow Up & Result
Western Mining Co. Pty Ltd; North Broken Hill Ltd; Norgold Ltd	Moonta-Wallaroo	1982–1987	EL01394	ENV 07001	Moonta Porphyry member, Doora Member, Wandearah Formation, Tickera Granite	Porphyry Cu-Mo	Alteration and mineralisation likened to porphyry Cu settings.	Typical grades 0.15% Cu and 0.07% Mo, not economically significant.
Minotaur Gold NL; Inca Resources Pty Ltd; Gawler Gold and Mineral Exploration NL; Minex Australia Pty Ltd	Bibliando Hill, eastern central Flinders Ranges	1996–2001	EL02229	ENV 09292	Wilyerpa Formation, Skillogalee Dolomite, Holowilena Ironstone	Olympic Dam-style Cu-Au and porphyry Cu mineralisation		
Peter S. and Gillian F. Forwood Pty Ltd	Wallaroo Bay, eastern Spencer Gulf	2002–2004	EL02963	ENV 09949	Tickera Granite , Wandearah Formation, Doora Member	Porphyry Cu-Au and Prominent Hill-style Cu-Au	North Wallaroo-Alford magnetic zone	No further work undertaken
Adelaide Exploration Ltd; Phelps Dodge Australasia Inc.; Red Metal Ltd	Wallaroo, northern Yorke Peninsula	2005	EL02885	ENV 11028		IOCG	Large gravity low anomaly within Alford structural corridor coincident with elevated Cu-Au soil geochemistry	Drilling intersected weakly copper mineralised basement characteristic of lithocap environment. Sub-economic copper mineralisation observed.
Giralia Resources Ltd; Pacific Magnesium Corp. Ltd	Anabama Hill, Blue Rose, Adelaide Geosyncline	2006	EL02938	ENV 11140	Anabama Granite	Porphyry Cu-Au	Remodelled and re-interpreted geological and geophysical signatures	
Giralia Resources Ltd	Netley Hill, Adelaide Geosyncline	2008	EL03848	ENV 11576	Anabama Granite	Porphyry Cu-Mo	Remodelled and re-interpreted geological and geophysical signatures	IP anomaly directly below Cu-Mo mineralisation was tested by 4 drill holes. Best intersection: 40 m @ 0.05% Mo and 1 g/t Ag from 11 m depth, including 7 m @ 0.07% Mo from 11 m depth, and 6 m @ 0.06% Mo from 22 m depth. Additional drill holes to define extent of Mo mineralisation.



Figure 18. Examples of alteration and mineralisation styles at the Netley Hill Prospect, photo source PacMag in Clifford (2008).

a) intense K-feldspar alteration in microveinlet (drill hole NTDD001 255.80 m); **b)** Near pervasive phyllic alteration (quartz-sericite-pyrite) overprinting earlier K-feldspar alteration (drill hole NTDD01 159.5 m); **c)** Quartz sericite zones overprinting K-feldspar rich zones forming the stockwork alteration (drill hole NTD001 106 m); **d)** quartz-magnetite vein at the centre of a discrete (10 cm wide) sericite alteration selvage; **e)** chalcopyrite-quartz vein at centre of K-feldspar alteration (drill hole NTD003 86 m); and **f)** disseminated bornite within sericite alteration zone. Scale: width of core = 5 cm diameter. (Photos 413613–413616, 407427 and 407428)

Exploration for porphyry-style mineralisation in the Curnamona Province began in the mid 90s when BHP Minerals identified anomalous magnetic features in the Benagerie Ridge region, interpreted to represent pyrrhotite or magnetite-rich mineralised systems, highlighting the potential for Cu-Au mineralisation (Cameron 1998).

Subsequent drilling identified anomalous gold (7 m averaging 0.15 g/t) and anomalous silver (40.4 m averaging 2.5 g/t) in one drill hole, highlighting the potential for porphyry-related mineralisation, endo-skarn type mineralisation, or Olympic Dam-type IOCG mineralisation in this region (Cameron 1998). Traces of pyrite-chalcopyrite-molybdenum-bornite mineralisation, akin to porphyry-style mineralisation, was observed within buried magnetic diorites in the Lake Charles area of the Benagerie Ridge (Cameron 1998). These diorites are interpreted to be 1590 Ma and

belong to the Lake Charles Diorite, Ninnerie Supersuite (Wade 2011), and represent medium- to fine-grained, quartz-biotite-hornblende bearing, diorite to granodiorite, locally affected by carbonate, chlorite and sericite alteration. Observed textures in some granodiorites suggest they were emplaced at shallow depths (Dugmore 1997). On magnetic imagery the Lake Charles Diorite is interpreted as several intrusive bodies which appear to be relatively undeformed, suggesting they were intruded late- to post-Olarian Orogeny (1620–1590 Ma).

Significant disseminated and vein-related mineralisation was found in propylitically-altered, medium-grained diorites which may be affiliated with porphyry Cu-Mo-Au mineralisation, skarn-related Cu-Au mineralisation or an Olympic Dam-style hydrothermal system (Cameron 1998). Hydrothermal alteration and brecciation is similar to that observed in calc-alkaline to alkaline porphyry Cu-Mo-Au systems, particularly overprinting of seritic and propylitic alteration on early potassium alteration (Cameron 1998). Despite these encouraging results, subsequent ground EM and gravity surveys did not reveal any drill targets (Cameron 1998).

Active exploration for epithermal silver, porphyry Cu and IOCG mineralisation is presently occurring on northern Eyre Peninsula and Yorke Peninsula by mineral exploration companies that include Investigator Resources, Trafford Resources, Menninnie Metals Pty Ltd and Tasman Resources.

In 2006, Tasman Resources NL made the discovery of epithermal-style Au-Ag mineralisation at their Parkinson Dam project near the southern margin of the Gawler Range Volcanics (Solomon 2006). Subsequent *PACE* funded drilling intersected anomalous gold and silver mineralisation, including 3 m at 80 g/t Ag and 3.4 g/t Au, within epithermal quartz veins (Tasman Resources NL 2006).

In 2011 Investigator Resources made the discovery of the Paris silver deposit and have since identified several other epithermal Ag/Au targets including Alexander, Hector and Morgans South. The targets occur in the NW-SE trending “Moonta Corridor” and are controlled by NW and NE trending structures. The corridor deepens to the south-east on Yorke Peninsula. The opportunity for a spectrum of deposit styles along this corridor, albeit covered by younger geology, makes the northern Eyre Peninsula and Yorke Peninsula a prospective area for IOCG deposit styles, epithermal Ag-Au adjacent to the Gawler Range Volcanics, porphyry Cu-Au, Cu-Fe skarns and carbonate replacement deposit styles.

Trafford Resources recently announced discovery of high-grade skarn-related Sn-W-Ag mineralisation at Wilcherry Hill which included 1 m @ 7.2% W with associated 41 m @ 56.2 g/t Ag at Golden Gate Prospect and 28 m @ 45.6 g/t Ag at the Ultima Dam West Prospect (Finch 2013).

STRATEGY FOR PORPHYRY Cu DEPOSITS IN SOUTH AUSTRALIA

In Table 11 a summary is provided of the key features (e.g. known deposits, geophysical anomalies, geochemical anomalies, alteration zones, breccias and veins and mineralising structures) and corresponding methods (e.g. literature review, prospecting, geochemical surveys, geophysical surveys, mapping and drilling) that can be used at different scales for porphyry Cu-(Au-Mo) exploration, ranging from regional to deposit scale objectives. Knowledge at every scale is essential for understanding the mineralising system which will help define future targets and further exploration.

Three main areas for exploration for porphyry Cu \pm Mo \pm Au, skarn Cu \pm Au, or high-sulphidation epithermal Au deposits, summarised from Sillitoe (2010b), include exploring in:

1. mature, well-endowed Cu or Au belts; a wise and successful exploration technique, e.g. El Indio-Maricunga belt in northern Chile;

2. emerging belts with less obvious metallogenetic credentials but having at least one important type of deposit that is sought; a less successful technique in areas that lack economically significant discoveries in the vicinity of isolated deposits; however, this greenfields exploration is still poorly defined in potential areas, i.e. magmatic arcs, or;
3. frontier terranes with geologic criteria that are considered to be perspective; high-risk exploration technique but has resulted in recent discoveries, e.g. Pebble, Oyu Tolgoi and Reko Diq.

Exploration programs for porphyry Cu \pm Mo \pm Au, skarn Cu \pm Au, or high-sulphidation epithermal Au deposits should understand the empirical relationship between magmatic arcs with known high-grade porphyry Cu and HS epithermal Au mineralisation and contractional tectonic settings. Such tectonic settings characterised by high surface uplift and denudation rates; evidence for shallow erosion, indicated by the preservation of lithocaps, particularly in arc segments where only minor volcanic rock volumes are contemporaneous with the development of porphyry Cu systems and; belts or districts where porphyry Cu stocks or dykes are overprinted on precursor plutons or where sedimentary rocks only slightly older than the porphyry Cu systems have been uplifted to \sim 1 km or more above sea level, may all prove useful for underexplored arc segments (Sillitoe 2010b).

Another highly effective exploration concept has focussed on the clustering or alignment of both porphyry Cu and high-sulphidation Au deposits, e.g. the recent porphyry Cu-Mo \pm Au discoveries in Collahuasi (Rosario Oeste), Chuquicamata (Toki cluster, Rivera and Pardo), Escondida (Pampa Escondida) and Los Bronces-Rio Blanco (Los Sulfatos) districts of Chile (Sillitoe 2010b). These recent discoveries are all within <1 to 3 km of the previously known deposit.

Determining erosion level will play a key role in type of mineralisation explored for; shallow parts of the lithocap may have the best potential for the discovery of high-sulphidation Au deposits, while deeply eroded lithocaps where quartz-pyrophyllite \pm muscovite \pm andalusite alteration is prominent is best for concealed porphyry Cu deposits beneath advanced argillic alteration (Sillitoe 2010b).

Table 12 summarises geological units in South Australia which fit several or more of the regional criteria listed above, as potential areas for possible porphyry system formation (Fig. 19). As previously mentioned, direct evidence for the formation of porphyry deposits may be masked by geological processes, including plate subduction, within a few million years of formation (Cooke et al. 2005). Therefore given the protracted geological history of South Australia, identifying conducive tectonic settings for porphyry formation (i.e. magmatic arcs) is challenging. Many of the older rocks in South Australia (Archaean to Mesoproterozoic) have been reworked and evidence of tectonic settings are inferred often by geochemical signatures, e.g. Devil's Playground Volcanics display a geochemical signature consistent with a back-arc geological setting (Swain et al. 2005).

Nonetheless igneous units which have been interpreted as forming in either convergent margin, syn, late, or post-orogenic or extensional tectonic settings with calc-alkaline affinities are listed in Table 12 and shown on Figure 19 and include:

- Cooyerdoo Granite: continental-arc setting at 3250–3150 Ma, (Fraser et al. 2010)
- Devil's Playground Volcanics: convergent margin environment, back-arc or arc-type setting at 2560 Ma (Swain et al. 2005)
- Aristarchus Prospect mafic and granitic rocks: syn-orogenic setting at 2480–2430 Ma, (Reid pers. comm., Wade 2012)
- Donington Suite: continental back-arc setting at 1850 Ma (Schaefer 1998)
- Poodla Granodiorite: extension or island-arc magmatism at 1720 Ma
- Tunkillia Suite: late- to post-orogenic setting at 1680 Ma (Payne et al. 2010)
- Tarcoola Formation: extension at 1650 Ma (Daly 1993)
- St Peter Suite: magmatic/volcanic-arc setting at 1620–1608 Ma (Swain et al. 2008)
- Hiltaba Suite, Gawler Range Volcanics and Ninnerie Supersuite: continental back-arc and syn-, late- to post-orogenic setting at 1590–1580 Ma (Blissett et al. 1993, Conor et al. 2006, Hand et al. 2008, Wade et al. 2012)

Table 11. Examples of methods used to detect specific features related to porphyry Cu deposits and their level of importance in exploration at various scales.

Scale objective	Look for	Methods	Target	Importance
<i>Regional</i>	Known deposits	Literature review	Exploration history, regional geological history	High
		Prospecting	Examine rock outcrops, exposure of mineral veins, hydrothermal alteration	High
	Alteration zones	Literature review	Exploration history, regional geological history	High
		Prospecting	Identify hydrothermal alteration in host rocks	High
		Satellite and aerial photograph studies	Airborne SWIR, ASTER	High
	Geochemical anomalies	Literature review	Exploration history, regional geological history, historical geochemical data	High
		Prospecting	Anomalous Au, As, Pb, Zn, Sb, Hg in host rocks	High
		Regional-scale surveys	Determine background values for each pathfinder	High
<i>District</i>	Known deposits	Literature review	Exploration history, district-scale geological history	High
		Prospecting	Examine rock outcrops, exposure of mineral veins, hydrothermal alteration	High
		Aerial photograph studies	Outcrop areas, sub-crop areas, no outcrop, alteration zones	High
	Alteration zones	Prospecting		High
		Ground surveys	Map hydrothermal mineral distribution	High
		Satellite and aerial photograph studies	Outcrop areas, sub-crop areas, no outcrop, identify alteration zones	High
	Geochemical anomalies	Stream and soil geochemical surveys	400m by 400m reconnaissance geochemical sample pattern	High
	Geophysical anomalies	Large-scale magnetic surveys	Major structures, structural intersections, oblique structures, deep intrusives	Low
		Large-scale gravity surveys	Major structures, structural intersections, oblique structures, deep intrusives, identify altered vs. unaltered host rocks, identify alteration zones in host rocks	High
		Large-scale EM surveys	Fault zones (low resistivity), igneous host rocks (highly resistive), quartz distribution (highly resistive), clays (conductive) and quartz (resistive) distribution in alteration zones	Moderate
		Spectral Mapping and remote sensing	Map hydrothermal minerals in sericitic, intermediate and advanced argillic and propylitic alteration; iron oxides and hydroxides; silica	High
<i>Prospect</i>	Veins, mineralised structures	Mapping	Map vein density as a vector towards mineralisation, map vein orientations, map vein generations and overprinting relationships, map mineralised structural orientations, generations and overprinting relationships	High
	Breccias	Mapping	Identify and describe breccias associated with hydrothermal system, use breccias to vector towards mineralisation, relative timing of mineralising events, brecciation and alteration	
	Alteration zones	Mapping	Map hydrothermal mineral distribution, map alteration types in host rocks and surrounding rocks, increasing biotite alteration towards core, quartz-sericite-pyrite and chlorite-epidote-actinolite in distal zones	High

Scale objective	Look for	Methods	Target	Importance
	Geochemical anomalies	Detailed soil and rock chip surveys	Anomalous distal Au-As (distal), Pb-Zn (halo), Sb-As-Hg (proximal to distal), Mn, Pb, An, As, Cs, Sb, Tl, Mo, Li increase outward to the margin of K silicate alteration, then outward at background values; Na-Ca alteration depletes rocks in Fe, K and trace elements, and enriches Sr, Ca, Na	High
	Geophysical anomalies	IP or resistivity surveys	Sulphide distribution in sericite alteration zone (conductive)	Moderate
		Radiometrics Spectral Mapping and remote sensing	Enhanced K content related to potassic alteration Map hydrothermal minerals in sericitic, intermediate and advanced argillic and propylitic alteration; iron oxides and hydroxides; and silica	Moderate High
Scale objective	Look for	Methods	Target	Importance
Deposit	Veins, mineralised structures	Mapping	Increasing Cu-Fe sulphides towards core; increasing vein abundance towards mineralisation	Very high
		Drill logging	Increasing Cu-Fe sulphides towards core; increasing vein abundance towards mineralisation	Very high
	Breccias	Mapping	Map relationship of breccias with other breccias, mineralised veins and structures, determine relative timing of mineralising events, brecciation and alteration. Intensity of brecciation, composition and texture can be used as vectors towards mineralisation	Very high
		Drill logging	Identify and describe breccias associated with hydrothermal system, relative timing of mineralising events, brecciation and alteration	Very high
	Alteration zones	Mapping	Increasing k-feldspar and biotite alteration towards core, increasing quartz-sericite-pyrite alteration and chlorite-epidote-actinolite alteration in annulus	Very high
		Drill logging	Chlorite-epidote-actinolite alteration in annulus, quartz-sericite-pyrite alteration distally, increasing K-feldspar biotite alteration towards core	Very high
	Geochemical anomalies	Detailed geochemistry of drill samples or outcrop	Increase in Cu and Au with depth until K-silicate zone then remain constant to base of system; Cu:Fe:S:As: Au ratios for sulphide mineralogy and distribution; depletion in Mn, Pb, Zn, As, Cs, Sb, Tl and Li in core; Vertical distribution of elements from porphyry Cu mineralisation to surface: Mo >5 ppm, Sn >5 ppm, Bi, Te > 1 ppm, As > 50 ppm, Sb >5 ppm, Tl >2 ppm	Very high
	Geophysical anomalies	Resistivity	Sulphide distribution in sericite alteration zone (conductive)	High
		Radiometrics	Enhanced K content related to potassic alteration in core	High
		Ground and airborne magnetics	Increasing magnetite in potassic core	High
		Magnetic susceptibility measurements	Differentiate hydrothermal alteration zones due to magnetite destruction, identify magnetite-rich zones where potassic alteration is preserved near surface	High
		Gravity	Increased density due to volume of fractures and dissolution vs. decreased density due to hydrothermal silicification	High
		IP	Sulphide distribution (conductive) increasing towards core	Very high
		Ground EM	Increased conductivity in upper parts and above deposit, increased resistivity in marginal parts and below lithocap corresponding to propylitic zone	Very high
		Spectral Mapping and remote sensing	Map hydrothermal minerals in sericitic, intermediate and advanced argillic and propylitic alteration; iron oxides and hydroxides; silica	Very high

- felsic gneisses of the Musgrave Province: volcanic-arc at 1590–1555 Ma (Wade et al. 2006)
- Anabama Granite: syn-orogenic setting at 450 Ma (Farrand and Preiss 1995).

As previously stated, extensional environments are less favourable for formation of porphyry deposits (Tosdal and Richards 2001) therefore the Tarcoola Formation and Poodla Granodiorite may be unlikely candidates for hosting or contributing to porphyry deposit formation. However, the Poodla Granodiorite has undergone intensive Na-K alteration and the contact zone of the granodiorite body is occupied by hydrothermal breccia (Payne 2003). The main body is crosscut by breccia bodies which are locally mineralised with pyrite-chalcopyrite (Conor et al. 2006) but may be part of IOCG-related mineralisation.

Of the remaining units, those which are found in areas that display evidence for porphyry-style mineralisation and alteration include parts of the GRV-Hiltaba Suite and Ninnerie Supersuite, e.g. southern margin of the GRV and southern margin of the Benagerie Ridge, Curnamona Province, and the 450 Ma Anabama Granite in the Adelaide Geosyncline.

Table 12. Summary of tectonic setting, magma composition, lithology and structural controls of various igneous units in South Australia to assess potential settings for porphyry Cu deposit formation.

	Age (Ma)	Tectonic setting	Magma composition	Lithology	Corresponding geological unit	Proximal structures
1	3250–3150	Continental arc	Calc-alkaline	Gneissic granite to granodiorite	Cooyerdoo Granite	N-S trending faults intersected by NE-SW faults
2	2560	Back-arc	Calc-alkaline I- to S- type	Andesites to basalts	Devil's Playground Volcanics	Neoproterozoic to mid-Mesoproterozoic NE/SW and NW-SE faults
3	2480–2430	Syn-orogenic	Calc-alkaline I type	Granite, norite, pyroxenite, gabbro	Aristarchus Prospect	NE-SW trending faults proximal to deposit; NW-SE trending faults 15 km to NE of the prospect; 15 km S of prospect intersecting faults
4	1850	Back-arc	Calc-alkaline I- type	Gabbro, gabbro-norite, charnockite, granodiorite, granite	Donington Suite	Kalinjala shear zone, NS to NE-SW
5	1720	Extension	Calc-alkaline I-type	Granodiorite, monzogranite	Poodla Granodiorite	NE-SW and EW trending faults that intersect to the north and the south of the Poodla Granodiorite body
6	1680	Late- to post orogenic	Alkaline to calc-alkaline I- type	Syenite, monzogranite, granodiorite and syenogranite	Tunkillia Suite	In the east, a strong structural control is apparent of N-S to E-W faults. To the northwest, NE-SW faults and shear zones
7	1650	Extension	Calc-alkaline I- to S-type	Basaltic to andesitic dykes/sills and dacitic tuffs	Tarcoola Formation	NW-SE and NE-SW trending faults at main Tarcoola Formation body, without intersections
8	1620	Volcanic arc	Calc-alkaline I-type	Granite, granodiorite, diorite, monzonite, monzodiorite, gabbro	St Peter Suite	N-S and N-E faults and fault intersections
9	1590	Continental back-arc	Calc-alkaline I- to S-type	Granite, granodiorite	Hiltaba Suite	NW-SE, EW and NE-SW faults and intersections between faults on southern margin of GRV
10	1590–1570	Late, syn- and post-orogenic, within plate	Calc-alkaline I- to S-type	Granite, granodiorite	Hiltaba Suite	NW-SE, EW and NE-SW faults and intersections between faults on southern margin of GRV
11	1590	Continental back-arc or Late, syn- and post-orogenic, within plate	Calc-alkaline I-type	Diorite, granodiorite	Lake Charles Diorite	Interpreted E-W to NE-SW trending faults with NW-SE intersecting faults
12	1590	Late, syn- and post-orogenic	Alkaline I-type	Syenite, ijolite, lamprophyre	Billeroo Intrusive Complex	NE-SW and EW trending faults intersect to the south of the complex

	Age (Ma)	Tectonic setting	Magma composition	Lithology	Corresponding geological unit	Proximal structures
13	1590–1555	Volcanic arc	Calc-alkaline I-type	Felsic gneiss	Unnamed, Musgrave Province	NW-SE, EW and NE-SW faults and intersections between faults
14	1580	Late, syn- and post-orogenic, within plate	I-type and S-type		Ninnerie Supersuite, Hiltaba Suite	NW-SE, EW and NE-SW faults and intersections between faults on southern margin of GRV and E-W to NE-SW trending faults with NW-SE intersecting faults in the Benagerie Ridge
15	480	?	Calc-alkaline	Diorite and basalt	€4/01	?
16	450	Syn-tectonic	S-type to I-type	Granite to granodiorite	Anabama Granite	Anabama Lineament, ENE-WSW

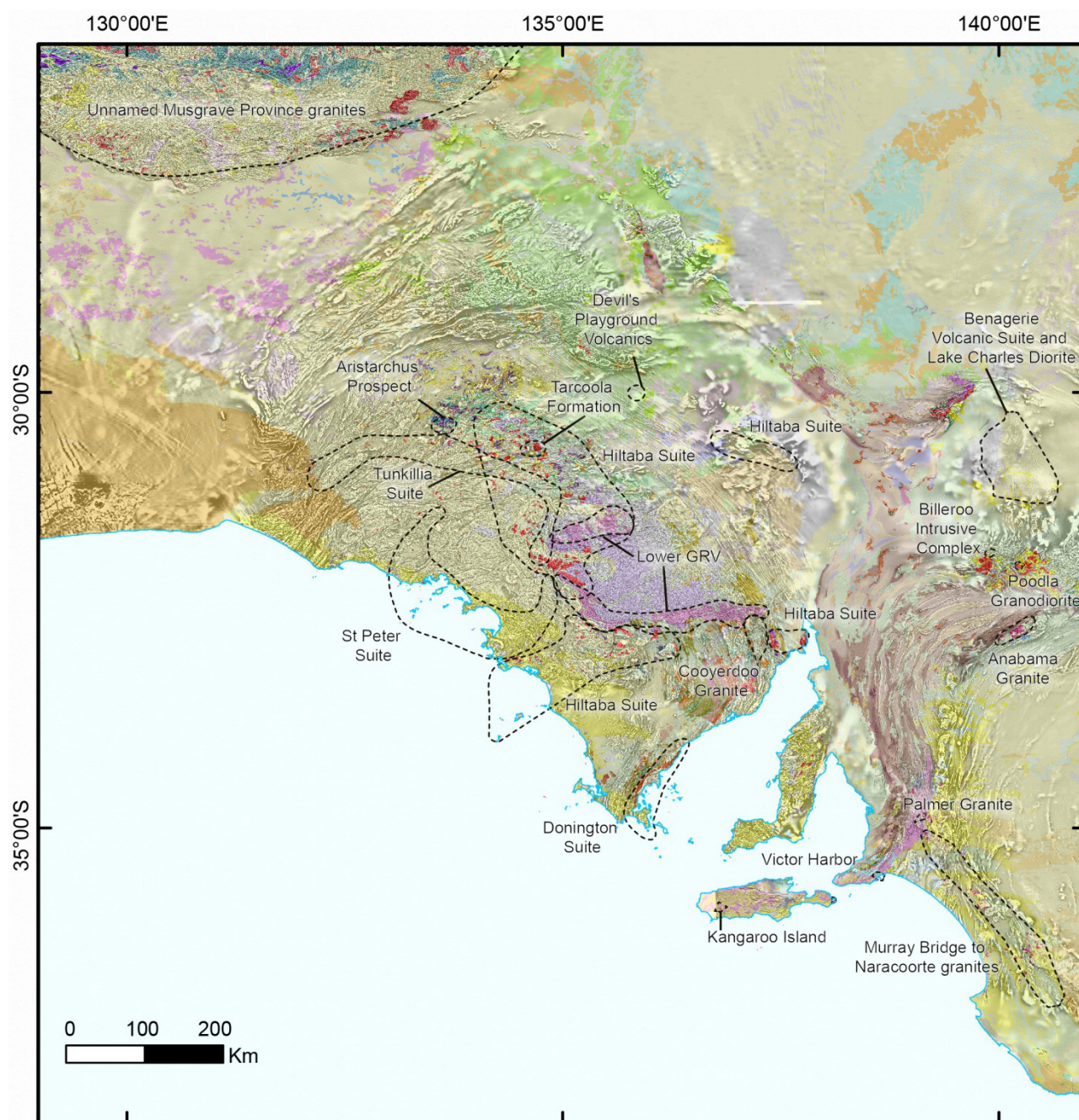


Figure 19. Location of various igneous units in South Australia which may be potential units that host porphyry Cu deposits, listed in Table 12.

ACKNOWLEDGEMENTS

Many aspects of this report were made possible by the author participating in a fieldtrip to Chile and Peru, South America, in March 2013 as part of the Master of Economic Geology degree run by ARC Centre of Excellence in Ore Deposits (CODES) at the University of Tasmania. Detailed course notes, group assignments and mine site presentations were provided to the participants, including the author, which have been incorporated, to some extent, into this report. Additional resources were provided from the attendance of short courses *A practical guide to porphyry Cu (-Mo-Au) deposits* presented by Richard Tosdal and Scott Halley in Perth, September 2012 and *Epithermal and Porphyry Ore Deposits: Field aspects for exploration geologists* presented by Greg Corbett in Adelaide, October 2013.

Bernd Michaelsen (GSSA) and Paul Magarey (DEWNR) are thanked for their thorough reviews and comments which have improved the content of this report. John Keeling and Wayne Cowley (GSSA) are also thanked for useful input.

REFERENCES

- Allis, R. G., (1990). Geophysical Anomalies over Epithermal Systems. *Journal of Geochemical Exploration* 36(1–3):339–374.
- Arribas, A., Hedenquist, J. W., Itaya, T., Okada, T., Concepción, R. A. and Garcia, J. S., (1995). Contemporaneous Formation of Adjacent Porphyry and Epithermal Cu-Au Deposits over 300 Ka in Northern Luzon, Philippines. *Geology* 23(4):337–340.
- Ashley, R. P., (1974). *Goldfield Mining District*. Nevada Bureau of Mines and Geology Report 19:49–66.
- Bailly, L., Stein, G. and Genna, A. (2002). Preliminary Microthermometric Measurements in Quartz, Sphallerite and Enargite from the Bor and Majdanpek Deposits, Serbia. *Geology and Metallogeny of Copper and Gold Deposits in the Bor Metallogenic Zone-Bor 100 Years International Symposium, Bor Lake, Yugoslavia, 2002*. Proceedings, p. 71–75.
- Bartlett, M. W., Enders, M. S., Volberding, J. E. and Wilkinson, W. H. (1995). The Geology of the McDonald Gold Deposit, Lewis and Clark County, Montana. In *Geology and Ore Deposits of the American Cordillera, Symposium*, p. 12.
- Behn, G., Camus, F. and Carrasco, P., (2001). Aeromagnetic Signature of Porphyry Copper Systems in Northern Chile and Its Geologic Implications. *Economic Geology* 96:239–248.
- Bissig, T., Clark, A. H., Lee, J. K. W. and Hodgson, C. J., (2002). Miocene Landscape Evolution and Geomorphologic Controls on Epithermal Processes in the El Indio-Pascua Au-Ag-Cu Belt, Chile and Argentina. *Economic Geology* 97:971–996.
- Bissig, T., Ullrich, T. D., Tosdal, R. M., Friedman, R. and Ebert, S., (2008). The Time-Space Distribution of Eocene to Miocene Magmatism in the Central Peruvian Polymetallic Province and Its Metallogenetic Implications. *Journal of South American Earth Sciences* 26(1):16–35.
- Blissett, A. H., Creaser, R. A., Daly, S., Flint, D. J. and Parker, A. J., (1993). Gawler Range Volcanics. In JF Drexel, WV Preiss and AJ Parker eds, *The geology of South Australia, Volume 1, The Precambrian*, Bulletin 54. Geological Survey of South Australia, Adelaide, pp. 107–131.
- Bonev, I. K., Kerestedijan, T., Atanassova, R. and Andrew, C. J., (2002). Morphogenesis and Composition of Native Gold in the Chelopech Volcanic-Hosted Au-Cu Epithermal Deposit, Srednogie Zone, Bulgaria. *Mineralium Deposita* 37:614–629.
- Bouse, R. M., Ruiz, J., Titley, S. R., Tosdal, R. M. and Wooden, J. L., (1999). Lead Isotope Compositions of Late Cretaceous and Early Tertiary Igneous Rocks and Sulfide Minerals in Arizona: Implications for the Sources of Plutons and Metals in Porphyry Copper Deposits. *Economic Geology* 94:211–244.
- Brathwaite, R. L. and Blattner, P., (1995). The Waihi Epithermal Gold-Silver-Quartz Vein System, New Zealand: A High-Throughput Geothermal System of Late Miocene Age. In Mauk JL and D, SGJ ed. *Proceedings of the 1995 PACRIM Congress, Melbourne*. Australasian Institute of Mining and Metallurgy, 75–80.
- Brimhall, G. H., Jr., (1977). Early Fracture-Controlled Disseminated Mineralization at Butte, Montana. *Economic Geology* 72:37–59.
- Bushnell, S. E., (1988). Mineralization at Cananea, Sonora, Mexico, and the Paragenesis and Zoning of Breccia Pipes in Quartzofeldspathic Rock. *Economic Geology* 83:1760–1781.
- Caira, N. M., Findlay, A., Delong, C. and Rebagliati, C. M., (1995). *Fish Lake Porphyry Copper-Gold Deposit, Central British Columbia*. Canadian Institute of Mining and Metallurgy Special Volume 46:327–342.
- Cameron, J., (1998). EL 1860 Lake Charles Area: Annual and Progress Reports for the Period 20/10/93 to 30/8/98 Submitted by Lynch Mining Pty Ltd and BHP Minerals Pty Ltd. Open File Envelope 8870 (unpublished). Department for Manufacturing, Innovation, Trade, Resources and Energy, South Australia, Adelaide. pp. 1–327.
- Camus, F., (2002). *The Andean Porphyry Systems*. University of Tasmania, Centre for Ore Deposit Research, Special Publication 4:5–22.
- Camus, F., (2005). The Andean Porphyry Systems. In TM Porter Ed. *Super Porphyry Copper and Gold Deposits: A Global Perspective*. PGC Publishing 1:45–63.
- Chang, Z., Hedenquist, J. W., White, N. C., Cooke, D. R., Roach, M., Deyell, C. L., Garcia, J., Gemmell, J. B., Mcknight, S. and Cuison, A. L., (2011). Exploration Tools for Linked Porphyry and Epithermal

- Deposits: Example from the Mankayan Intrusion-Centered Cu-Au District, Luzon, Philippines. *Economic Geology* 106(8):1365–1398.
- Clark, A. H., Farrar, E. and Kents, P., (1977). Potassium-Argon Age of the Cerro Colorado Porphyry Copper Deposit, Panama. *Economic Geology* 72:1154–1158.
- Clark, A. H., Tosdal, R. M., Farrar, E. and Plazolles, A. V., (1990). Geomorphological Environment and Age of Supergene Enrichment of the Cuajone, Quellaveco, and Toquepala Porphyry Copper Deposits, Southeastern Peru. *Economic Geology* 85:1604–1628.
- Clifford, M., (2006). EL 2938 Wadnaminga Pace Initiative: Theme 2, Year 3 Drilling Partnership – Blue Rose Mineral Prospect Target 1 (Porphyry-Style Cu-Au-Mo) Project Final Report. Pacific Magnesium Corp. Ltd. Open File Envelope 11140. Department for Manufacturing, Innovation, Trade, Resources and Energy, South Australia, Adelaide. p. 116
- Clifford, M., (2008). EL 3848 Wadnaminga Pace Initiative: Theme 2, Year 5 Drilling Partnership – Netley Hill Porphyry-Style Cu-Mo Mineral Prospect Project Final Report. PacMag Metals Ltd, Open File Envelope 11576. Department for Manufacturing, Innovation, Trade, Resources and Energy, South Australia, Adelaide. p. 127.
- Cohen, J. (2011). Mineralogy and Geochemistry of Hydrothermal Alteration at the Ann-Mason Porphyry Copper Deposit, Nevada: Comparison of Large-Scale. Masters Thesis, unpublished, Oregon State University. p. 599.
- Conor, C. H. H., Ashley, P. M., Bierlein, F. B., Cook, N. D. J., Crooks, A. F., Lawie, D. C., Plimer, I. R., Preiss, W. V., Robertson, R. S. and Skirrow, R. G., (2006). *Geology of the Olary Domain, Curnamona Province, South Australia*. Report Book, 2006/00013. Department of Primary Industries and Resources South Australia, Adelaide. p. 1–95.
- Cooke, D. R., (2013). Ore Deposits of South America: Short Course Manual. CODES, ARC Centre of Excellence on Ore Deposits, University of Tasmania, March 2013. p. 300.
- Cooke, D. R. and Bloom, M. S., (1990). Epithermal and Sub-Jacent Porphyry Mineralisation, Acupan, Baguio District, Philippines: A Fluid-Inclusion and Paragenetic Study. *Journal of Geochemical Exploration* 35:297–340.
- Cooke, D. R., Hollings, P. and Walshe, J. L., (2005). Giant Porphyry Deposits: Characteristics, Distribution, and Tectonic Controls. *Economic Geology* 100(5):801–818.
- Cooke, D. R., Mcphail, D. C. and Bloom, M. S., (1996). Epithermal Gold Mineralization, Acupan, Baguio District, Philippines: Geology, Mineralization, Alteration, and the Thermochemical Environment of Ore Deposition. *Economic Geology* 91:243–272.
- Cooke, D. R. and Simmons, S. F., (2000). Characteristics and Genesis of Epithermal Gold Deposits. *Reviews in Economic Geology* 13:221–244.
- Corbett, G., (2009). Anatomy of Porphyry-Related Au-Cu-Ag-Mo Mineralised Systems: Some Exploration Implications. In (Ed), *Australian Institute of Geoscientists North Queensland Exploration Conference June 2009, North Queensland*. Australian Institute of Geoscientists, 13 p.
- Cornejo, P., Tosdal, R. M., Mpodozis, C., Tomlinson, A. J., Rivera, O. and Fanning, C. M., (1997). El Salvador, Chile Porphyry Copper Deposit Revisited: Geologic and Geochronologic Framework. *International Geology Review* 39(1):22–54.
- Cuadra, P. and Camus, F., (1998). The Radomiro Tomic Porphyry Copper Deposit, Northern Chile. In Porter, T. M. (Ed), *Porphyry and hydrothermal copper and gold deposits: A global perspective*. Perth, 1998, Conference Proceedings, Glenside, South Australia, Australian Mineral Foundation, pp. 99–109.
- Daly, S. J., (1993). Tarcoola Formation. In JF Drexel, WV Preiss and AJ Parker eds, *The geology of South Australia, Volume 1, The Precambrian*, Bulletin 54. Geological Survey of South Australia, Adelaide, pp. 68–69.
- Depaolo, D. J., (1981). Trace Element and Isotopic Effects of Combined Wallrock Assimilation and Fractional Crystallization. *Earth and Planetary Science Letters* 53(2):189–202.
- Dilles, J. H., (1987). Petrology of the Yerington Batholith, Nevada; Evidence for Evolution of Porphyry Copper Ore Fluids. *Economic Geology* 82(7):1750–1789.
- Djouka-Fonkwé, M. L., Kyser, K., Clark, A. H., Urqueta, E., Oates, C. J. and Ihlenfeld, C., (2012). Recognizing Propylitic Alteration Associated with Porphyry Cu-Mo Deposits in Lower Greenschist Facies Metamorphic Terrain of the Collahuasi District, Northern Chile-Implications of Petrographic and Carbon Isotope Relationships. *Economic Geology* 107:1457–1478.

- Dugmore, M., (1997). El 1860 "Lake Charles" South Australia: Annual Report for the Period Ended 29 August 1996: Appendix 5 Petrology *In*: Teale, G. S. (Ed), El 1860 Lake Charles Area Annual and Progress Reports for the Period 10/10/93 to 30/8/98. Lynch Mining Pty Ltd and BHP Minerals Pty Ltd, Open File Envelope 8870 (unpublished). Department for Manufacturing, Innovation, Trade, Resources and Energy, South Australia, Adelaide. pp. 259–264.
- Einaudi, M. T. and Burt, D. M., (1982). Introduction; Terminology, Classification, and Composition of Skarn Deposits. *Economic Geology* 77(4):745–754.
- Einaudi, M. T., Hedenquist, J. W. and Inan, E. E., (2003). *Sulfidation State of Fluids in Active and Extinct Hydrothermal Systems: Transitions from Porphyry to Epithermal Environments*. Society of Economic Geologists Special Publication 10:285–313.
- Farrand, M. G. and Preiss, W. V., (1995). Delamerian Igneous Rocks. In JF Drexel and WV Preiss eds, *The geology of South Australia, Vol. 2, The Phanerozoic*, Bulletin 54. Geological Survey of South Australia, Adelaide. pp. 54–57.
- Finch, I., (2013). *Trafford Plans 2000m Drilling Program Targeting High Grade Tin, Tungsten and Silver Discoveries at Wilcherry Hill*. ASX Announcement. 14 May 2013.
- Fraser, G., McAvaney, S., Neumann, N., Szpunar, M. and Reid, A., (2010). Discovery of Early Mesoarchean Crust in the Eastern Gawler Craton, South Australia. *Precambrian Research* 179:1–21.
- Garcia, J. S., (1991). *Geology and Mineralisation Characteristics of the Mankayan Mineral District, Philippines*. Japan Geological Survey Report 277:21–30.
- Garwin, S., (2002). *The Geological Setting of Intrusion-Related Hydrothermal Systems near the Batu Hijau Porphyry Copper-Gold Deposit, Sumbawa, Indonesia*. Society of Economic Geologists Special Publication 9:333–366.
- Geyne, A. R., Fries, C., Jr., Segerstrom, K., Black, R. F. and Wilson, I. F., (1963). *Geology and Mineral Deposits of the Pachuca-Real del Monte District, State of Hidalgo, Mexico*. Consejo de Recursos Naturales No Renovables Publication 5E:203.
- Gustafson, L. B. and Hunt, J. P., (1975). The Porphyry Copper Deposit at El Salvador, Chile. *Economic Geology* 70(5):857–912.
- Gutscher, M.-A., Maury, R., Eissen, J., -P. and Bourdon, E., (2000). Can Slab Melting Be Caused by Flat Subduction? *Geology* 28:535–538.
- Halter, W. E., Bain, N., Becker, K., Heinrich, C. A., Landtwing, M., Vonquadt, A., Clark, A. H., Sasso, A. M., Bissig, T. and Tosdal, R. M., (2004). From Andesitic Volcanism to the Formation of a Porphyry Cu-Au Mineralizing Magma Chamber: The Farallón Negro Volcanic Complex, Northwestern Argentina. *Journal of Volcanology and Geothermal Research* 136(1–2):1–30.
- Hand, M., Reid, A., Szpunar, M., Direen, N. G., Wade, B., Payne, J. and Barovich, K., (2008). Crustal Architecture During the Early Mesoproterozoic Hiltaba-Related Mineralisation Event: Are the Gawler Range Volcanics a Foreland Basin Fill? *MESA Journal* 51:19–24. Department of Primary Industries and Resources South Australia, Adelaide.
- Harris, L., Livermore, D., Santa Cruz, C. and Diaz, M., (1994). *The Yanacocha Project*. p.Preprint 94–74.
- Harvey, B. A., Myers, S. A. and Klein, T., (1999). Yanacocha Gold District, Northern Peru. *Pacrim '99 Congress*, Bali, Indonesia, 1999, Proceedings. Australasian Institute of Mining and Metallurgy, 445–459.
- Hedenquist, J. W., Arribas, A. and Reynolds, T. J., (1998). Evolution of an Intrusion-Centered Hydrothermal System: Far Southeast-Lepanto Porphyry and Epithermal Cu-Au Deposits, Philippines. *Economic Geology* 93:373–404.
- Hedenquist, J. W., Matsuhisa, Y., Izawa, E., White, N. C., Giggenbach, W. F. and Aoki, M., (1994). Geology, Geochemistry, and Origin of High Sulfidation Cu-Au Mineralization in the Nansatsu District, Japan. *Economic Geology* 89:1–30.
- Holliday, J. R. and Cooke, D. R., (2007). Advances in Geological Models and Exploration Methods for Copper ± Gold Porphyry Deposits. In Milkereit, B. (Ed), *Exploration in the New Millennium*, Proceedings of Exploration 07: Fifth Decennial International Conference on Mineral Exploration, pp. 791–809.
- Hollings, P. and Cooke, D. R., (2005). Regional Geochemistry of Tertiary Igneous Rocks in Central Chile: Implications for the Geodynamic Environment of Giant Porphyry Copper and Epithermal Gold Mineralization. *Economic Geology* 100:887–904.

- Hudson, D. M., (1993). *The Comstock District Nevada. Crustal Evolution of the Great Basin and the Sierra Nevada: Cordilleran/Rocky Mountain Section*, Geo-Logical Society of America Guidebook, Department of Geological Sciences, University of Nevada, Reno, pp. 481–496,
- Irvine, R. J. and Smith, M. J., (1990). Geophysical Exploration for Epithermal Gold Deposits. *Journal of Geochemical Exploration* 36(1–3):375–412.
- Izawa, E., Kurihara, M. and Itaya, T., (1993). K-Ar Ages and the Initial Ar Isotopic Ratio of Adularia-Quartz Veins from the Hishikari Gold Deposit, Japan. In Shikazono, N., Naito, K. and Izawa, E. (Ed), High Grade Epithermal Gold Mineralization-the Hishikari Deposit. *Resource Geology Special Issue* 14:63–69.
- Izawa, E., Urashima, Y., Ibaraki, K., Suzuki, R., Yokoyama, T., Kawasaki, K., Koga, A. and Taguchi, S., (1990). The Hishikari Gold Deposit: High-Grade Epithermal Veins in Quaternary Volcanics of Southern Kyushu, Japan. *Journal of Geochemical Exploration* 36:1–56.
- James, D. and Sacks, I. S., (1999). *Cenozoic Formation of the Central Andes: A Geophysical Perspective*. Society of Economic Geologists Special Publication 7:1–25.
- Jankovic, S. R., Jelenkovic, R. J. and Kozelj, D., (2002). *The Bor Copper and Gold Deposit: Bor, Serbia*. QWERTY, 298.
- Jannas, R. R., Bowers, T. S., Petersen, U. and Beane, R. E., (1999). *High-Sulfidation Deposit Types in the El Indio District, Chile*. Society of Economic Geologists Special Publication 7:219–266.
- John, D. A., Ayuso, R. A., Barton, M. D., Blakely, R. J., Bodnar, R. J., Dilles, J. H., Gray, F., Graybeal, F. T., Mars, J. C., McPhee, D. K., Seal, R. R., Taylor, R. D. and Vikre, P. G., (2010). *Porphyry Copper Deposit Model, Chap. B of Mineral Deposit Models for Resource Assessment*. U.S. Geological Survey Scientific Investigations Report, 2010-5070-B, 169.
- Kay, S. M. and Mpodozis, C., (2002). Magmatism as a Probe to the Neogene Shallowing of the Nazca Plate beneath the Modern Chilean Flat-Slab. *Journal of South American Earth Sciences* 15(1):39–57.
- Kelley, K. D., Eppinger, R. G., Lang, J., Smith, S. M. and Fey, D. L., (2011). *Porphyry Cu Indicator Minerals in Till as an Exploration Tool: Example from the Giant Pebble Porphyry Cu-Au-Mo Deposit, Alaska, USA*. *Geochemistry: Exploration, Environment, Analysis* 11(4):321–334.
- Kerrick, R., Goldfarb, R., Groves, D. and Garwin, S., (2000). The Geodynamics of World-Class Gold Deposits: Characteristics, Space-Time Distributions, and Origins. *Reviews in Economic Geology* 13:501–551.
- Kesler, S. E., (1973). Copper, Molybdenum and Gold Abundances in Porphyry Copper Deposits. *Economic Geology* 68(1):106–112.
- Kesler, S. E., Sutter, J. F., Issigonis, M. J., Jones, L. M. and Walker, R. L., (1977). Evolution of Porphyry Copper Mineralization in an Oceanic Island Arc, Panama. *Economic Geology* 72:1142–1153.
- Kirkham, R. V. and Dunne, K. P. E., (2000). *World Distribution of Porphyry, Porphyry-Associated Skarn, and Bulk-Tonnage Epithermal Deposits and Occurrences*. Geological Survey of Canada Open File 3792a, 26.
- Langton, J. M. and Williams, S. A., (1981). Structural, Petrological and Mineralogical Controls for the Dos Pobres Orebody, Lone Star Mining District, Graham County, Arizona. In: Titley, S. R. (Ed). *Advances in Geology of the Porphyry Copper Deposits-Southwestern North America: Tuscon, Arizona*. pp. 335–352.
- Lowell, J. D. and Guilbert, J. M., (1970). Lateral and Vertical Alteration-Mineralization Zoning in Porphyry Ore Deposits. *Economic Geology* 65(4):373–408.
- Meyer, C., Shea, E. P., Goddard, J. R. and Staff, (1968). *Ore Deposits at Butte, Montana. Ore deposits of the United States, 1933-1967* (Graton-Sales volume). American Institute of Mining, Metallurgical, and Petroleum Engineers 2:1373–1416.
- Middleton, C., Buenavista, A., Rohrlach, B., Gonzales, J., Subang, L. and Moreno, G., (2004). *A Geological Review of the Tampakan Copper-Gold Deposit, Southern Mindanao, Philippines*. Melbourne, Australian Institute of Mining and Metallurgy Publication Series 5/2004:173–187.
- Mines, I., (2004). *The Oyu Tolgoi Copper and Gold Deposits, South Gobi, Mongolia*. University of Tasmania, Centre for Ore Deposit Research Special Publication 5:35–40.
- Moritz, R., Chambefort, I., Jacquat, S., Petrunov, R., Georgieva, S. and Stoykov, S., (2002). Gold-Copper Epithermal Deposits in the Cretaceous Banat-Srednogie Belt, Eastern Europe: Lessons from the High-Sulphidation Chelopech Deposit, Panagyurishte District, Bulgaria. In *GEODE study centre on geodynamics and ore deposit evolution, near Grenoble, France, 2002*. Working Group discussion paper. 3.

- Morris, B. J., (1981). Porphyry Style Copper/Molybdenum Mineralisation at Anabama Hill. *Mineral Resources Review*, South Australia 150:5–24.
- Moyle, A. J., Doyle, B. J., Hoogvliet, B. H. and Ware, A. R., (1990). Ladolam Gold Deposit, Lihir Island. In Hughes, F. E. (Ed), *Geology of the Mineral Deposits of Australia and Papua New Guinea*, V. 2. Australasian Institute of Mining and Metallurgy Monograph 14:1793–1805.
- Mumin, A. H., Btirran Jones, A. K. S., Corriveau, L., Ootes, L. and Camier, J., (2010). The locg-Porphyry-Epithermal Continuum in the Great Bear Magmatic Zone, Northwest Territories, Canada. In Corriveau, L. and Mumin, A. H. (Ed), *Exploring for Iron Oxide Copper-Gold Deposits: Canada and Global Analogues*. Geological Association of Canada, Mineral Deposits Division Short Course Volume, pp. 57–76.
- Muntean, J. L., Kesler, S. E., Russell, N. and Polanco, J., (1990). Evolution of the Monte Negro Acid Sulfate Au-Ag Deposit, Pueblo Viejo, Dominican Republic: Important Factors in Grade Development. *Economic Geology* 85:1738–1758.
- Mutschler, F. E., Ludington, S. and Bookstrom, A. A., (1999). *Giant Porphyryrelated Metal Camps of the World-a Database*. USGS Open-File Report 99-556, 6 p. (<http://geopubs.wr.usgs.gov/open-file/of99-556/>).
- Oviedo, L., Fiister, N., Tschischow, N., Ribba, L., Zuccone, A., Grez, E. and Aguilar, A., (1991). The General Geology of La Coipa Precious Metal Deposit, Atacama, Chile. *Economic Geology* 86:1287–1300.
- Payne, J. (2003). *The Poodla Granite in the Olary Domain, South Australia: Intrusive Relationships, Alteration and Implications for Cu-Au Mineralisation*. Adelaide University, Unpublished Honours Thesis, 70.
- Payne, J. L., Ferris, G., Barovich, K. M. and Hand, M., (2010). Pitfalls of Classifying Ancient Magmatic Suites with Tectonic Discrimination Diagrams: An Example from the Paleoproterozoic Tunkillia Suite, Southern Australia. *Precambrian Research* 177:227–240.
- Perelló, J., Cox, D., Garamjav, D., Sanjdori, S., Diakov, S., Schissel, D., Munkhbat, T. O. and Oyun, G., (2001). Oyu Tolgoi, Mongolia: Siluro-Devonian Porphyry Cu-Au-(Mo) and High-Sulfidation Cu Mineralization with a Cretaceous Chalcocite Blanket. *Economic Geology* 96:1407–1428.
- Porter, M., (1998). An Overview of the World's Porphyry and Other Hydrothermal Copper and Gold Deposits and Their Distribution. In Porter, T. M. (Ed), *Porphyry and hydrothermal copper and gold deposits: A global perspective*, Perth, 1998, Conference Proceedings, Glenside, South Australia, Australian Mineral Foundation, pp. 3–17.
- Pour, A. B. and Hashim, M., (2011). Identification of Hydrothermal Alteration Minerals for Exploring of Porphyry Copper Deposit Using Aster Data, Se Iran. *Journal of Asian Earth Sciences* 42(6):1309–1323.
- Pour, A. B. and Hashim, M., (2012). The Application of Aster Remote Sensing Data to Porphyry Copper and Epithermal Gold Deposits. *Ore Geology Reviews* 44(0):1–9.
- Rainbow, A., Clark, A. H., Kyser, T. K., Gaboury, F. and Hodgson, C. J., (2005). The Pierina Epithermal Au–Ag Deposit, Ancash, Peru: Paragenetic Relationships, Alunite Textures, and Stable-Isotope Geochemistry. *Chemical Geology* 215(1–4):235–252.
- Richards, J. P., (2003). Tectono-Magmatic Precursors for Porphyry Cu-(Mo-Au) Deposit Formation. *Economic Geology* 98(8):1515–1533.
- Richards, J. P., (2011a). High Sr/Y Arc Magmas and Porphyry Cu ± Mo ± Au Deposits: Just Add Water. *Economic Geology* 106(7):1075–1081.
- Richards, J. P., (2011b). Magmatic to Hydrothermal Metal Fluxes in Convergent and Collided Margins. *Ore Geology Reviews* 40(1):1–26.
- Richards, J. P. and Kerrich, R., (1993). The Porgera Gold Mine, Papua New Guinea: Magmatic-Hydrothermal to Epithermal Evolution of an Alkalic Type Precious Metal Deposit. *Economic Geology* 88:1017–1052.
- Russell, N. and Kesler, S. E., (1991). *Geology of the Maar-Diatreme Complex Hosting Precious Metal Mineralization at Pueblo Viejo, Dominican Republic*. Geological Society of America Special Paper 262, pp. 203–215.
- Rutherford, L., Burt, A. C., Barovich, K. and Hand, M., (2003). Alkalic Magmatism in the Olary Domain; Genesis and Implications for Cu/Ag Mineralisation. In Peljo, M. (Ed), *Broken Hill Exploration Initiative: abstracts from the July 2003 conference*. Geoscience Australia. Canberra, Australia. 2003. 2003/13,
- Salas, G. P., (1991). *Cananea Copper Deposit, Sonora*. Geological Society of America, Geology of North America, P-3, pp. 199–200.

- Samani, B., (1998). Distribution, Setting and Metallogenesis of Copper Deposits in Iran. In Porter, T. M. (Ed), *Porphyry and hydrothermal copper and gold deposits: A Global Perspective*, Perth, 1998, Conference Proceedings, Glenside, South Australia, Australian Mineral Foundation, pp. 135–158.
- Sander, M. V. and Einaudi, M. T., (1990). Epithermal Deposition of Gold During Transition from Propylitic to Potassic Alteration at Round Mountain, Nevada. *Economic Geology* 85:285–311.
- Sawkins, F. J., O'neil, J. R. and Thompson, J. M., (1979). Fluid Inclusion and Geochemical Studies of Vein Gold Deposits, Baguio District, Philippines. *Economic Geology* 74(6):1420–1434.
- Schaefer, B. F. (1998). *Insights into Proterozoic Tectonics from the Southern Eyre Peninsula, South Australia*. PhD Thesis, University of Adelaide, p. 131.
- Seedorff, E., Dilles, J. H., Proffett, J., John M., Einaudi, M. T., Zurcher, L., Stavast, W. J. A., Johnson, D. A. and Barton, M. D., (2005). Porphyry Deposits: Characteristics and Origin of Hypogene Features. *Economic Geology* 100:251–298.
- Shikazono, N. and Nagayama, T., (1993). *Origin and Depositional mechanism of the Hishikari Gold-Quartz-Adularia Mineralization*. Resource Geology (Japan), Special Issue 14:47–6.
- Shikazono, N., Naito, K. and Izawa, E., (1993). *Editor's Preface*. Resource Geology (Japan) Special Issue 14:iii-v.
- Siddleley, G. and Araneda, R., (1986). Theel Indio-El Tambo Gold Deposits, Chile. In Macdonald, A. J. (Ed), *Gold '86*: Willowdale, Ontario, Konsult International, pp. 445–456.
- Sillitoe, R. H., (1972). A Plate Tectonic Model for the Origin of Porphyry Copper Deposits. *Economic Geology* 67(2):184–197.
- Sillitoe, R. H., (1994). Erosion and Collapse of Volcanoes: Causes of Telescoping in Intrusion-Centered Ore Deposits. *Geology* 22(10):945–948.
- Sillitoe, R. H., (1997). Characteristics and Controls of the Largest Porphyry Copper-Gold and Epithermal Gold Deposits in the Circum-Pacific Region. *Australian Journal of Earth Sciences* 44(3):373–388.
- Sillitoe, R. H., (1999). Styles of High-Sulfidation Gold, Silver and Copper Mineralization in Porphyry and Epithermal Environments. *PACRIM Congress '99, Bali, Indonesia, 1999*. Conference Proceedings. Australian Institute of Mining and Metallurgy, 29–44.
- Sillitoe, R. H., (2010a). Iron Oxide-Copper-Gold Deposits: An Andean View. *Mineralium Deposita* 38:787–812.
- Sillitoe, R. H., (2010b). Porphyry Copper Systems. *Economic Geology* 105(1):3–41.
- Sillitoe, R. H. and Hedenquist, J. W., (2003). *Linkages between Volcanotectonic Settings, Ore-Fluid Compositions, and Epithermal Precious Metal Deposits*. Society of Economic Geologists Special Publication 10:315–343.
- Sillitoe, R. H. and Lorson, R. C., (1994). Epithermal Gold-Silver-Mercury Deposits at Paradise Peak, Nevada: Ore Controls, Porphyry Gold Association, Detachment Faulting and Supergene Oxidation. *Economic Geology* 89:1228–1249.
- Sillitoe, R. H. and Mortensen, J. K., (2010). Longevity of Porphyry Copper Formation at Quellaveco, Peru. *Economic Geology* 105(6):1157–1162.
- Sillitoe, R. H. and Perelló, J., (2005). Andean Copper Province: Tectonomagmatic Settings, Deposit Types, Metallogeny, Exploration, and Discovery. *Economic Geology*, 100th Anniversary Volume, pp. 845–890.
- Sillitoe, R. H., Steele, G. B., Thompon, J. F. H. and Lang, J. R., (1998). Advanced Argillic Lithocaps in the Bolivian Tin-Silver Belt. *Mineralium Deposita* 33:539–546.
- Sinclair, W. D., (2007). *Porphyry Deposits. Mineral Deposits of Canada: A Synthesis of Major Deposit-Types, District Metallogeny, the Evolution of Geological Provinces, and Exploration Methods*. Geological Association of Canada, Mineral Deposits Division, Special Publication 5:223–243.
- Smith, D. M., Jr., Albinson, T. and Sawkins, F. J., (1982). Geologic and Fluidinclusion Studies of the Tayoltita Silver-Gold Vein Deposit, Durango, Mexico. *Economic Geology* 77:1120–1145.
- Sokolov, A. L., (1998). The Regional and Local Controls on Gold and Copper Mineralization in Central Asia and Kazakhstan. In Porter, T. M. (Ed), *Porphyry and hydrothermal copper and gold deposits: A global perspective*, Perth, 1998, Conference Proceedings, Glenside, South Australia, Australian Mineral Foundation, pp. 181–189.

- Solomon, G. H., (2006). *Tasman Resources NI, Sulphide-Rich Epithermal Veining Intersected*. Australian Stock Exchange Announcement, Exploration Update. 11th October 2006.
- Steele, G. B. (1996). *Metallogenesis and Hydrothermal Alteration at Cerro Rico, Bolivia*. Ph.D. thesis, University of Aberdeen, p. 435.
- Swain, G., Barovich, K., Hand, M., Ferris, G. and Schwarz, M., (2008). Petrogenesis of the St Peter Suite, Southern Australia: Arc Magmatism and Proterozoic Crustal Growth of the South Australian Craton. *Precambrian Research* 166:283–296.
- Swain, G., Woodhouse, A., Hand, M., Barovich, K., Schwarz, M. and Fanning, C. M., (2005). Provenance and Tectonic Development of the Late Archaean Gawler Craton, Australia; U-Pb Zircon, Geochemical and Sm-Nd Isotopic Implications. *Precambrian Research* 141:106–136.
- Tasman Resources NI, (2006). *Evaluation of Newly Discovered and Untested Epithermal Gold-Silver Mineralisation near Parkinson Dam, S.A.* Unlocking South Australia's Mineral & Energy Potential A Plan for Accelerating Exploration Theme 2: Drilling Partnerships with PIRSA and Industry. Tasman Resources NL: Interim Drilling Report: Parkinson Dam Project DPY3-10. ENV 11121, 109.
- Thompson, T. B., (1992). Mineral Deposits of the Cripple Creek District, Colorado. *Mining Engineering* 44:135–138.
- Tingley, J. V. and Berger, B. R., (1985). *Lode Gold Deposits of Round Mountain, Nevada*. Nevada Bureau of Mines and Geology, Report 100.
- Tosdal, R. M., (2012). *Tectonics and the Porphyry-Epithermal Transition*. Proceedings of the 34th International Geological Congress 2012, 1810.
- Tosdal, R. M. and Richards, J. P., (2001). Magmatic and Structural Controls on the Development of Porphyry Cu ± Mo ± Au Deposits. *Reviews in Economic Geology* 14:157–181.
- Ulrich, T. and Heinrich, C. A., (2001). Geology and Alteration Geochemistry of the Porphyry Cu-Au Deposit at Bajo De La Alumbrera, Argentina. *Economic Geology* 96:1719–1742.
- Van Leeuwen, T. M., Leach, T. M., Hawke, A. A. and Hawke, M. M., (1990). The Kelian Disseminated Gold Deposit, East Kalimantan, Indonesia. *Journal of Geochemical Exploration* 35:1–61.
- Vikre, P. G., (1989a). Fluid-Mineral Relations in the Comstock Lode. *Economic Geology* 84:1574–1613.
- Vikre, P. G., (1989b). Ledge Formation at the Sandstorm and Kendall Gold Mines, Goldfield, Nevada. *Economic Geology* 84:2115–2138.
- Vikre, P. G., Mckee, E. H. and Silberman, M. L., (1988). Chronology of Miocene Hydrothermal and Igneous Events in the Western Virginia Range, Washoe, Storey, and Lyon Counties, Nevada. *Economic Geology* 83(4):864–874.
- Vry, V. H., Wilkinson, J. J., Seguel, J. and Millán, J., (2010). Multistage Intrusion, Brecciation, and Veining at El Teniente, Chile: Evolution of a Nested Porphyry System. *Economic Geology* 105(1):119–153.
- Wade, B., Barovich, K., Hand, M., Scrimgeour, I. R. and Close, D. F., (2006). Evidence for Early Mesoproterozoic Arc-Related Magmatism in the Musgrave Block, Central Australia: Implications for Proterozoic Crustal Growth and Tectonic Reconstructions of Australia. *Journal of Geology* 114:43–63.
- Wade, C. E., (2011). Definition of the Mesoproterozoic Ninnerie Supersuite, Curnamona Province, South Australia. *MESA Journal* 62:35–52. Department for Manufacturing, Innovation, Trade, Resources and Energy, South Australia, Adelaide.
- Wade, C. E., (2012). *Geochemistry of Pre-1570 Ma Mafic Magmatism within Southern Australia: Implications for Possible Tectonic Settings and of Major Mineralisation Events in South Australia*, Report Book 2012/00019. Department for Manufacturing, Innovation, Trade, Resources and Energy, South Australia, Adelaide.
- Wade, C. E., Reid, A., Wingate, M. T. D., Jagodzinski, E. A. and Barovich, K., (2012). *Geochemistry and Geochronology of the C. 1585 Ma Benagerie Volcanic Suite, Southern Australia: Relationship to the Gawler Range Volcanics and Implications for the Petrogenesis of a Mesoproterozoic Silicic Large Igneous Province* *Precambrian Research*, 206–207, 17–35.
- Wilson, A. J., R., C. D. and Richards, T., (2004). *Veins, Pegmatites and Breccias: Examples from the Alkalic Cadia Quarry Au-Cu Porphyry Deposit, NSW, Australia*. University of Tasmania, Centre for Ore Deposit Research Special Publication 5:45–56.